THE EFFECT OF MACROPHAGE-SECRETED FACTORS ON PREADIPOCYTE SURVIVAL

André Molgat

Thesis submitted to the

Faculty of Graduate and Postdoctoral Studies

In partial fulfillment of the requirements

For the Ph.D. degree in Biochemistry

Department of Biochemistry, Microbiology and Immunology

Faculty of Medicine

University of Ottawa

ABSTRACT

Adipose tissue (AT) expansion and remodeling that maintains healthy function relies on stromal preadipocytes capable of differentiating into new adipocytes (adipogenesis). During chronic positive energy balance, a relative deficit in adipogenesis, from either a decrease in preadipocyte number or their capacity to differentiate, leads to excessive adipocyte hypertrophy and AT dysfunction. AT contains macrophages whose number and activation state is dynamically regulated with changes in AT mass. This study aims to investigate the effect of macrophage-secreted factors on preadipocyte survival.

To assess the effect of macrophage-secreted factors on preadipocytes, murine 3T3-L1 preadipocytes or human primary preadipocytes were incubated with macrophage-conditioned medium (MacCM), prepared from either murine (J774A.1, RAW264.7, bone marrow-derived) or human (THP-1, monocyte-derived) macrophage models, respectively. MacCM inhibited preadipocyte apoptosis and activated pro-survival signaling in both preadipocyte models. Inhibition of PDGFR, Akt, or ERK1/2 reduced the pro-survival effect of MacCM in 3T3-L1 preadipocytes. Inhibition of reactive oxygen species (ROS) generation, or enhancement of ROS clearance, reduced MacCM-dependent 3T3-L1 preadipocyte survival. Whereas anti-inflammatory activated macrophages retained the ability to prevent preadipocyte apoptosis, pro-inflammatory activated macrophages did not. TNF-α immunoneutralization restored the survival activity of pro-inflammatory MacCM on 3T3-L1 preadipocytes.

These studies reveal a novel pro-survival effect of MacCM on preadipocytes, and identify signaling molecules (PDGF, Akt, ERK1/2, and ROS) that underlie this action. Macrophage activation was found to regulate the pro-survival activity of MacCM. These *in vitro* cell culture

studies are consistent with a model in which the extent of preadipocyte apoptosis *in vivo* may determine preadipocyte number and the ability of AT to expand while maintaining healthy function during chronic positive energy balance.

ACKNOWLEDGMENTS

I would like to thank my supervisor and mentor Dr. Alexander Sorisky for his guidance, support, and patience throughout my training. I am grateful to have had the opportunity to study in his laboratory. Thank you to all of the members of the lab for creating a very stimulating and enjoyable research environment. Specifically, I would like to acknowledge the invaluable advice and assistance provided by Dr. AnneMarie Gagnon, and the excellent technical assistance of Anne Landry. Lastly, thank you to my mother, father, sister, and Cassandra for their support and encouragement.

TABLE OF CONTENTS

LIST OF ABBREVIATIONS

α-SMA	Alpha-smooth muscle actin
ANOVA	Analysis of variance
AT	Adipose tissue
ATE	Adipose tissue eosinophil
ATGL	Adipose triglyceride lipase
ATL	Adipose tissue lymphocyte
ATL-B	Adipose tissue B lymphocyte
ATL-T	Adipose tissue T lymphocyte
ATM	Adipose tissue macrophage
BAT	Brown adipose tissue
BMD-macrophages	Bone marrow-derived macrophages
BMI	Body mass index
BSA	Bovine serum albumin
CCL	Chemokine C-C motif ligand
CCR	Chemokine C-C motif receptor
CD	Cluster of differentiation
Cdk	Cyclin-dependent kinase
C/EBP	CCATT-enhancer-binding protein
CHX	Cycloheximide
CLS	Crown-like structure
CS	Calf serum
CVD	Cardiovascular disease
DEXA	Dual-energy X-ray absorptiometry
DG	Diacylglycerol
DHR123	Dihydrorhodamine 123
DMEM	Dulbecco's modified Eagle's medium
DMSO	Dimethyl sulfoxide
DPI	Diphenyleneiodonium
ECM	Extracellular matrix
EGTA	Ethylene glycol tetraacetic acid
ELISA	Enzyme-linked immunosorbent assay
ER	Endoplasmic reticulum
ERK1/2	Extracellular signal-regulated kinase 1/2
FABP4	Fatty acid binding protein 4
FAS	Fatty acid synthase
FBS	Fetal bovine serum
FLICE	Fas-associated protein with death domain-like interleukin-1 beta-converting enzyme
GLUT4	Glucose transporter type 4
GM-CSF	Granulocyte-macrophage colony-stimulating factor
Gr1	Granulocyte differentiation antigen 1
Grb2	Growth factor receptor-bound protein 2

GWAS	Genome-wide association studies
HBSS	Hank's buffered salt solution
HIF-1α	Hypoxia-inducible factor-1 alpha
HRP	Horseradish peroxidase
HSL	Hormone-sensitive lipase
IFNγ	Interferon gamma
IGF-1	Insulin-like growth factor 1
IgG	Immunoglobulin G
IKKβ	Inhibitor of kappa B kinase beta
IL	Interleukin
IOD	Integrated optical density
IRS-1	Insulin receptor substrate-1
JNK	c-Jun N-terminal kinase
LD	Lipid droplet
LPS	Lipopolysaccharide
MacCM	Macrophage-conditioned medium
MCE	Mitotic clonal expansion
MCP-1	Monocyte chemotactic protein-1
MD-macrophages	Monocyte-derived macrophages
MEK1/2	Mitogen-activated protein kinase kinase
MG	Monoacylglycerol
MGL	Monoacylglycerol lipase
MHO	Metabolically healthy obese
MRI	Magnetic resonance imaging
mTORC2	Mammalian target of rapamycin complex 2
NAC	N-acetyl cysteine
NADPH	Nicotinamide adenine dinucleotide phosphate
NEFA	Non-esterified fatty acids
NFκB	Nuclear factor κ B
NOX	Nicotinamide adenine dinucleotide phosphate oxidase
NP-40	Nonidet P-40
PBMC	Peripheral blood mononuclear cell
PBS	Phosphate buffered saline
PDGF	Platelet-derived growth factor
PDGFRβ	Platelet-derived growth factor receptor beta
PDK1	Phosphoinositide-dependent kinase-1
PI	Propidium iodide
PI3K	Phosphoinositide 3-kinase
PKA	Protein kinase A
PPARγ	Peroxisome proliferator-activated receptor gamma
PTEN	Phosphatase and tensin homolog
Romo1	Reactive oxygen species modulator 1
ROS	Reactive oxygen species
RPMI	Roswell Park Memorial Institute
RQ	Relative quantification
RT-PCR	Real time-polymerase chain reaction

sAT	Subcutaneous adipose tissue
SDS-PAGE	Sodium dodecyl sulfate polyacrylamide gel electrophoresis
Sfrp5	Secreted frizzled-related protein 5
SGBS	Simpson-Golabi-Behmel syndrome
Sos	Son of sevenless
SREBP-2	Sterol-regulatory binding protein 2
SVF	Stromal-vascular fraction
T2D	Type 2 diabetes
TCR	T cell receptor
TG	Triacylglycerol
Th1	T helper 1
TNF-α	Tumor necrosis factor-alpha
TPA	12-O-tetradecanoylphorbol-13-acetate
Tregs	T regulatory cells
UPR	Unfolded protein response
vAT	Visceral adipose tissue
WHO	World Health Organization

LIST OF FIGURES

2.0 MANUSCRIPT #1

3.0 MANUSCRIPT #2

4.0 MANUSCRIPT #3

5.0 GENERAL DISCUSSION

1.0 GENERAL INTRODUCTION

OBESITY

Definition and assessment

Obesity is an excess accumulation of fat mass (adipose tissue; AT). Estimates from 2009 indicate that ~24% of Canadians are obese, representing a large increase from ~14% in 1989 (Shields et al., 2011). This condition can be quantified by numerous methods; the most routine is the body mass index (BMI) calculated by dividing the subject's body mass in kg by the subject's height in m^2. The World Health Organization (WHO) classifies individuals with a BMI $\geq$25kg/m^2 as overweight. A BMI $\geq$ 30kg/m^2 is considered obese. Calculation of BMI is rapid and does not require sophisticated equipment, making it suitable for population studies. However, body mass is influenced by changes in non-fat mass (ie. muscle and bone). Consequently, BMI does not always reflect an increase in AT mass. Unlike more sophisticated measures, BMI does not provide any information regarding the distribution of body fat. Waist circumference and waist to hip ratio measurements are other relatively rapid methods to estimate adiposity.

Other more accurate measures of AT mass require time, expertise, and/or expensive equipment, and are more appropriate for smaller studies. Caliper measurement of skin fold thickness is used to estimate body fat percentage, though this method only measures subcutaneous fat, and therefore does not account for intra-abdominal (visceral) fat stores. Underwater weighing, based on the Archimedes' principle of floating bodies,

is a procedure that is considered a gold standard for calculating body density, which can then be used to estimate fat mass. The precision of this technique is lowered by variation in skeletal mass, and a required mathematical correction for lung volume (Brozek et al., 1963). Dual-energy X-ray absorptiometry (DEXA) and magnetic resonance imaging (MRI) are accurate and rapid body imaging alternatives. DEXA quantifies bone mineral density and lean soft tissue, from which AT mass is indirectly estimated (Manninen, 2006). MRI allows for the accurate imaging of AT, and provides spatial detail of fat accumulation (Tinsley et al., 2004).

Causes of obesity

AT mass depends on the relative intake versus expenditure of calories. In a state of chronic positive energy balance, in which caloric intake exceeds energy expenditure, AT expands and obesity develops. Both the environment and the genome can have a profound influence on energy balance. Principal environmental factors contributing to obesity include the consumption of energy-rich foods and physical inactivity. Genetic influences on obesity have been estimated to contribute 40-70% to the variation in body weight within a population, by affecting energy intake and expenditure (Tung and Yeo, 2011). Although obesity is generally considered a multifactorial disease, rare monogenic forms of obesity exist. Monogenic forms of obesity usually result in an early-onset severe form of weight gain. Melanocortin 4 receptor loss-of-function mutations represent the most common monogenic form of obesity, accounting for ~5% of severe early onset obesity (Farooqi et al., 2003). This hypothalamic receptor binds to α-melanocyte

stimulating hormone and normally functions to decrease food intake (Farooqi et al., 2003). Loss-of-function mutations in the leptin gene or the leptin receptor account for ~3% of severe cases of obesity (Farooqi et al., 2002). Leptin, acting on its hypothalamic receptor, reduces appetite (Montague et al., 1997). It is therefore believed that the remaining heritability lies within a large number of genetic variants affecting multiple genes (Ramachandrappa and Farooqi, 2011). In order to identify genetic mutations that associate with obesity, genome-wide association studies (GWAS) have been conducted. GWAS have currently identified ~30 genetic loci affecting the risk of developing obesity (McCarthy, 2010). The first and strongest identified association between body weight and multiple variants in genetic loci was the fat mass and obesity associated FTO gene. Mutations in the FTO loci are associated with a 3 kg increase in body weight and a 1.7-fold increased risk of obesity (Frayling et al., 2007). Currently, loci identified by GWAS account for ~10% of the heritability of obesity (Ramachandrappa and Farooqi, 2011).

Complications of obesity

Obesity is a concern because it is associated with many morbidities. For example, obesity correlates with an increased risk for developing dyslipidemia, hypertension, type 2 diabetes (T2D), cardiovascular disease (CVD), and several types of cancer (Conway and Rene, 2004; Khandekar et al., 2011). In Canada, T2D, CVD, and cancer represent the top three causes of death (WHO, 2004).

Increased adiposity is associated with an impaired sensitivity to the action of insulin in peripheral tissues (insulin resistance), resulting in the aberrant release of non-

esterified fatty acids (NEFA) from AT, an increased production of hepatic very low density lipoprotein and glucose, and a reduced uptake of circulating glucose into muscle. Insulin resistance is caused by chronic low-grade inflammation due to the overproduction of pro-inflammatory cytokines both locally within AT and systemically (as discussed below).

ADIPOSE TISSUE

Forms and functions:

Brown versus white adipose tissue

AT exists in two forms, brown (BAT) and white, each possessing unique functions. BAT is a thermogenic organ producing heat by uncoupling mitochondrial electron transport from adenosine triphosphate production. This function is made possible by the unique expression of uncoupling protein-1 in the mitochondria of brown adipocytes (Cannon et al., 1982). Although long thought to disappear after birth, recent positron emission tomography imaging studies have revealed functional BAT in adult humans, located primarily in the neck region (Cypess et al., 2009; van Marken Lichtenbelt et al., 2009; Virtanen et al., 2009). In response to cold exposure, an increase in the uptake of glucose and NEFA from the circulation into BAT occurs. Uncoupled oxidation of NEFA within brown adipocytes significantly contributes to whole body energy expenditure during cold exposure (Ouellet et al., 2012).

White AT (referred to here as AT) is the body's major energy storage organ, and is the form of AT that defines obesity. AT serves a critical role in energy homeostasis during periods of fasting and feeding. In the fed state, insulin increases energy uptake and storage in AT (lipogenesis) and decreases energy breakdown and release from AT (lipolysis) (Frayn et al., 2003). In the fasting state, and during periods of exercise, sympathetic innervation releases norepinephrine within AT to stimulate lipolysis (Frayn et al., 2003). The presence and function of AT is evolutionarily conserved, with energy storage being allocated to AT in animals as primitive as fish (Gesta et al., 2007).

Adipose tissue depots

AT forms distinct depots, distributed within subcutaneous and visceral regions, each with a unique structure and function. Visceral AT (vAT) contains more blood vessels and neuronal innervation. These differences, in combination with a relatively higher sensitivity for β-adrenoceptor activation, result in greater lipolysis from vAT versus subcutaneous AT (sAT) depots (Tran et al., 2008). In contrast, sAT is thought to be more efficient at lipid storage. Functionally, these differences may contribute to the strong positive correlation between vAT and cardiometabolic disease (including insulin resistance, T2D, hypertension, and CVD) (Tran and Kahn, 2010). Differences in the cellular composition of the vAT and sAT have also been noted, with greater numbers of infiltrated leukocytes and lower numbers of preadipocytes (discussed below) in vAT (Tchoukalova et al., 2010a; Weisberg et al., 2003). AT remodeling, discussed below, differs between vAT and sAT.

The concept of distinct origins of adipocytes within different depots has recently emerged. Adipocyte precursor cells isolated from vAT versus sAT differ with respect to their ability to proliferate and differentiate into adipocytes (Macotela et al., 2012; Tchkonia et al., 2007). Furthermore, lineage tracing experiments have suggested distinct progenitor subpopulations may give rise to adipocytes in different depots (Seale et al., 2011), supporting earlier mRNA analyses of adipocytes from vAT vs sAT indicating differential expression of developmental genes (Gesta et al., 2006). Distinct adipocyte origins may contribute to the differences in metabolic activity of each AT depot

The secretory function of the adipose tissue

In addition to storing energy, AT is a highly active endocrine organ, responsible for secreting many molecules that impact the function of other tissues (Lago et al., 2007). These AT-derived molecules are collectively referred to as adipokines. The archetypal adipokine, leptin, was discovered in 1994 by Freidman and his research group (Zhang et al., 1994). The cloning of leptin from adipocytes explained the genetic basis for the obese phenotype in a mutant mouse, ob, generated in 1950 (Ingalls et al., 1950). Freidman's studies followed earlier work by Coleman's group showing that the mutation in ob mice resulted in the loss of a circulating hormone affecting satiety (Coleman, 1973). The regulation of feeding by leptin is mediated through signaling events in leptin receptor-expressing neurons within the hypothalamus (Bjorbaek and Kahn, 2004). Leptin has more recently been shown to exert pleiotropic effects on metabolism and energy balance by acting on both central and peripheral tissues (Bjorbaek and Kahn, 2004; Lago et al.,

2007). Subsequent to the discovery of leptin, numerous other adipokines have been identified (Muoio and Newgard, 2005). The effects of adipokines are diverse, affecting muscle insulin sensitivity and glucose uptake, liver metabolism, and the vasculature (Lau et al., 2005; Mora and Pessin, 2002). Additionally, adipokines are emerging as important immune regulatory molecules, acting as either anti-inflammatory (adiponectin, Interleukin (IL)-10, secreted frizzled-related protein 5; Sfrp5), or pro-inflammatory (IL-6, IL-1β, tumor necrosis factor-α; TNF-α) autocrine/paracrine signals (Bradley et al., 2008; Hotamisligil et al., 1995; Ouchi et al., 2010; Turer and Scherer, 2012). These molecules are produced from a variety of cell types within the AT, including adipocytes, preadipocytes, and AT leukocytes.

Cellular composition of the AT

AT can be separated into adipocyte and non-adipocyte fractions by filtration and centrifugation, based on the buoyant nature of the lipid-filled adipocyte (Skurk and Hauner, 2012). Adipocytes comprise between 50 – 70% of the cellular mass of AT. Within the non-adipocyte fraction (aka stromal-vascular fraction; SVF), there exists a heterogeneous collection of cells, composed of preadipocytes (20 – 40%), vascular endothelial cells (1-10%), and leukocytes (10-50%) (Hauner, 2005).

Adipocytes

The adipocyte serves as the energy reservoir within AT, possessing the capacity to store an estimated 3μg of lipid (Danforth, 2000). The bulk of the adipocyte's mass derives from a single lipid droplet (LD), consisting of a phospholipid monolayer encapsulating a neutral lipid core. The lipid core is composed primarily of triacylglycerol (TG), and a small amount of cholesteryl ester (Frayn et al., 2003).

TG is synthesized when energy is in excess. Fatty acids delivered to the adipocyte from circulating lipoproteins are esterified onto glycerol molecules by specific acyltransferases to form monoacylglycerol (MG), diacylglycerol (DG), or TG. Glycerol is derived from glycolysis, or synthesized from oxaloacetate, through glyceroneogenesis. De novo synthesized fatty acids from glucose also contribute to the fatty acid pool, albeit to a lesser extent (Reshef et al., 2003).

Lipolysis in the adipocyte LD, defined as the breakdown of TG into glycerol and individual NEFA, occurs to meet energy demand. The phospholipid monolayer of the LD is the site of action for many proteins that regulate the enzymatic digestion of the inner lipids. Examples of these proteins include monoacylglycerol lipase (MGL), hormone-sensitive lipase (HSL), and adipose triglyceride lipase (ATGL). ATGL catalyzes the hydrolysis of the initial fatty acid from TG, forming DG. Though expressed in most cell types, ATGL is enriched in AT. Upon interaction of ATGL with the LD-associated protein, comparative gene identification-58, TG hydrolase activity of ATGL is greatly enhanced (Zechner et al., 2012). Negative regulation of ATGL activity occurs in part through its interaction with G_0/G_1 switch gene 2 (Yang et al., 2010). Subsequent

hydrolysis of DG to MG occurs through the action of HSL. HSL is selectively expressed in adipocytes and steroidogenic tissues, and regulated by protein kinase A (PKA)-dependent phosphorylation, which promotes its recruitment to the LD. PKA also phosphorylates and triggers the dissociation of perilipin from the LD, which facilitates HSL access to lipid substrate (Frayn et al., 2003). MGL, abundantly expressed in most cell types and not rate-limiting, catalyzes the hydrolysis of the third fatty acid from MG, releasing glycerol (Thiele and Spandl, 2008).

Adipocyte turnover

Recent investigations using novel methods of cellular dating have revealed a homeostatic turnover of adipocytes. A comparison of ^{14}C levels in adipocyte genomic DNA with declining atmospheric ^{14}C levels (since cessation of above-surface atomic bomb testing), has estimated that ~10% of adipocytes within human sAT turn over each year (Spalding et al., 2008). Other strategies involving the labeling of proliferating preadipocytes with either bromodeoxyuridine or $^{2}H_2O$, followed by the assessment of the label's presence in mature adipocytes, have been performed in both mice and humans (Neese et al., 2002; Rigamonti et al., 2011; Strawford et al., 2004). These studies support the concept of constant adipocyte production in adulthood, though the estimated turnover rates derived from these alternative methods are higher than those derived from ^{14}C cellular dating. All measurements to date have been made using stable-weight mice and humans, during which AT mass was not changing; adipocyte turnover may be much greater during AT expansion. Due to the post-mitotic nature of these mature cells,

adipocyte generation occurs not by proliferation but via the recruitment and differentiation of adipogenic progenitors.

Adipogenesis

Adipocytes arise from the differentiation of preadipocytes, stromal progenitor cells committed to the adipocyte lineage. Adipocyte differentiation, termed adipogenesis, is a regulated process occurring in two phases; mitotic clonal expansion (MCE), and terminal differentiation. MCE is initiated by mitogenic signals that stimulate a limited phase of preadipocyte proliferation (Festa et al., 2011; Tang et al., 2003). During MCE, chromatin remodeling provides access for transcription factor binding to the promoter regions of adipocyte-specific genes (Farmer, 2006). An orchestrated sequence of transcriptional regulation, involving E2F and pocket proteins, prepares the preadipocyte for terminal differentiation. Prior to adipogenic induction, E2F4, complexed with the pocket protein p130, interacts with histone deacetylase 3 on the promoter of peroxisome proliferator-activated receptor γ (PPARγ) 1, maintaining its transcriptional repression (Reichert and Eick, 1999). E2F1 is simultaneously sequestered away from its DNA response elements through its interaction with retinoblastoma protein (Rb). Following adipogenic induction, p130 and the cyclin-dependent kinase (Cdk) inhibitor, $p27^{kip}$, are downregulated, leading to PPARγ1 transcription and Cdk activation (Patel and Lane, 2000; Richon et al., 1997). Rb is sequentially phosphorylated by cyclin D1/Cdk4/6, cyclin E/Cdk2, and cyclin A/Cdk2 complexes, releasing E2F1 and allowing for the

expression of genes required for cell cycle entry (Lundberg and Weinberg, 1998). Following preadipocyte expansion, terminal differentiation proceeds.

Induction of early-phase transcription factors, CCATT-enhancer-binding protein (C/EBP) β and δ, occurs through an early growth response protein 2-dependent pathway (Chen et al., 2005). C/EBPβ and δ drive the expression of PPARγ and C/EBPα, master regulators of adipogenesis (Rosen et al., 2002). PPARγ and C/EBPα reciprocally upregulate each other, and initiate transcription of adipocyte-specific genes such as those involved in lipid accumulation (ie. fatty acid binding protein 4, FABP4; fatty acid synthase, FAS) and adipokine production (ie. leptin, adiponectin); resulting in the mature insulin-responsive adipocyte phenotype.

Preadipocytes

AT contains stromal progenitors at various stages of adipogenic commitment. Less committed progenitors, referred to as mesenchymal stem cells, have the capacity to differentiate into osteoblasts, chrondrocytes, and adipocytes when provided with the appropriate signals. As such, these progenitors are multipotent, and their molecular signature is beginning to be defined. Methods for AT progenitor identification vary due to a lack of cell surface markers capable of distinguishing multipotent cells from committed preadipocytes. Peadipocytes are currently defined as either adherent stromal cells possessing adipogenic potential, or as stromal cells expressing a limited number of cell surface proteins (Decaunes et al., 2011; Rodeheffer et al., 2008; Tchoukalova et al., 2007; Tran et al., 2012).

In mice, positive selection for a combination of cluster of differentiation (CD) 29, CD34, CD24, and stem cell antigen-1; or platelet-derived growth factor receptor β (PDGFRβ), α-smooth muscle actin (α-SMA), and NG2, isolates a population of cells capable of forming functional fat pads upon transplantation, and possessing multipotent differentiation capacity *in vitro* (Rodeheffer et al., 2008; Tang et al., 2008). In human AT, stromal cells expressing CD34 but not CD31 or CD14, may represent a similar progenitor, not fully committed to the adipocyte lineage, but capable of robust adipogenesis *in vitro* (Maumus et al., 2011).

Emerging evidence suggests the *in situ* location of adipose progenitors is near, or on, the tissue microvasculature (Maumus et al., 2011; Rodeheffer et al., 2008; Tang et al., 2008). The close interplay between the adipose microvasculature and adipogenesis has been further supported by recent lineage tracing analyses that suggest endothelial cells and preadipocytes may share a common progenitor (Gupta et al., 2012; Tran et al., 2012). Indeed, the above-mentioned combination of PDGFRβ, α-SMA, and NG2, are markers of vascular support cells termed pericytes (Armulik et al., 2011).

Adipose tissue growth and remodeling:

Adipose tissue expansion

AT expansion leading to obesity occurs through coordinated increases in both adipocyte size (hypertrophy) and number (hyperplasia) (Alligier et al., 2012). Hyperplastic AT expansion involves the recruitment and differentiation of preadipocytes

into adipocytes. Expansion predominantly through hyperplasia distributes the excess energy among many newly generated adipocytes, which serves to maintain the metabolic function of each adipocyte. Hypertrophic AT expansion occurs when the excess energy is stored as TG in the existing adipocytes, resulting in hypertrophy e.g. an increase in cell volume (Heilbronn et al., 2004). Hypertrophy has been linked to adipocyte dysfunction, AT inflammation, insulin resistance, and an increased risk of developing T2D (Heilbronn et al., 2004). Weight gain through AT hyperplasia is thought to be more favourable, and is commonly seen in metabolically healthy obese (MHO) patients, which represent up to 25% of obese individuals (Bluher, 2010; Kloting et al., 2010). Therefore hypertrophic AT can be thought of as dysfunctional fat, whereas hyperplastic AT represents a functional form of fat.

Careful examination of weight gain in a high fat-fed mouse model has revealed the temporal coordination between AT hyperplasia and hypertrophy (Strissel et al., 2007). Early expansion of the AT occurs through adipocyte hypertrophy, with little change in adipocyte number. Following hypertrophy is a transient phase of adipocyte death resulting in a marked (up to 80%) decline in the number of adipocytes. This phase coincides with the infiltration of leukocytes and robust remodeling of the AT extracellular matrix (ECM), involving the deposition of collagen proteins, an event linked with adipogenesis (Divoux et al., 2010). Remodeling events also coincide with the proliferation of preadipocytes, a prerequisite for adipocyte differentiation (Festa et al., 2011; Suga et al., 2010). Indeed, subsequent to adipocyte death, significant increases in adipocyte number occur, due to the presence of preadipocytes and their differentiation into adipocytes (Strissel et al., 2007). Recent investigations in humans support many of

these observations. Overfeeding humans for two months in a controlled experimental setting results in depot-selective increases in adipocyte size and number (Tchoukalova et al., 2010b); concomitantly, increased ECM gene expression and collagen deposition is seen (Alligier et al., 2012).

Evidence of an adipogenic deficit

A deficit in the number of preadipocytes and/or their adipogenic capacity would be expected to impair the late phase of hyperplasic AT growth, described by Strissel et al. Consequently, an adipogenic deficit would favour AT expansion predominantly through hypertrophy (Danforth, 2000; Heilbronn et al., 2004). Several observations have suggested an adipogenic deficit may exist in obese humans. The number of preadipocytes per gram of AT is reduced in obese humans compared to lean controls (Onate et al., 2012; Tchoukalova et al., 2007). Marked adipocyte hypertrophy is evident in AT sections from obese patients, which correlates with an impaired adipogenic capacity of isolated preadipocytes from humans with a high BMI (Kloting et al., 2010; van Harmelen et al., 2003). Expression analyses of AT from insulin-resistant obese individuals has revealed that adipocyte-related genes are downregulated relative to MHO (Kloting et al., 2010). Obese patients with hypertrophic AT and insulin resistance generate 70% fewer adipocytes each year compared to MHO patients with hyperplastic AT (Arner et al., 2010). Taken together, the number of preadipocytes and their adipogenic capacity may represent critical determinants of AT function.

ADIPOSE TISSUE DYSFUNCTION

Molecular mechanisms of adipocyte dysfunction

Aberrant NEFA release from hypertrophied adipocytes results in ectopic lipid accumulation, primarily in the muscle and liver. The accumulation of ectopic lipids, particularly DG and ceramides derived from long chain acyl-CoA species, interferes with normal muscle and liver function. Through the activation of serine/threonine kinases (ie. protein kinase C; c-Jun N-terminal kinase, JNK; and inhibitor of kappa B kinase beta, IKKβ), ectopic lipids promote the inhibitory phosphorylation of the insulin receptor and IRS-1. Consequently, insulin promotes less glucose uptake into myocytes, fails to suppress hepatic glucose production, and increases hepatic lipid synthesis, contributing to hyperglycemia and dyslipidemia (Bremer et al., 2012). The molecular mechanism by which adipocyte hypertrophy results in dysfunctional AT is complex. Lipid overload within the adipocyte has been demonstrated to trigger membrane cholesterol depletion, endoplasmic reticulum (ER) stress, and hypoxia, all of which converge on the over-production of pro-inflammatory cytokines.

Cholesterol imbalance

Accumulation of intracellular TG is accompanied by a proportional increase in unesterified cholesterol on the surface of the LD (Krause and Hartman, 1984). During

adipocyte hypertrophy, to maintain a constant TG to cholesterol ratio on the LD, a relative depletion of membrane cholesterol occurs (Guerre-Millo et al., 1994). Membrane cholesterol levels are sensed through sterol-regulatory binding protein 2 (SREBP-2) (Radhakrishnan et al., 2008). When membrane cholesterol levels decline, SREBP-2 translocates to the nucleus where it is active. In hypertrophied adipocytes, an accumulation of nuclear SREBP-2 is seen (Le Lay et al., 2001). Enhanced SREBP-2 activation results in over-production of pro-inflammatory, insulin de-sensitizing cytokines (e.g. IL-6 and TNF-α), and the down-regulation of mediators of insulin action (e.g. Glucose transporter type 4; GLUT4) (Le Lay et al., 2001).

ER stress

The storage and handling of intracellular lipids requires the synthesis of many proteins necessary for fatty acid transport, modification, esterification, and packaging within the LD. The ER is the site responsible for synthesizing nascent proteins by translating messenger RNA into a polypeptide sequence. Increased levels of intracellular lipid increase the demand for protein synthesis (Boden, 2009). When the demand for protein synthesis exceeds the capacity of the ER, an unfolded protein response (UPR) is initiated. The UPR involves the activation of double-stranded RNA-dependent protein kinase-like ER kinase, inositol-requiring protein-1, and activating transcription factor 6, which collectively act to restore ER function by upregulating protein chaperones, stimulating ER biogenesis, and inhibiting protein translation (Boden, 2009). A pathologic UPR, as occurs when the elevated demand for protein synthesis persists, leads to ER

stress. ER stress activates JNK and IKKβ which promote pro-inflammatory cytokine production and impair insulin action (Hirosumi et al., 2002; Jiao et al., 2011). ER stress is evident in AT of insulin-resistant obese mice and humans, and inhibition of ER stress in mice improves insulin sensitivity (Boden, 2009; Ozcan et al., 2004; Ozcan et al., 2006).

Hypoxia

AT expansion relies heavily on concomitant vascularization of the growing tissue. Insufficient vascularization results in an inadequate supply of O_2, resulting in hypoxia. Localized regions of hypoxia have been found in AT of obese animals, and have been causally linked to insulin resistance. Hypoxia has been documented by a reduction in the interstitial partial pressure of O_2, by increased chemical staining with hypoxia-specific probes, and by increased expression of the hypoxia-dependent protein, hypoxia-inducible factor-1 alpha (HIF-1α) in hypertrophied adipocytes (Rausch et al., 2008). The main function of HIF-1α signaling is to promote vascularization through the upregulation of pro-angiogenic genes. However, HIF-1α also signals through the pro-inflammatory transcription factor, nuclear factor kappa B (NFκB), turning on the expression of a myriad of insulin desensitizing pro-inflammatory genes (e.g. TNF-α, IL-1β, IL-6, and monocyte chemotactic protein-1; MCP-1). Adipocyte-selective deletion of HIF-1α protects animals from obesity-associated insulin resistance (Jiang et al., 2011).

ADIPOSE TISSUE INFLAMMATION

Adipose tissue leukocytes

Within AT, numerous leukocytes reside whose number and activity are dynamically regulated. The composition of AT leukocytes includes myeloid cells from the innate immune system (ie. macrophages and eosinophils) and lymphoid cells from the adaptive immune system (ie. T and B lymphocytes). AT leukocytes can be broadly classified into pro-inflammatory and anti-inflammatory populations; their relative balance appears to influence AT function.

Adipose tissue macrophages

AT macrophages (ATMs) are by far the most numerous, comprising ~ 50% of the total AT leukocyte population. ATMs were first identified in 2003 by the research groups of Ferrante and Chen, and found to be of bone-marrow origin (Weisberg et al., 2003; Xu et al., 2003). The ATM population has been broadly defined by reactivity with F4/80 antibody (aka epidermal growth factor-like module-containing mucin-like hormone receptor-like 1, in humans). The number of ATMs was shown to dramatically increase with obesity in both mice and humans, ranging from 5% of the SVF in lean subjects to upwards of 50% in obese. In addition to adiposity, ATM number varies according to age, gender, and the particular adipose depot examined (Lumeng et al., 2011; Ortega Martinez

de Victoria et al., 2009; Tam et al., 2012). ATMs are most abundant in vAT, peak in humans between 30-35 years of age, and have been found to be more numerous in females. ATM content positively correlates with the degree of insulin resistance (Wentworth et al., 2010).

Subsequent studies have refined the origins and phenotypes of ATMs and revealed these cells to be complex and highly heterogeneous. With respect to their influence on AT function, the activation state of the ATM appears to be paramount. Macrophages are reactive cells, altering their phenotype and function in response to their local environment (Gordon, 2003). Two divergent activation states, M1 and M2, are commonly used to classify macrophages. M1 macrophages result from activation with interferon γ (IFNγ) or lipopolysaccharide (LPS), and display a pro-inflammatory phenotype. M2 macrophages result from activation with IL-4 or IL-13, and display an anti-inflammatory phenotype (Gordon, 2003). Many researchers describe ATMs using the M1/M2 system, though this classification does not recognize the heterogeneity within the ATM population (Romeo et al., 2012). Nevertheless, this system provides a general framework for the discussion of dominant ATM activation states. ATM subpopulations will herein be described using the pro-inflammatory (M1) or anti-inflammatory (M2) nomenclature.

The rise in ATM number observed with increasing adiposity primarily represents an accumulation of pro-inflammatory macrophages (Lumeng et al., 2007b). A causal link between pro-inflammatory ATMs and obesity-associated insulin resistance in mice has been demonstrated (Patsouris et al., 2008). The accumulation of pro-inflammatory ATMs occurs as a result of monocyte influx from the circulation, via a recruitment system

principally involving signaling between adipose-secreted MCP-1 and chemokine C-C motif receptor 2 (CCR2), expressed on the cell surface of blood monocytes (Oh et al., 2012; Weisberg et al., 2006). Other recruitment systems have also been suggested to contribute to ATM accumulation. Upregulation of various chemokines (MCP-2, MCP-3, chemokine C-C motif ligand 3; CCL3, and CCL5) and chemokine receptors (CCR1, CCR2, CCR3 and CCR5) have been observed in the circulation and AT of obese mice and humans (Kanda et al., 2006; Kitade et al., 2012; Zeyda et al., 2010). Genetic disruption of CCR5 expression either globally, or selectively in bone marrow cells, was found to prevent pro-inflammatory ATM accumulation in obese mice (Kitade et al., 2012).

Whether the infiltrating monocytes are predisposed to a pro-inflammatory fate, or acquire a pro-inflammatory phenotype within AT, is a subject of ongoing research. In support of the concept of pro-inflammatory predisposition, phenotypic heterogeneity among circulating monocytes has been documented in both mice and humans. Murine monocytes expressing granulocyte differentiation antigen 1 (Gr1) or human monocytes expressing CD14 and CD16, secrete high amounts of pro-inflammatory cytokines, and may possess a propensity to become pro-inflammatory tissue macrophages (van de Veerdonk and Netea, 2010). MCP-1 has been shown to selectively recruit Gr1-expressing monocytes to sites of infection (Dunay et al., 2008). However, *in vivo* monocyte tracking experiments in a mouse model of obesity have demonstrated blood monocytes only acquire pro-inflammatory activity after their recruitment into AT (Oh et al., 2012). Numerous molecules present within AT have been proposed to act as pro-inflammatory activators of recruited ATMs. These include, but are not limited to: adipocyte-derived

NEFA, preadipocyte and adipocyte-derived TNF-α, IL-1β, and IFN-γ (Mayi et al., 2012; Suganami et al., 2005).

In contrast to the pro-inflammatory ATMs that dominate in obese animals, anti-inflammatory ATMs are dominant in lean animals. An overall ATM phenotypic switch occurs with the transition from lean to obese states (Lumeng et al., 2007a). In contrast to the detrimental effects of pro-inflammatory ATMs on AT function, anti-inflammatory ATMs have been suggested to maintain AT homeostasis (Wu et al., 2011). This switch in ATM phenotype with obesity is the result of pro-inflammatory ATM accumulation, and not due to a decline in anti-inflammatory ATM number (Lumeng et al., 2008).

Anti- and pro-inflammatory ATMs exist in distinct tissue environments. Pro-inflammatory ATMs accumulate around large adipocytes that appear to be dying, and form what has been termed a crown-like structure (CLS) (Cinti et al., 2005). Anti-inflammatory ATMs reside within the interstitial spaces of the AT (Lumeng et al., 2008). The regulation of anti-inflammatory ATMs is poorly understood. Local proliferation of anti-inflammatory macrophages in non-adipose tissues has recently been demonstrated (Davies et al., 2011; Jenkins et al., 2011). Local production of IL-4 and IL-13, secreted from eosinophils, T lymphocytes, and adipocytes, may control anti-inflammatory ATM content (Fujisaka et al., 2009; Kang et al., 2008; Wu et al., 2011).

Through paracrine signaling, ATMs influence AT function. Macrophage-secreted factors can directly impair insulin-stimulated glucose uptake in adipocytes by downregulating GLUT4 and inhibiting insulin stimulated insulin receptor substrate-1 (IRS-1) tyrosine phosphorylation (Lumeng et al., 2007c). Macrophage-secreted factors interfere with lipid synthesis and stimulate lipolysis from adipocytes (Kurokawa et al.,

2010). Adipocyte-derived NEFA can then feedback on macrophages and further stimulate lipolytic cytokine release, establishing a paracrine loop between the adipocyte and the ATM (Suganami et al., 2005). Furthermore, macrophage-secreted factors disrupt adipokine production, alter preadipocyte proliferation, and block the differentiation of preadipocytes into adipocytes (Constant et al., 2006; Ichioka et al., 2011; Lacasa et al., 2007; Maumus et al., 2008). Anti-inflammatory macrophage activation can attenuate their anti-adipogenic influence on preadipocytes (Lu et al., 2010; Stienstra et al., 2008). These effects of ATMs on adipocytes position the ATM as a critical regulator of AT expansion and homeostasis.

Adipose tissue eosinophils

Eosinophils, associated with allergy and parasitic infection, are detectable within AT. In contrast to ATMs, AT-eosinophils (ATEs) decline in number with enlarging adipose mass. Through the secretion of IL-4, ATEs appear to support the anti-inflammatory activation of ATMs. Sustaining the ATE population in obese mice using helminth infection improves whole body insulin sensitivity and promotes anti-inflammatory activation of ATMs (Wu et al., 2011). The ATE has therefore emerged as a critical player in AT biology, through its influence on ATM activation.

Adipose tissue T lymphocytes

The innate immune cells operating within AT are integrated with adaptive immune cells. The adaptive immune system includes T and B lymphocytes, which respond to specific antigen, generating complementary cell surface receptors. T lymphocytes were first identified within the AT in 2007 based on the detection of AT CD3 expression, a component of the T cell receptor (TCR) that is present on all T lymphocyte subpopulations (Wu et al., 2007). AT T lymphocytes (ATL-Ts) exist as both resident and recruited populations. In lean mice and humans, a subpopulation of T lymphocytes known as T regulatory cells (Tregs) for their ability to dampen innate and adaptive immune reactions, represents ~ 3% of all AT-lymphocytes (ATLs) (Feuerer et al., 2009; Sun et al., 2012). Obesity is accompanied by a decline in AT Treg number which is associated with an increase in AT inflammation (Feuerer et al., 2009; Nishimura et al., 2009). As obesity develops, pro-inflammatory ATL-Ts accumulate, localizing within the CLS. ATL-T recruitment may occur in part through a system involving adipocyte-secreted CCL20 and CCR6 expressed on circulating T lymphocytes (Duffaut et al., 2009).

Recruited ATL-Ts include IFN-γ-producing CD4-positive ATL-Ts, which activate ATMs, and MCP-1-producing CD8-positive ATL-Ts, which may promote ATM recruitment (Kintscher et al., 2008). In support of this model in which ATL-Ts serve to recruit and activate ATMs, several studies have noted ATL-T accumulation precedes ATM recruitment (Duffaut et al., 2009; Kintscher et al., 2008; Nishimura et al., 2009), though other investigations have questioned this sequence of events (Strissel et al., 2010).

In either case, once present in AT, pro-inflammatory ATL-Ts contribute to AT inflammation and the development of insulin resistance (Ilan et al., 2010; Nishimura et al., 2009; Winer et al., 2009). ATL-Ts express a limited selection of TCRs, which suggests activation by a restricted variety of antigens (Feuerer et al., 2009), which possibly include AT-derived lipids (Ji et al., 2012).

Adipose tissue B lymphocytes

B lymphocytes, defined by the expression of CD19, are present in AT of mice and humans, and quickly increase in number as obesity develops (Duffaut et al., 2009). The accumulation of AT B lymphocytes (ATL-Bs) has been shown to occur immediately prior to ATL-T recruitment, though the consequences of this temporal sequence of ATL trafficking is unknown (Duffaut et al., 2009). ATL-Bs, like ATL-Ts and pro-inflammatory ATMs, localize within the CLS (McDonnell et al., 2012; Winer et al., 2011). ATL-Bs contribute to the development of obesity-associated insulin resistance and AT inflammation (McDonnell et al., 2012). This effect is largely mediated through ATL-B-dependent activation of ATL-Ts and ATMs (Winer et al., 2011). Furthermore, obese insulin resistant mice and humans have increased levels of pathogenic immunoglobulin G (IgG) autoantibodies (Winer et al., 2011).

RATIONALE

The above mentioned observations support the concept that distinct macrophage subsets, defined by a pro- or anti-inflammatory phenotype, serve unique functions in regulating AT expansion. Whereas pro-inflammatory ATMs may promote hypertrophic AT expansion through the inhibition of preadipocyte proliferation and differentiation, anti-inflammatory ATMs may promote hyperplastic and metabolically functional AT expansion through the maintenance of an adequate number of responsive preadipocytes.

The implication of macrophage-secreted factors in the regulation of preadipocyte differentiation and proliferation suggests that further regulation of preadipocyte number may occur through their influence on a third fate, namely preadipocyte survival. Promoting preadipocyte survival through the inhibition of apoptosis would be expected to maintain a population of preadipocytes capable of expanding the adipocyte pool through adipogenesis. In contrast, loss of preadipocytes through unsuppressed apoptosis would contribute to an adipogenic deficit, resulting in excess adipocyte hypertrophy and dysfunctional AT. Through paracrine signaling, ATMs may communicate with preadipocytes to suppress or promote apoptosis.

HYPOTHESIS

I hypothesize that macrophage-secreted factors regulate preadipocyte number by influencing preadipocyte survival.

CELL MODELS USED

3T3-L1 preadipocytes

3T3-L1 cells are a clonal line derived from 17 to 19 day old digested Swiss mouse embryos, selected for their spontaneous accumulation of intracellular TG following contact growth inhibition (Green and Kehinde, 1975; Todaro and Green, 1963). While fibroblast-like in their undifferentiated state, these cells assume a round adipocyte morphology while accumulating lipid. Differentiated 3T3-L1 adipocytes respond appropriately to lipolytic hormone treatment (Green and Goldberg, 1964, 1965; Green and Kehinde, 1975; Green and Meuth, 1974). The adipocyte conversion of 3T3-L1 cells can be enhanced with the addition of defined chemicals, making this cell line an excellent and widely used preadipocyte model (Student et al., 1980). Nevertheless, during initial selection, chromosomal duplications arose resulting in an aneuploid karyotype; confirmatory studies in primary preadipocyte cultures are therefore warranted (Todaro and Green, 1963).

Human primary preadipocytes

Human primary preadipocytes are isolated by centrifugation from the stromal-vascular fraction of digested sAT (Skurk and Hauner, 2012). These adherent cells represent a heterogeneous mixture, all possessing a fibroblast-like morphology and not

completely defined with respect to cell surface protein expression (Decaunes et al., 2011; Zimmerlin et al., 2010). Human primary preadipocytes have limited proliferative capacity, yet can be efficiently differentiated into adipocytes following treatment with defined chemicals (Skurk and Hauner, 2012). While a valuable human preadipocyte model, cell responses may be variable, as expected from donor heterogeneity in a primary cell population.

J774A.1 macrophages

J774A.1 cells are a clonal histiocyte line isolated from a reticulum cell sarcoma in Balb/c mice (Ralph et al., 1975). J774A.1 cells possess macrophage function (e.g. a high phagocytic capacity, activation by cytokines and antibody, and lysozyme expression), phenotype, and morphology (Ralph and Nakoinz, 1975). Basally J774A.1 macrophages secrete very low amounts of pro-inflammatory cytokines and large amounts of IL-1β (Lachman and Metzgar, 1980).

RAW264.7 macrophages

RAW264.7 macrophages are derived from a tumor isolated from the peritoneal cavity of Abelson murine leukemia virus-infected BAB/14 mice (Raschke et al., 1978). These adherent cells display phagocytic activity, secrete lysozyme, express macrophage cell surface proteins, and display elevated tumoricidal activity (Raschke et al., 1978).

RAW264.7 cells can be activated towards a pro-inflammatory phenotype upon appropriate chemical treatment, but secrete low levels of pro-inflammatory cytokines when unstimulated (Ralph and Nakoinz, 1977).

Bone marrow-derived macrophages

Bone marrow-derived macrophages (BMD-macrophages) are generated from murine BM progenitor cells, differentiated in culture dishes towards a macrophage cell fate by the presence of macrophage colony-stimulating factor (M-CSF)-containing L929 fibroblast-conditioned medium (Weischenfeldt and Porse, 2008). Following culture for 7 days, cells are considered fully differentiated, expressing macrophage surface proteins and cytokines, and displaying phagocytic function. Basally, BMD-macrophages are slightly skewed to an anti-inflammatory activation state, characterized by intermediate CD206 expression and undetectable nitric oxide production (Modolell et al., 1995).

THP-1 macrophages

THP-1 cells are derived from blood monocytes of a one year old boy with acute monocytic leukemia (Tsuchiya et al., 1980). Grown in suspension, THP-1 cells acquire plastic adherence and undergo macrophage differentiation following treatment with phorbol esters (Tsuchiya et al., 1982). Characterization of phorbol ester-treated THP-1 cells has demonstrated macrophage function (e.g. a high phagocytic capacity, activation

by cytokines and antibody, and lysozyme expression), phenotype, and morphology (Tsuchiya et al., 1982). Though certain differentiation protocols have been demonstrated to activate these cells, basally, low levels of pro-inflammatory cytokine (e.g. TNF-α) and anti-inflammatory surface marker expression (e,g, CD206) occur with the differentiation method employed in my studies (Daigneault et al., 2010). Their human origin and ability to be extensively passaged make the THP-1 cell line a valuable monocyte/macrophage model.

Monocyte-derived macrophages

Human monocyte-derived macrophages (MD-macrophages) are isolated from the peripheral blood mononuclear cell (PBMC) layer following Ficoll-gradient centrifugation of whole blood (Johnson et al., 1977). Following seeding into culture dishes, adherent cells represent a heterogenous population composed primarily of monocytes (Norris et al., 1979). A macrophage phenotype and morphology is acquired during culture in serum-supplemented medium (Daigneault et al., 2010). MD-macrophages can be activated towards pro- or anti-inflammatory phenotypes with different cytokine treatments; basally, MD-macrophages are mildly skewed towards an anti-inflammatory activation state (Daigneault et al., 2010; Martinez et al., 2006). The MD-macrophage is a valuable primary human macrophage cell model; however donor-related experimental variability is expected.

OBJECTIVES

Objective 1: Determine the effect of macrophage-secreted factors on preadipocyte survival.

Objective 2: Identify the anti-apoptotic signaling pathways mediating macrophage-dependent preadipocyte survival.

Objective 3: Determine the effect of macrophage activation on macrophage-dependent preadipocyte survival.

2.0 MANUSCRIPT #1

Preadipocyte apoptosis is prevented by macrophage-conditioned medium in a PDGF-dependent manner.

STATEMENT OF AUTHOR CONTRIBUTIONS

André S.D. Molgat is the first author on this publication. He performed all experiments, participated in the design of the experiments, performed the data analysis, and wrote the manuscript. **Dr. AnneMarie Gagnon** is the research associate in Dr. Alexander Sorisky`s laboratory. She participated in the design of the experiments, performed data analysis, and assisted in the editing and revising of the manuscript. **Dr. Alexander Sorisky** is the PhD supervisor of André Molgat. He contributed to the design of the experiments, analysis of results, and revising the manuscript.

SUMMARY

The following manuscript entitled "Preadipocyte apoptosis is prevented by macrophage-conditioned medium in a PDGF-dependent manner" was published in Am J Physiol Cell Physiol [(2009) 296, 757-765]. The objective of manuscript #1 was to determine the effect of macrophage-secreted factors on preadipocyte survival. This study was conducted using the 3T3-L1 preadipocyte cell model, and the J774A.1 and RAW264.7 macrophage cell models. MacCM was prepared and applied to confluent 3T3-L1 preadipocyte cultures. 3T3-L1 preadipocytes were induced to undergo apoptosis

by serum withdrawal. Preadipocyte apoptosis was assessed by enumeration of viable cells, staining and quantification of apoptotic nuclei with Hoechst 33342, and quantification of Annexin V/propidium iodide (PI) positive cells by flow cytometry. This study revealed that MacCM protects preadipocytes from apoptosis, and identified PDGF as the macrophage-derived factor responsible for the pro-survival effect.

Preadipocyte apoptosis is prevented by macrophage-conditioned medium in a PDGF-dependent manner.

André SD Molgat, AnneMarie Gagnon, Alexander Sorisky

Departments of Medicine and of Biochemistry, Microbiology, and Immunology, University of Ottawa, and Chronic Disease Program, Ottawa Health Research Institute, Ottawa ON Canada

Running Head: Macrophage-secreted PDGF prevents preadipocyte apoptosis.

Contact information

Dr. Alexander Sorisky, Ottawa Health Research Institute, 725 Parkdale Avenue, Ottawa ON K1Y 4E9 Canada; Tel: 613-798-5555 #17572; Fax: 613-761-4355;

email: asorisky@ohri.ca

ABSTRACT

Obesity is associated with macrophage accumulation and inflammation in adipose tissue. Macrophage-secreted factors have been reported to inhibit the differentiation of preadipocytes into adipocytes and to modulate adipogenic extracellular matrix gene expression. To enlarge our understanding of macrophages and the scope of their interactions with preadipocytes, we investigated their effect on preadipocyte survival. Acute exposure of 3T3-L1 preadipocytes to J774A.1 macrophage-conditioned medium (MacCM) stimulated platelet-derived growth factor receptor (PDGFR) tyrosine phosphorylation by 4.1-fold. There were significant increases in the phosphocontent of downstream PDGFR targets, Akt and ERK1/2 (5.3 fold and 2.4 fold, respectively), that were inhibited by PDGF immunoneutralization or by the selective PDGFR inhibitor imatinib. Serum-free J774A.1-MacCM or RAW264.7-MacCM completely prevented 3T3-L1 preadipocyte apoptosis normally induced by serum deprivation. Addition of PDGF alone to serum-free control medium was sufficient to prevent 3T3-L1 preadipocyte apoptosis. Inhibition of PDGFR activation by MacCM, either by addition of imatinib or by PDGF immunodepletion of MacCM, effectively disrupted the pro-survival effect. In summary, our data indicate that MacCM promotes preadipocyte survival in a PDGF-dependent manner.

KEYWORDS: apoptosis, macrophage, preadipocyte, PDGF

INTRODUCTION

Obesity, defined as an increase in adiposity, results from a chronic positive energy balance. Expansion of adipose tissue occurs through the formation of new adipocytes, via the differentiation of stromal precursor preadipocytes, and the enlargement of existing adipocytes (Gesta et al., 2007). Deficiency in the number of preadipocytes, or their capacity to differentiate, may lead to excessively hypertrophied and dysfunctional adipocytes that overproduce immune cell chemoattractant proteins (Despres and Lemieux, 2006; Heilbronn et al., 2004; Jiao et al., 2008). Concomitantly, the population of adipose tissue macrophages rises due to monocyte infiltration. This abnormal cellular remodeling of adipose tissue is associated with low-grade inflammation and insulin resistance (Weisberg et al., 2003).

Paracrine communication between macrophages, adipocytes, and preadipocytes is believed to contribute to obesity-associated adipose tissue dysfunction (Gustafson et al., 2007). We and others have reported that macrophages produce anti-adipogenic factors that restrain the differentiation of preadipocytes into adipocytes (Constant et al., 2006; Constant et al., 2008; Keophiphath et al., 2009; Lacasa et al., 2007; Stienstra et al., 2008; Yarmo et al., 2009). Macrophage-secreted factors have also been observed to have variable effects on preadipocyte proliferation (Lacasa et al., 2007; Maumus et al., 2008). Apoptosis, the other key preadipocyte fate pertinent to adipose tissue remodeling (Guo et al., 2007; Magun et al., 1998b; Prins and O'Rahilly, 1997), has not been evaluated with respect to potential macrophage paracrine interactions.

The precise identity of the macrophage products influencing preadipocyte responses is not known. Here, we demonstrate that macrophage-conditioned medium (MacCM) activates platelet-derived growth factor (PDGF) signaling in 3T3-L1 preadipocytes. Our studies indicate that serum-free MacCM prevents apoptosis of preadipocytes undergoing serum deprivation, and that this pro-survival effect depends on the presence of PDGF.

MATERIALS AND METHODS

Preparation of MacCM.

J774A.1 (from ATTC, Manasas, VA) and RAW264.7 (from Dr. X. Zha, Ottawa, Canada) macrophages were grown in DMEM supplemented with 10% fetal bovine serum (FBS) and antibiotics (100U/ml penicillin, 0.1mg/ml streptomycin). At confluence, the medium was replaced with fresh growth medium, or serum-free medium, and collected 24 h later. MacCM was centrifuged at 200 *g* for 5 minutes, and the supernatant was stored at -20^{0}C until use for preadipocyte studies. Control medium (serum-supplemented or serum-free, but not exposed to macrophages) was processed in parallel. Immunodepletion of PDGF was performed by incubating serum-free control medium and serum-free MacCM with 10μg/ml of neutralizing anti-PDGF antibody (R&D Systems, Minneapolis, MN) or non-specific goat IgG for 1 h at room temperature. Medium was subsequently incubated with protein A sepharose (~10μl/ml medium) for 30 min.

Samples were then centrifuged at 3000 *g* for 15 min and supernatants were applied to preadipocyte cultures.

Preadipocyte signal transduction studies.

Low passage 3T3-L1 preadipocytes (ATCC) were grown in DMEM supplemented with 10% calf serum (CS) and antibiotics. Confluent 3T3-L1 preadipocytes were either placed in serum-supplemented MacCM or control medium with or without 20ng/ml human recombinant PDGF (Calbiochem, Gibbstown, NJ or Millipore, Billerica, MA) for the time periods shown. Where indicated, preadipocytes were pretreated with 10μM imatinib mesylate (kindly provided by Novartis, Basel, Switzerland) for 90 min. To interfere with PDGF action, MacCM was incubated with 0-20μg/ml neutralizing anti-PDGF antibody (R&D Systems, Minneapolis, MN) for 1 h at room temperature prior to addition to preadipocyte cultures. Preadipocyte signaling was also assessed following exposure to serum-free MacCM immunodepleted of PDGF.

Immunoblot analysis of cell lysates and conditioned medium.

Following stimulation, cells were lysed in 1X Laemmli buffer (Laemmli, 1970) supplemented with 5% β-mercaptoethanol, 1mM sodium orthovanadate, 5mM EGTA (pH 8.0), 50mM sodium fluoride, and 5mM sodium pyrophosphate. Protein was measured using the Dc Protein Assay (Bio-Rad, Hercules, CA) with bovine serum albumin (BSA) as a standard. Equal amounts of solubilised protein (10-50μg), or equal

volumes of immunoprecipitated protein, were resolved by SDS-PAGE and transferred to a nitrocellulose membrane. Membranes were incubated for 1 h in 5% skim milk or 3% BSA to block non-specific binding sites, and then probed as indicated with the following primary antibodies directed against: Akt1 (C-20; goat polyclonal; 1:1000), PDGF receptor (PDGFR)-β (rabbit polyclonal; 1μg/ml; both from Santa Cruz Biotechnology, Santa Cruz, CA), phosphotyrosine (PY20, mouse monoclonal; 1:1000; BD Biosciences, Mississauga, ON, Canada), ERK1/2 (1.0μg/ml; Upstate Biotechnology, Charlottesville, VA), phospho-ERK1/2 (pERK1/2; Thr202/Tyr204; 1:1000), phospho-Akt (pAkt; Ser473; rabbit polyclonal; 1:1000; all from Cell Signaling Technology, Beverly, MA). This was followed by incubation with the appropriate horseradish peroxidase-conjugated secondary antibody. Signal detection was performed using Immobilon Western chemiluminescence HRP Substrate (Millipore). Relative intensity of the bands was quantified using AlphaEaseFC software (Alpha Innotech, San Leandro, CA) and expressed as integrated optical density (I.O.D.) units.

Serum-free medium, control or conditioned by J774A.1 macrophages, was concentrated with a 3kDa cut-off filter (Millipore). Media was centrifuged at 3000 *g* for 6 h. Retentate was collected by inverting the column and centrifuging at 2000 *g* for 10 min. The retentate was diluted in an equal volume of 2X Laemmli buffer and an aliquot was resolved by SDS-PAGE under non-reducing conditions, and immunoblotted with anti-PDGF antibody (R&D Systems, 2μg/ml).

Immunoprecipitation.

Cells were lysed in PBS (pH 7.4) containing 1% NP-40, 50mM sodium fluoride, 5mM sodium pyrophosphate, 0.1mg/ml phenylmethyl-sulfonylfluoride, 200mM sodium orthovanadate, 10μg/ml aprotinin, 10μg/ml leupeptin, 4μg/ml benzamidine, and 1mM β-glycerophosphate. Lysates (~0.5mg protein, assayed by Micro BCA protein assay, Pierce, Rockford, IL), were precleared with protein A-sepharose beads, and incubated with 1μg anti-PDGFRβ antibody complexed to protein A-sepharose beads. Immunoprecipitated proteins were washed and solubilized in 1X Laemmli containing 1 mM sodium orthovanadate. Immunoprecipitated proteins were subsequently analyzed by immunoblot analysis as described above.

Analysis of cell death.

Confluent 3T3-L1 preadipocytes were placed in control medium or MacCM containing 10% FBS or serum-free. Where indicated, the PDGFR-selective inhibitor, imatinib (10μM), or 0.1% DMSO (vehicle control) was added to these media. After 6 h, floating cells were removed, and adherent cells were trypsinized and stained with 0.2% trypan blue dye. Viable cells (trypan blue exclusion) were counted in duplicate using a Neubauer hemacytometer. Each treatment was performed in triplicate.

To visualize and quantify apoptotic changes in cell nuclei, confluent 3T3-L1 preadipocytes, grown on coverslips, were exposed to the same media for 3 h. Cells were then fixed in 10% formaldehyde for 1 h, followed by staining for 10 min with 1μg/ml

Hoechst 33342 in a humid chamber. Individual coverslips were mounted onto glass slides using Moviol. Cells were visualized and photographed (400x magnification) with a Zeiss Axioplan 2 microscope equipped with an Axiocam digital camera (Carl Zeiss, Toronto, Canada). Ten random fields were photographed for each of the three coverslips used per treatment. Counts of all stained nuclei and apoptotic nuclei were performed by 2 independent observers. Data are represented as % apoptosis, calculated by dividing the total number of apoptotic nuclei by the total number of nuclei, multiplied by 100.

Annexin V binding was assessed using the Vybrant Apoptosis Assay kit #2 (Molecular Probes, Eugene, Oregon). Confluent 3T3-L1 preadipocytes were exposed to the same media for 3 h. Adherent cells were trypsinized and combined with the floating cell population. Cells were centrifuged at 500 g for 5 min, washed, resuspended, and stained with annexin V and propidium iodide (PI) for 15 min, as per the manufacturer's protocol. Annexin V binding and propidium iodide staining was quantified with a Beckman Coulter Epics XL-MCL flow cytometer.

Statistical Analysis.

Comparison of means was performed by ANOVA ($P<0.05$ taken as significant), followed by the post-hoc Newman-Keuls test to assess differences between individual means using GraphPad InStat v3.05 (GraphPad Software Inc., San Diego, CA).

RESULTS

Macrophage-secreted products induce PDGFR signaling in 3T3-L1 preadipocytes.

To assess potential deregulated signaling in preadipocytes triggered by macrophage-derived factors, we conducted a time-course stimulation on 3T3-L1 preadipocytes exposed to J774A.1-MacCM. We observed a time-dependent increase in the tyrosine phosphorylation of a 180kDa protein in preadipocytes exposed acutely (0-60 min) to MacCM (indicated by arrow in Fig. 1A, $P<0.05$). To determine whether this might be due to phosphorylation of the PDGFR, we stimulated 3T3-L1 preadipocytes for 5 min with 20ng/ml PDGF, J774A.1-MacCM, or control medium. Solubilised proteins were immunoprecipitated with an anti-PDGFRβ antibody, followed by antiphosphotyrosine immunoblot analysis. A 4.1-fold increase in PDGFR phosphorylation occurred upon treatment with MacCM (Fig. 1B, $P<0.05$, MacCM vs control).

We next investigated whether MacCM was capable of activating signaling molecules downstream of the PDGFR. A 15 min stimulation of 3T3-L1 preadipocytes was performed with either control medium, medium supplemented with PDGF, or MacCM, in the presence or absence of the PDGFR-selective inhibitor, imatinib (Buchdunger et al., 2002). MacCM stimulated the tyrosine phosphorylation of the PDGFR (Fig. 2A, $P<0.001$), and phosphorylation of Akt and ERK1/2 (Fig. 2A, 5.3 fold increase in pAkt $P<0.05$, 2.4 fold increase in pERK1/2 $P<0.05$, MacCM vs. control). PDGF treatment produced similar results (Fig. 2A). The phosphorylation of Akt and of

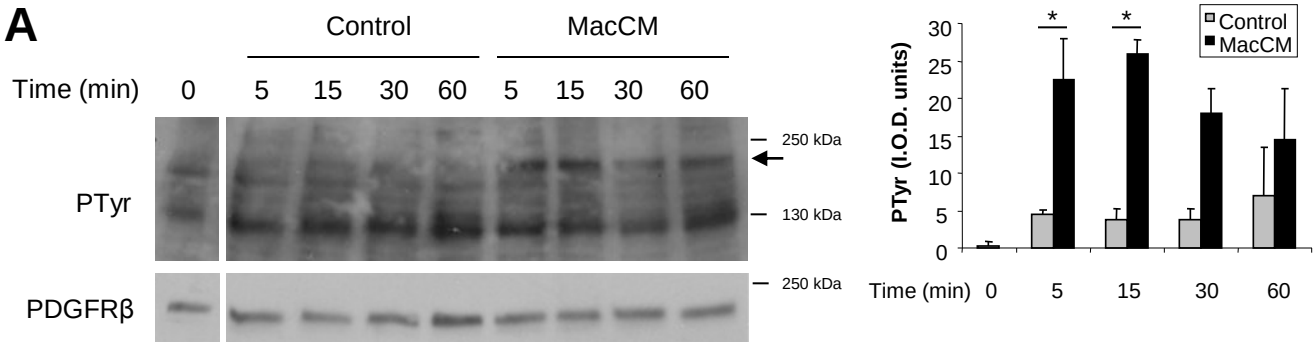
A
Control
MacCM
Time (min)
0
5
15
30
60
5
15
30
60
PTyr
PDGFRβ
250 kDa
130 kDa
250 kDa
PTyr (I.O.D. units)
Control
MacCM
*
*
Time (min) 0 5 15 30 60

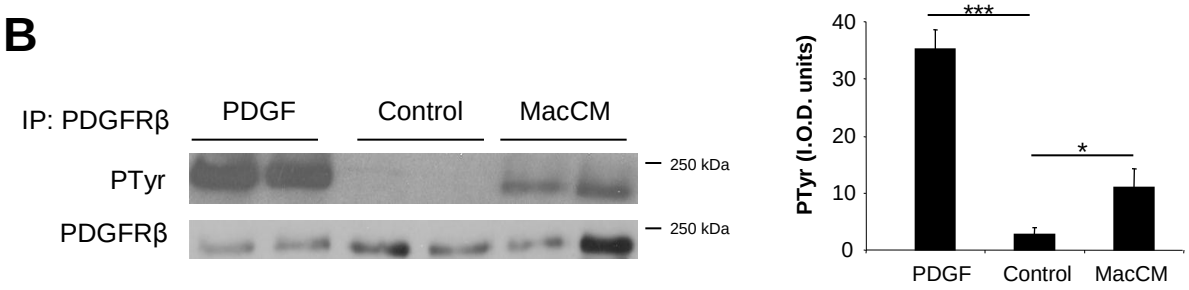
B
IP: PDGFRβ
PDGF
Control
MacCM
PTyr
PDGFRβ
250 kDa
250 kDa
PTyr (I.O.D. units)
***
*
PDGF
Control
MacCM

Figure 1. Macrophage-conditioned medium (MacCM) stimulates PDGFR tyrosine phosphorylation. A. Confluent 3T3-L1 preadipocytes were placed in control medium or J774A.1-MacCM, each containing serum, for the indicated times. Cell lysates were separated by SDS-PAGE and immunoblotted with the indicated antibodies. Representative immunoblots are shown. Densitometric data from three independent experiments are expressed as mean ± SE. **P*<0.05. B. Confluent 3T3-L1 preadipocytes were placed in control medium (with or without 20ng/ml PDGF) or J774A.1-MacCM, each containing serum, for 5 min. Lysates were immunoprecipitated with anti-PDGFRβ antibody. Immunoprecipitated proteins were separated by SDS-PAGE followed by immunoblotting with the indicated antibodies. Representative immunoblots of duplicate samples are shown. Densitometric data from three independent experiments are expressed as mean ± SE. **P*<0.05, ****P*<0.001.

ERK1/2 by MacCM was inhibited by pretreatment with imatinib, indicating that this was a PDGF-dependent response (Fig. 2A). Under control conditions, Akt phosphorylation was not detected, and the basal level of ERK1/2 phosphorylation appeared to be independent of PDGFR activation, as it was not inhibited by imatinib (Fig. 2A).

To confirm, by a second strategy, that acute MacCM-stimulated phosphorylation of Akt and ERK1/2 was mediated through PDGFR activation, we incubated MacCM with increasing concentrations of PDGF neutralizing antibody prior to exposure to 3T3-L1 preadipocytes. PDGF immunoneutralization of MacCM significantly decreased PDGFR phosphorylation (Fig. 2B), and this was accompanied by a significant inhibition of Akt and ERK1/2 phosphorylation (Fig. 2B).

MacCM-induced PDGFR signaling protects 3T3-L1 preadipocytes from apoptosis.

Since Akt and ERK1/2 signaling pathways have been implicated in cell survival, we therefore investigated whether MacCM-induced signaling could protect preadipocytes from cell death. MacCM was generated from J774A.1 or RAW 264.7 macrophages under serum-free conditions. Serum-free MacCM was then compared to serum-supplemented MacCM and serum-supplemented control medium with respect to their ability to preserve cell viability upon serum deprivation (growth factor withdrawal) of 3T3-L1 preadipocytes. The apoptotic response of 3T3-L1 preadipocytes to serum withdrawal has been reported previously (Magun et al., 1998a; Magun et al., 1998b; Niesler et al., 2000). Following 6 h of serum withdrawal, we observed a 50% reduction in the total number of viable cells, assessed by the enumeration of adherent cells excluding trypan blue dye

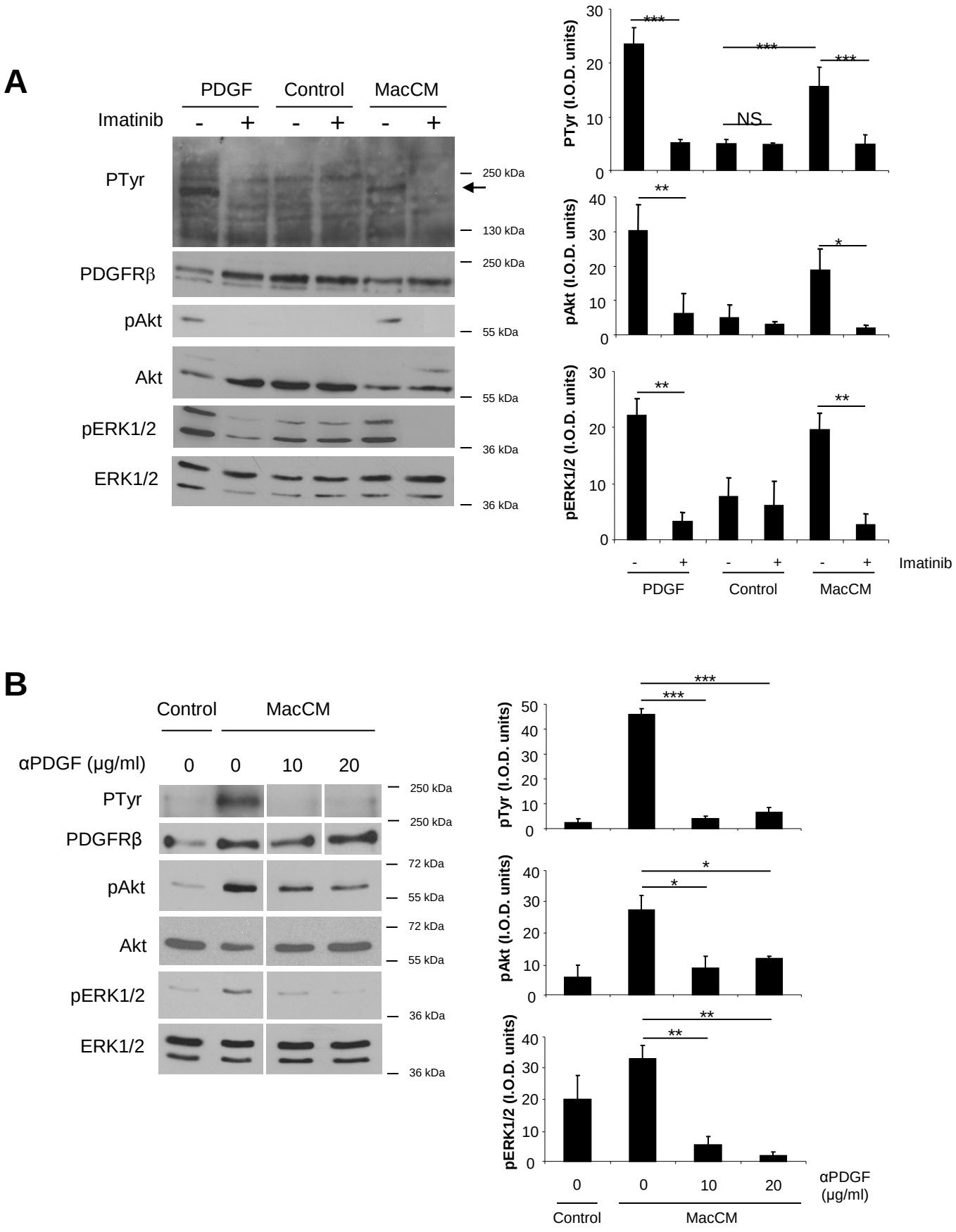
A
PDGF
Control
MacCM
Imatinib
- + - + - +
PTyr
PDGFRβ
pAkt
Akt
pERK1/2
ERK1/2
250 kDa
130 kDa
250 kDa
55 kDa
55 kDa
36 kDa
36 kDa
PTyr (I.O.D. units)
pAkt (I.O.D. units)
pERK1/2 (I.O.D. units)
***
***
***
NS
**
*
**
**
Imatinib
B
Control
MacCM
αPDGF (μg/ml)
0 0 10 20
PTyr
PDGFRβ
pAkt
Akt
pERK1/2
ERK1/2
250 kDa
250 kDa
72 kDa
55 kDa
72 kDa
55 kDa
36 kDa
36 kDa
pTyr (I.O.D. units)
pAkt (I.O.D. units)
pERK1/2 (I.O.D. units)
***
***
*
*
**
**
αPDGF (μg/ml)

Figure 2. Phosphorylation of Akt and ERK1/2 by MacCM requires PDGFR activation. A. Confluent 3T3-L1 preadipocytes were placed in serum-containing control medium (with or without 20ng/ml PDGF) or J774A.1-MacCM, for 15 min, in the presence of 10μM imatinib or vehicle (0.1% DMSO). Cell lysates were separated by SDS-PAGE and immunoblotted with the indicated antibodies. Representative immunoblots are shown. Densitometric data from five independent experiments are expressed as mean ± SE. $^{**}P<0.01$. B. Confluent 3T3-L1 preadipocytes were placed in control medium or J774A.1-MacCM that had been incubated or not with PDGF neutralizing antibody, each containing 10% FBS, for 5 min. Cell lysates were separated by SDS-PAGE and immunoblotted with the indicated antibodies. Representative immunoblots are shown. Densitometric data from three independent experiments are expressed as mean ± SE. $^{*}P<0.05$, $^{**}P<0.01$, $^{***}P<0.001$.

(Fig. 3A and B, control medium with serum vs. without, $P<0.001$). In contrast, there was no decrease in the number of viable cells following the same time period of serum withdrawal when in the presence of serum-free MacCM from either macrophage cell model. Hoechst staining of nuclei following 3 h of serum deprivation confirmed the pro-survival effect (Fig. 3C). To further demonstrate the anti-apoptotic effect of MacCM, 3T3-L1 preadipocytes were stained with both annexin V and PI. A significant increase in annexin V staining was observed following serum withdrawal (Fig. 3D, annexin V+/PI- for serum-containing vs serum-free control medium, $P<0.001$). In contrast, there was no increase in annexin V staining for cells placed in serum-free MacCM. PI staining, an indicator of necrosis, was minimal and not significantly changed with any of the treatments, suggesting 3T3-L1 preadipocytes were strictly undergoing apoptosis when serum-deprived.

To determine whether J774A.1-MacCM contained detectable amounts of PDGF, serum-free control medium or MacCM was immunoblotted with anti-PDGF antibody; human recombinant PDGF served as a standard. Bands (30-36kDa) were detected in the PDGF and MacCM lanes (Fig. 4A). The slight mobility difference observed here has been reported previously by others comparing PDGF in conditioned medium to recombinant PDGF (Fenstermaker et al., 1993).

PDGF is known to promote cell survival (Tallquist and Kazlauskas, 2004). To assess whether PDGF alone is sufficient to protect 3T3-L1 preadipocytes from apoptosis induced by growth factor withdrawal, preadipocytes were placed in serum-free medium supplemented with increasing concentrations of recombinant PDGF. A significant and dose-dependent protection from serum withdrawal-induced cell loss was

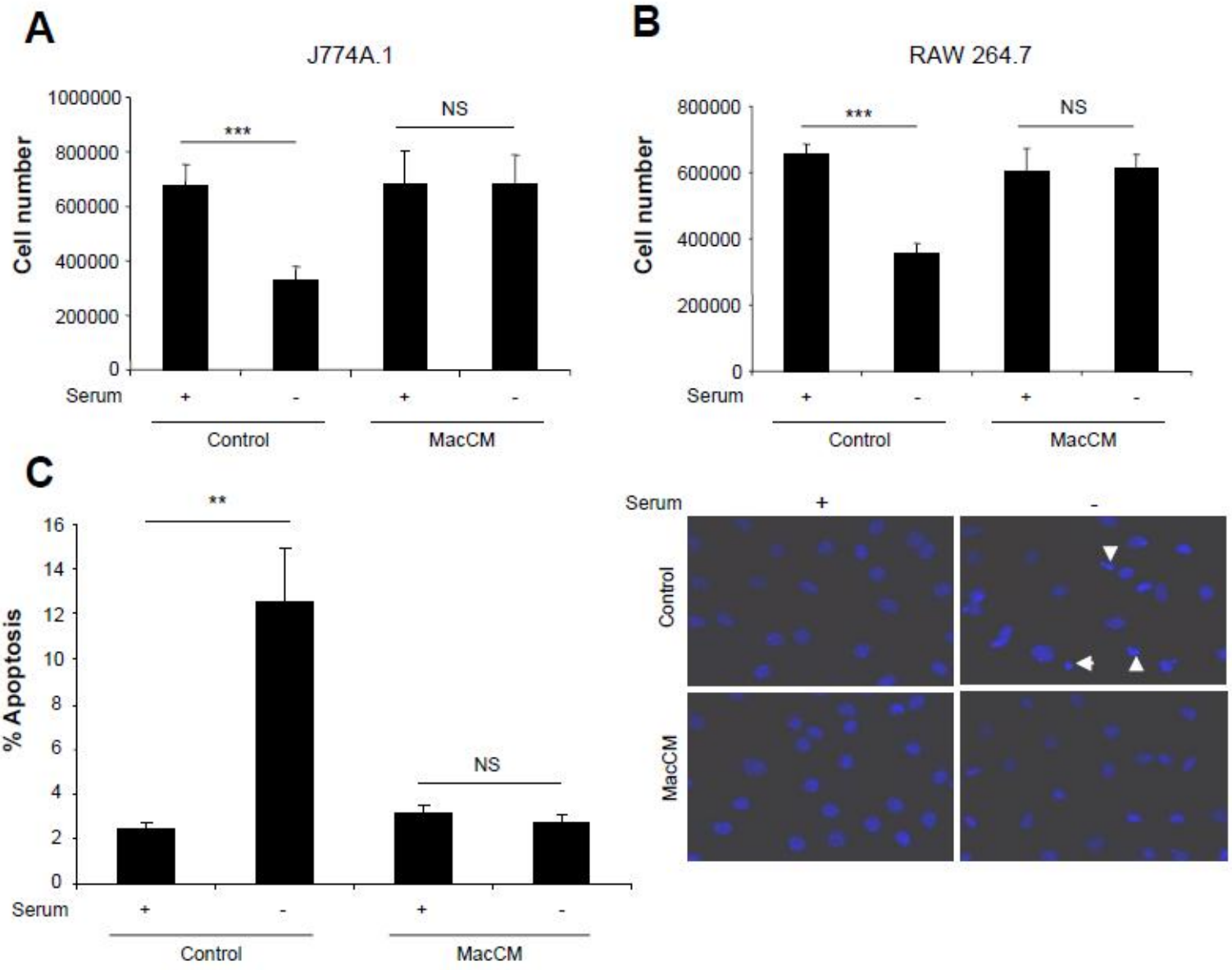

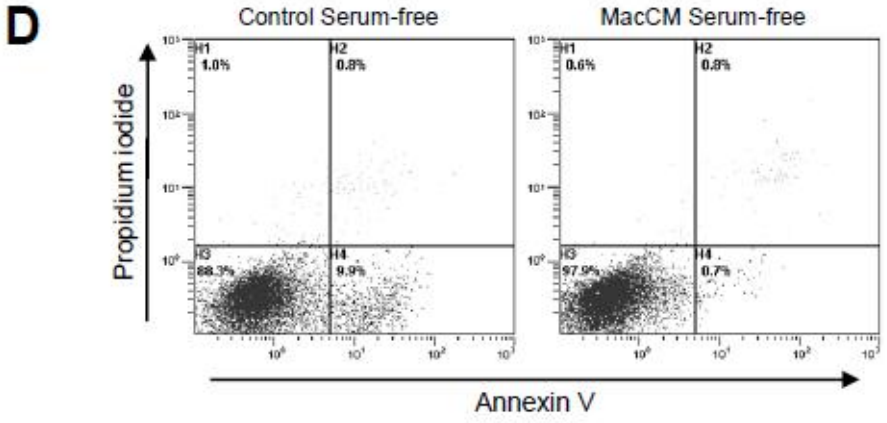

	Control		MacCM	
Serum	+	-	+	-
Population				
Annexin V+/PI-	1.23 ± 0.22	7.06 ± 1.15[a]	1.23 ± 0.34	0.88 ± 0.23
Annexin V-/PI+	0.57 ± 0.20	1.65 ± 0.77	1.10 ± 0.45	0.95 ± 0.16
Annexin V+/PI+	0.80 ± 0.11	0.60 ± 0.19	0.70 ± 0.20	1.20 ± 0.28
Annexin V-/PI-	97.37 ± 0.42	90.63 ± 1.41[a]	96.95 ± 0.47	96.97 ± 0.45

Figure 3. MacCM protects 3T3-L1 preadipocytes from serum withdrawal-induced cell death. A,B. Confluent 3T3-L1 preadipocytes were placed in the indicated media for 6 h. Cells were trypsinized, stained with 0.2% Trypan blue, and viable cells were counted. Data are expressed as the mean number of viable cells ± SE (n=3, each performed in triplicate, ***P<0.001). C. Confluent 3T3-L1 preadipocytes were placed in the indicated media for 3 h. Cells were then fixed in 10% formalin and stained with 1μg/ml Hoechst dye. The number of apoptotic preadipocytes (arrows) is expressed as the mean % of total preadipocytes ± SE (n=3, each performed in triplicate, **P<0.01). Representative images are shown (400x magnification). D. Confluent 3T3-L1 preadipocytes were placed in the indicated media for 3 h. Cells were then stained with annexin V and propidium iodide. Representative flow cytometry plots are shown for control and MacCM conditions, both serum-free. Data for all conditions are shown in the accompanying table as mean ± SE (n=3, each performed in duplicate, [a]P<0.001).

observed with concentrations of PDGF as low as 1ng/ml (Fig. 4B, $P<0.05$, PDGF vs. serum free).

To determine whether MacCM-mediated preadipocyte PDGFR activation was required for the pro-survival effect, 3T3-L1 preadipocytes were placed in serum-free MacCM in the presence of imatinib. As before, serum withdrawal in the absence of macrophage-secreted factors resulted in a 50% reduction in the number of viable cells (Fig. 4C, $P<0.01$, serum-containing vs serum-free control medium). The protection by macrophage-derived factors was lost in the presence of imatinib (Fig. 4C, $P<0.01$, serum-free MacCM vs serum-free MacCM + imatinib). Imatinib, added to serum-supplemented control medium, did not result in any 3T3-L1 preadipocyte death, and it did not aggravate cell loss when added to serum-free control medium (Fig 4D). Hoechst staining of nuclei further indicated that imatinib blocked MacCM-dependent cell survival (Fig. 4E, $P<0.001$).

We next sought to confirm the importance of PDGF signaling in preadipocyte survival by using PDGF-immunodepleted MacCM. Following immunodepletion (Fig. 5A), MacCM was no longer capable of stimulating PDGFR tyrosine phosphorylation (Fig. 5B, $P<0.01$). Incubation of serum-free MacCM with non-specific IgG did not alter the ability of MacCM to completely prevent 3T3-L1 preadipocyte cell loss (Fig. 5C). In contrast, serum deprivation of preadipocytes in the presence of PDGF-immunodepleted MacCM led to 30% cell death (Fig. 5C, MacCM serum-free IgG vs MacCM serum-free αPDGF, $P<0.001$). Additionally, there were significantly more apoptotic nuclei observed when serum deprivation was performed in PDGF-depleted MacCM compared to MacCM (Fig. 5D, $P<0.001$).

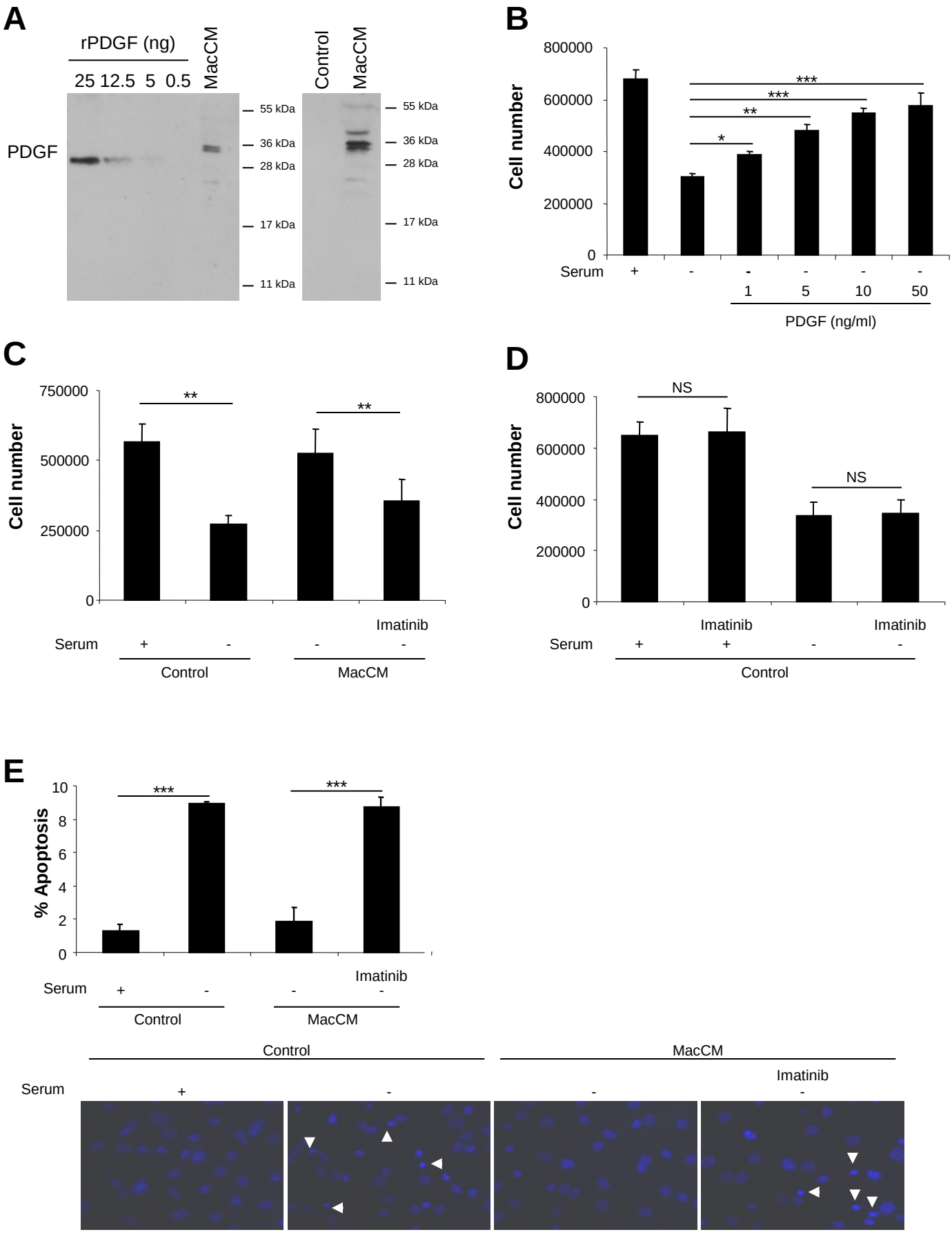
A
rPDGF (ng)
25 12.5 5 0.5
MacCM
Control
MacCM
PDGF
55 kDa
36 kDa
28 kDa
17 kDa
11 kDa
B
Cell number
800000
600000
400000
200000
0
***
***
**
*
Serum + - - - - -
1 5 10 50
PDGF (ng/ml)
C
Cell number
750000
500000
250000
0
**
**
Imatinib
Serum + - - -
Control
MacCM
D
Cell number
800000
600000
400000
200000
0
NS
NS
Imatinib
Imatinib
Serum + + - -
Control
E
% Apoptosis
10
8
6
4
2
0
***
***
Imatinib
Serum + - - -
Control
MacCM
Control
MacCM
Serum
Imatinib
+ - - -

Figure 4. Imatinib inhibits MacCM protection of 3T3-L1 preadipocytes from serum withdrawal-induced cell death. A. MacCM (serum-free) was concentrated; proteins were separated by SDS-PAGE and then immunoblotted with anti-PDGF antibody. The immunoblot on the left is representative of three independent experiments. The immunoblot on the right confirms the absence of PDGF in serum-free control medium. B, C and D. Confluent 3T3-L1 preadipocytes were placed in the indicated media for 6 h Cells were then trypsinized, stained with 0.2% Trypan blue, and viable cells were counted. Data are expressed as the mean number of viable cells ± SE (n=3, performed in duplicate (B) or triplicate (C and D), *P<0.05, **P<0.01, ***P<0.001). E. Confluent 3T3-L1 preadipocytes were placed in the indicated media for 3 h. Cells were then fixed in 10% formalin and stained with 1μg/ml Hoechst dye. The number of apoptotic preadipocytes (arrows) is expressed as the mean % of total preadipocytes, ± SE (n=3, performed in triplicate, ***P<0.001). Representative images are shown (400x magnification).

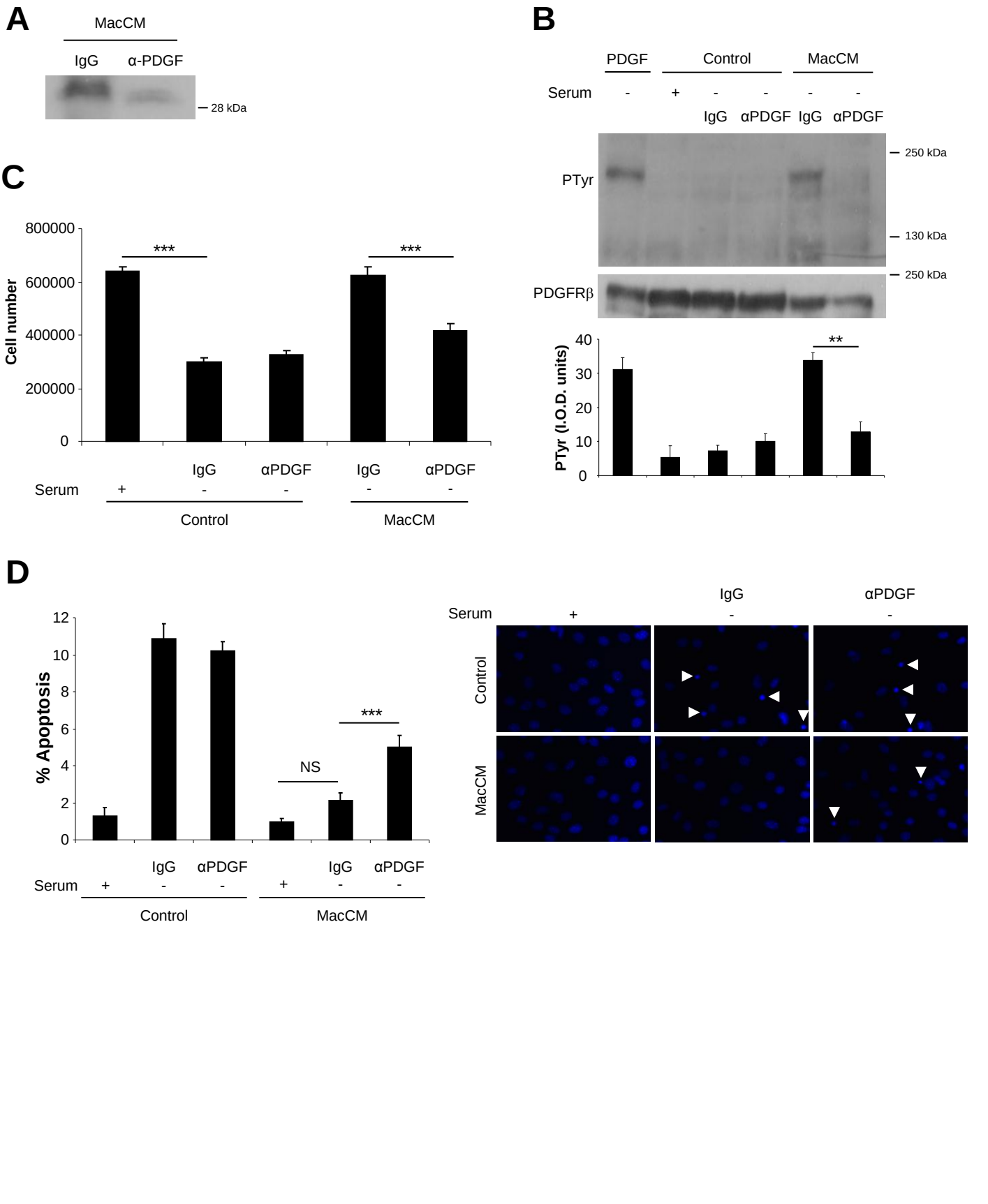
A
MacCM
IgG
α-PDGF
28 kDa
B
PDGF
Control
MacCM
Serum
IgG
αPDGF
PTyr
PDGFRβ
250 kDa
130 kDa
PTyr (I.O.D. units)
C
Cell number
Serum
Control
MacCM
D
% Apoptosis
NS
Control
MacCM

Figure 5. PDGF-immunodepleted MacCM fails to protect 3T3-L1 preadipocytes from serum withdrawal-induced cell death. A. PDGF-immunodepleted MacCM or MacCM (both serum-free) were concentrated; proteins were separated by SDS-PAGE and then immunoblotted with anti-PDGF antibody. B. 3T3-L1 preadipocytes were placed in the indicated media for 5 min, lysed, and then subjected to antiphosphotyrosine immunoblot analysis. Representative immunoblots are shown. Densitometric data from three independent experiments are expressed as mean ± SE, $^{**}P<0.01$. C. Confluent 3T3-L1 preadipocytes were placed in the indicated media for 6 h. Following treatment, cells were trypsinized, stained with 0.2% Trypan blue, and viable cells were counted. Data are expressed as the mean number of viable cells ± SE (n=3, ***P<0.001). D. Confluent 3T3-L1 preadipocytes were placed in the indicated media for 3 h. Following treatment, cells were fixed in 10% formalin and stained with 1μg/ml Hoechst dye. Representative images are shown (400x magnification). The number of apoptotic preadipocytes (arrows) is expressed as the mean % of total preadipocytes, ± SE (n=3, performed in triplicate, $^{***}P<0.001$).

DISCUSSION

Our studies demonstrate that MacCM contains PDGF and activates PDGFR signaling pathways in 3T3-L1 preadipocytes. We have shown that MacCM prevents 3T3-L1 preadipocyte apoptosis induced by growth factor withdrawal, and PDGF is sufficient and necessary for this effect. This novel interaction between macrophages and preadipocytes hints at the growing complexity of adipose tissue remodeling.

The recognition that obesity promotes an increase in the number of adipose tissue macrophages has initiated a new way of understanding adipose tissue inflammation and insulin resistance (Schenk et al., 2008; Weisberg et al., 2003; Xu et al., 2003). Several potential roles for this population of macrophages have been proposed, such as direct release of pro-inflammatory cytokines into the circulation, or inhibition of mature adipocyte insulin-regulated glucose and lipid metabolism (Lumeng et al., 2007c; Permana et al., 2006; Suganami et al., 2005).

Regulation of preadipocyte fate with respect to adipose tissue remodeling and expansion is thought to be important to maintain adipose tissue function and result in the metabolically healthy obese phenotype (Heilbronn et al., 2004). Inhibition of adipogenic capacity and the resulting decreased formation of new adipocytes (hyperplasia) would predispose to exaggerated adipocyte hypertrophy and dysfunction (Danforth, 2000; Heilbronn et al., 2004). Paracrine communication between macrophages and stromal progenitor preadipocytes has been proposed by us and others (Constant et al., 2006; Lacasa et al., 2007; Maumus et al., 2008). The nature of such interactions may alter the functionality of adipose tissue. We have reported that MacCM from mouse J774 and human THP-1 macrophage cell lines inhibit the differentiation of mouse 3T3-L1 and

human primary preadipocytes into adipocytes (Constant et al., 2006; Constant et al., 2008; Yarmo et al., 2009). Conditioned medium from human monocyte-derived macrophages and from human adipose tissue macrophages is similarly anti-adipogenic (Keophiphath et al., 2009; Lacasa et al., 2007). A recent report has also demonstrated the same phenomenon in a mouse model (Stienstra et al., 2008).

The effects of MacCM on preadipocyte proliferation have also been studied, with both pro- and anti-proliferative effects described (Keophiphath et al., 2009; Lacasa et al., 2007; Maumus et al., 2008). The reasons for the discrepancy are not clear at present, but progress in this area is needed, as proliferation capacity would be expected to exert an important influence of the size of the preadipocyte pool in the stromal fraction.

Another influential process on preadipocyte number is apoptotic susceptibility, but there are no reports in the literature examining macrophage-secreted factors on preadipocyte survival. It has been shown, by us and others, that 3T3-L1 preadipocytes are susceptible to apoptosis induced by serum withdrawal (Magun et al., 1998a; Magun et al., 1998b; Niesler et al., 2000). Therefore, we addressed this question using the established and widely used mouse J774A.1 macrophage, RAW264.7 macrophage, and 3T3-L1 preadipocyte cell line models. Our data show a clear, consistent, and potent anti-apoptotic effect of MacCM on serum-deprived preadipocytes. Although macrophages are known to produce many pro-inflammatory factors that might have been predicted to favour cell death, the survival effect we saw indicated to us that a macrophage-secreted growth factor might be implicated.

Our acute signaling preadipocyte studies with MacCM revealed that the PDGFR was activated, including stimulation of the classical downstream kinases, Akt and

ERK1/2. We also demonstrated the presence of PDGF in MacCM, and that immuno-based neutralization of PDGF in the MacCM rendered it incapable of PDGF receptor activation.

PDGF activation of Akt, NFκB and ERK1/2 has been shown to mediate its pro-survival activity in other cell types (Arase et al., 2000; Romashkova and Makarov, 1999; Vantler et al., 2005). Signaling through these pathways has been shown to regulate Bcl protein expression and caspase activity (Tallquist and Kazlauskas, 2004). The effect of MacCM on these intracellular targets in serum-deprived preadipocytes remains to be identified.

PDGF gene expression has been shown to be elevated in alternatively activated macrophages (Song et al., 2000), while treatment of macrophages with the Th1 cytokine, IFNγ, suppresses PDGF expression (Kosaka et al., 1992). Hypoxia, which is a feature of the obese adipose tissue (Trayhurn et al., 2008), has also been shown to increase PDGF expression in macrophages (Pang et al., 2008).

Our study is limited to the use of macrophage and preadipocyte cell lines that are established *in vitro* models for inflammation and metabolic research. It should be noted that macrophages are highly influenced by the local environment in vivo, with different classes of cytokines resulting in pro-inflammatory (classic) versus anti-inflammatory (alternate) states of macrophage activation (Gordon, 2003). Indeed, some investigators describe adipose tissue macrophages in intermediate states between these two extremes (Bourlier et al., 2008; Lumeng et al., 2008; Lumeng et al., 2007b). Furthermore, human preadipocytes have been reported to be less susceptible to apoptosis induced by serum deprivation *in vitro* (Papineau et al., 2003). It will therefore be important to conduct

similar experiments with human primary cell cultures to explore the impact of human macrophages on human preadipocyte apoptosis. As discussed above, it should be noted that adipogenesis studies using either cell lines or primary cell cultures have been very consistent.

To date, identifying the role of specific secreted macrophage products for any preadipocyte response has been elusive. Therefore, it is significant that we have discovered that PDGF is the critical factor for this newly described anti-apoptotic effect of MacCM. Our data show that PDGF is clearly both sufficient and required for the anti-apoptotic effect. We have demonstrated that blocking PDGF receptor activation by imatinib interfered with the ability of MacCM to prevent preadipocyte apoptosis. Imatinib, though selective for the PDGF receptor kinase, is also known to inhibit c-Abl and c-Kit (Buchdunger et al., 2002) Neither of these two kinases have been implicated in preadipocyte survival responses. In any case, to more precisely implicate PDGFR, we immunodepleted the MacCM of PDGF by immunoprecipitation with PDGF antibody, an approach used by others (Ray et al., 2005). PDGF-immunodepleted MacCM was unable to stimulate tyrosine phosphorylation acutely, and could no longer sustain preadipocytes subjected to serum withdrawal over the 6 h time period.

In conclusion, our findings suggest a novel role for macrophages in protecting preadipocytes from death. Furthermore, we have identified PDGF as a factor that is sufficient and necessary for this effect. These results add to a growing body of knowledge concerning macrophage-preadipocyte interactions and adipose tissue remodeling.

GRANTS

This work was supported by grant MOP-43850 from the Canadian Institutes for Health Research (to A. Sorisky) and a Heart and Stroke Foundation of Ontario Master's Studentship (to A.S.D. Molgat).

ACKNOWLEDGMENTS - none

DISCLOSURES - none

3.0 MANUSCRIPT #2

Macrophage-induced preadipocyte survival depends on signaling through Akt, ERK1/2, and reactive oxygen species.

STATEMENT OF AUTHOR CONTRIBUTIONS

André S.D. Molgat is the first author on this publication. He performed all experiments, participated in the design of the experiments, performed the data analysis, and wrote the manuscript. **Dr. AnneMarie Gagnon** is the research associate in Dr. Alexander Sorisky`s laboratory. She participated in the design of the experiments, performed data analysis, and assisted in the editing and revising of the manuscript. **Dr. Alexander Sorisky** is the PhD supervisor of André Molgat. He contributed to the design of the experiments, analysis of results, and revising the manuscript.

SUMMARY

The following manuscript entitled "Macrophage-induced preadipocyte survival depends on signaling through Akt, ERK1/2, and reactive oxygen species" was published in Exp Cell Res [(2011) 317, 521-530]. The objective of manuscript #2 was to identify the anti-apoptotic signaling pathways mediating MacCM-dependent preadipocyte survival. This study was conducted using the 3T3-L1 preadipocyte model, and the J774A.1 and BMD-macrophage cell models. MacCM was prepared and applied to

confluent 3T3-L1 preadipocyte cultures. 3T3-L1 preadipocytes were induced to undergo apoptosis by serum withdrawal. Preadipocyte apoptosis was assessed by enumeration of viable cells, and quantification of Annexin V/PI positive cells by flow cytometry. Reactive oxygen species (ROS) were quantified using a dihydrorhodamine 123 (DHR123) fluorescent probe. This study revealed that MacCM protects preadipocytes from apoptosis through the activation of Akt, ERK1/2, and the production of ROS.

Macrophage-Induced Preadipocyte Survival Depends on Signaling through Akt, ERK1/2, and Reactive Oxygen Species

André S.D. Molgat, AnneMarie Gagnon, Alexander Sorisky*

Chronic Disease Program, Ottawa Hospital Research Institute, Departments of Medicine and of Biochemistry, Microbiology & Immunology, University of Ottawa, Ottawa, Ontario, Canada.

*Corresponding author: Alexander Sorisky, Ottawa Hospital Research Institute, General campus, 501 Smyth Road, Ottawa, Ontario, Canada, K1H 8L6, Phone: 613-737-8899 #73320; Fax: 613-737-8803; E-mail asorisky@ohri.ca

Abstract

Obesity is associated with adipose tissue remodeling, characterized by macrophage accumulation, adipocyte hypertrophy, and apoptosis. We previously reported that macrophage-conditioned medium (MacCM) protects preadipocytes from apoptosis, due to serum withdrawal, in a platelet-derived growth factor (PDGF)-dependent manner. We have now investigated the role of intracellular signaling pathways, activated in response to MacCM versus PDGF, in promoting preadipocyte survival. Exposure of 3T3-L1 preadipocytes to J774A.1-MacCM or PDGF strongly stimulated Akt and ERK1/2 phosphorylation from initially undetectable levels. Inhibition of the upstream regulators of Akt or ERK1/2, i.e. phosphoinositide 3-kinase (PI3K; using wortmannin or LY294002) or MEK1/2 (using UO126 or PD98509), abrogated the respective phosphorylation responses, and significantly impaired pro-survival activity. J774A.1-MacCM increased reactive oxygen species (ROS) levels by 3.4-fold, and diphenyleneiodonium (DPI) or N-acetyl cysteine (NAC) significantly inhibited pro-survival signaling and preadipocyte survival in response to J774A.1-MacCM. Serum withdrawal itself also increased ROS levels (2.1-fold), and the associated cell death was attenuated by DPI or NAC. In summary, J774A.1-MacCM-dependent 3T3-L1 preadipocyte survival requires the Akt and ERK1/2 signaling pathways. Furthermore, ROS generation by J774A.1-MacCM is required for Akt and ERK1/2 signaling to promote 3T3-L1 preadipocyte survival. These data suggest potential mechanisms by which macrophages may alter preadipocyte fate.

Key words: preadipocyte; macrophage; apoptosis; PDGF; reactive oxygen species.

Introduction

Obesity is a major risk factor for insulin resistance, type 2 diabetes, and cardiovascular disease. Chronic positive caloric balance leads to increased adipose tissue accumulation through increases in adipocyte size (hypertrophy) and number (hyperplasia). Differentiation of preadipocytes to form new adipocytes (adipogenesis) is believed to be critical to maintain healthy adipose tissue function (Heilbronn et al., 2004). Insulin sensitivity is preserved in animal models of obesity characterized by adipose tissue hyperplasia (Kim et al., 2007).

Recent studies have demonstrated there is an annual 10% turnover of adipocytes, with cell number staying constant in steady-state due to a balance between adipogenesis and apoptosis (Spalding et al., 2008). However, a relative deficit in preadipocyte number or their capacity to differentiate into adipocytes is associated with the development of dysfunctional hypertrophied adipocytes, leading to low-grade inflammation and insulin resistance in obese humans (Arner and Spalding, 2010; Heilbronn et al., 2004; Kim et al., 2007; Spalding et al., 2008). Adipose tissue macrophages, more numerous in this setting, may be in a pro-inflammatory state (M1) or in an alternatively activated state (M2) associated with tissue remodeling and resolution of inflammation (Bourlier et al., 2008; Shaul et al., 2010; Weisberg et al., 2003; Xu et al., 2003; Zeyda et al., 2007). Apoptosis has also been noted in adipose tissue of obese mice and humans, but the precise role played by macrophages in this process remains unclear (Alkhouri et al., 2010; Cinti et al., 2005). Preadipocyte susceptibility to cell death is routinely assessed in primary culture (Prins et al., 1997; Tchoukalova et al., 2007), although histological evidence of apoptosis

is currently lacking. Overall, adipose tissue macrophages may have a complex paracrine influence on preadipocytes and adipose tissue remodeling.

We have previously demonstrated that medium conditioned by macrophages (MacCM) inhibits the ability of preadipocytes to differentiate into adipocytes, and this effect was subsequently observed by other groups using a wide variety of preadipocyte and macrophage experimental models (Constant et al., 2006; Constant et al., 2008; Keophiphath et al., 2009; Lacasa et al., 2007; Lu et al., 2010; Stienstra et al., 2008; Yarmo et al., 2009). More recently, we discovered that J774A.1 and RAW264.7 MacCM inhibit 3T3-L1 preadipocyte apoptosis induced by serum deprivation, and identified platelet-derived growth factor (PDGF) as the principal anti-apoptotic macrophage-secreted factor (Molgat et al., 2009). The precise survival signals activated in preadipocytes by MacCM in this context remain to be delineated. Since PDGF-mediated survival in other cell systems requires Akt, ERK1/2, or reactive oxygen species (ROS) generation (Arase et al., 2000; Lei and Kazlauskas, 2009; Romashkova and Makarov, 1999), we have evaluated these signaling pathways in serum-deprived preadipocytes to determine how MacCM induces preadipocyte survival.

Materials and methods

Preparation of MacCM.

J774A.1 mouse macrophages (from ATCC, Manassas, VA) were grown in DMEM supplemented with 10% FBS and antibiotics (100U/ml penicillin, 0.1mg/ml

streptomycin). At confluence, cells were rinsed and placed in serum-free medium that was collected 24 h later. J774A.1-MacCM was centrifuged at 200 x g for 5 min, and the supernatant was stored at -20 ^{o}C until use for preadipocyte studies. Control medium (not exposed to macrophages) was processed in parallel. PDGF immunodepletion of J774A.1-MacCM was performed as previously described (Molgat et al., 2009). MacCM from murine bone marrow-derived macrophages (BMD-MacCM) was a kind gift from Dr. Y. Marcel (University of Ottawa Heart Institute, Ottawa, Canada). Bone marrow hematopoietic cells were differentiated as previously described (Ouimet et al., 2008), and BMD-MacCM was prepared as described above.

Preadipocyte studies on signal transduction and cell death.

Low-passage 3T3-L1 mouse preadipocytes (ATCC) were grown in DMEM supplemented with 10% calf serum (CS) and antibiotics (growth medium). Confluent 3T3-L1 preadipocytes were placed in J774A.1-MacCM or DMEM supplemented with 20 ng/ml human recombinant PDGF-BB (Millipore, Billerica, MA), for the indicated time periods. Cells were then processed for immunoblot analysis. For cell enumeration studies, confluent 3T3-L1 preadipocytes were placed in control medium or MacCM, each either supplemented with 10% FBS or maintained serum-free. Where indicated, confluent 3T3-L1 preadipocytes were placed in serum-free medium supplemented, or not, with 20 ng/ml PDGF-BB. After 6 h, floating cells were removed, and adherent cells were trypsinized and stained with 0.2% trypan blue dye. Viable cells (trypan blue exclusion) were counted in duplicate using a Neubauer hemacytometer. Each treatment was performed in

triplicate. For annexin V studies, confluent 3T3-L1 preadipocytes were placed in the above media for 3 h. Adherent cells were trypsinized, combined with floating cells, and were centrifuged at 500 x g for 5 min, washed, resuspended, and exposed to annexin V and propidium iodide (PI) for 15 min (Vybrant Apoptosis Assay Kit No. 2; Molecular Probes, Eugene, OR). Annexin V binding and PI staining were quantified with a Beckman Coulter Epics XL-MCL flow cytometer, or Beckman Coulter Cell Lab Quanta SC MPL flow cytometer, for wortmannin and diphenyleneiodonium (DPI) studies, respectively (Beckman Coulter, Brea, CA).

Where indicated, preadipocytes were pretreated with the following inhibitors added to growth medium: 100 nM wortmannin (Kamita Biomedical Co., Thousand Oaks, CA), 10 mM N-acetyl cysteine (NAC), 10 μM LY294002, 10 μM DPI (all from Sigma Aldrich), 10 μM UO126, or 50 μM PD98059 (all from Calbiochem). Vehicle controls were 0.1% DMSO for all inhibitors except for NAC which was 20 mM HEPES.

Immunoblot analysis

Following stimulation, cells were lysed in 1X Laemmli buffer (Laemmli, 1970) supplemented with 5% β-mercaptoethanol, 1 mM sodium orthovanadate, 5 mM EGTA (pH 8.0), 50 mM sodium fluoride, and 5 mM sodium pyrophosphate. Protein was measured using the Dc Protein Assay (Bio-Rad, Hercules, CA) with BSA as a standard. Equal amounts (25 μg) of solubilized protein were resolved by SDS-PAGE and transferred to a nitrocellulose membrane. Membranes were incubated for 1 h in 5% skim milk or 3% BSA to block non-specific binding sites, and then probed as indicated with

the following primary antibodies directed against: PDGF receptor (PDGFR)-β (rabbit polyclonal; 1 μg/ml; Santa Cruz Biotechnology, Santa Cruz, CA), phosphotyrosine (PY20; mouse monoclonal; 1:1000; BD Biosciences, Mississauga, ON, Canada), ERK1/2 (rabbit polyclonal**;** 0.25 μg/ml; Upstate Biotechnology, Charlottesville, VA), phospho-ERK1/2 (pERK1/2; Thr202/Tyr204; rabbit polyclonal; 1:2000), Akt (rabbit polyclonal; 1:1000), phospho-Akt (pAkt; Ser473; rabbit polyclonal; 1:1000; all from Cell Signaling Technology, Beverly, MA). This was followed by incubation with the appropriate horseradish peroxidase (HRP)-conjugated secondary antibody. Signal detection was performed using Immobilon Western chemiluminescence HRP Substrate (Millipore). Relative intensity of the bands was quantified using AlphaEaseFC software (Alpha Innotech, San Leandro, CA) and expressed as integrated optical density (I.O.D.) units.

Measurement of ROS

Confluent 3T3-L1 preadipocytes were washed with DMEM and placed in control medium or J774A.1-MacCM, depleted or not of PDGF, and supplemented with 10% FBS or left serum-free, all in the presence of 10 μM dihydrorhodamine 123 (DHR123), for 15 min. All cells were then washed twice in ice-cold PBS and scraped in 1 ml of PBS on ice. Collected cells were disrupted by sonication, on ice, for 10 s, with a Vibra cell sonicator (Sonics & Materials Inc., Newtown, CT), set at 25% amplitude. Fluorescence was assayed in triplicate, using a FLUOstar Galaxy plate reader (BMG Labtechnologies, Germany), with excitation and emission wavelengths of 505 nm and 538 nm,

respectively, and was corrected for background non-specific fluorescence signal, measured from cells not exposed to DHR123.

Statistical analysis

Comparison of means was performed by ANOVA followed by the post-hoc Newman-Keuls test to assess differences between individual means using GraphPad InStat v3.05 (GraphPad Software Inc., San Diego, CA). A value of $p<0.05$ was taken as significant.

Results

MacCM-induced preadipocyte survival is reduced by phosphoinositide 3-kinase (PI3K) inhibitors

We evaluated the dependence of J774A.1-MacCM-induced 3T3-L1 preadipocyte survival on the phosphorylation of Akt and ERK1/2. Parallel studies were conducted with PDGF, since we have identified PDGF as a component of J774A.1-MacCM that is responsible for its pro-survival effect (Molgat et al., 2009). Resting levels of phosphorylated Akt and ERK1/2 were barely detectable, and increased strongly upon stimulation with J774A.1-MacCM or PDGF (Fig. 1). The PI3K inhibitor wortmannin completely reduced Akt phosphorylation in response to J774A.1-MacCM (Fig. 1A; $p<0.01$). J774A.1-MacCM-stimulated ERK1/2 phosphorylation was equally inhibited by

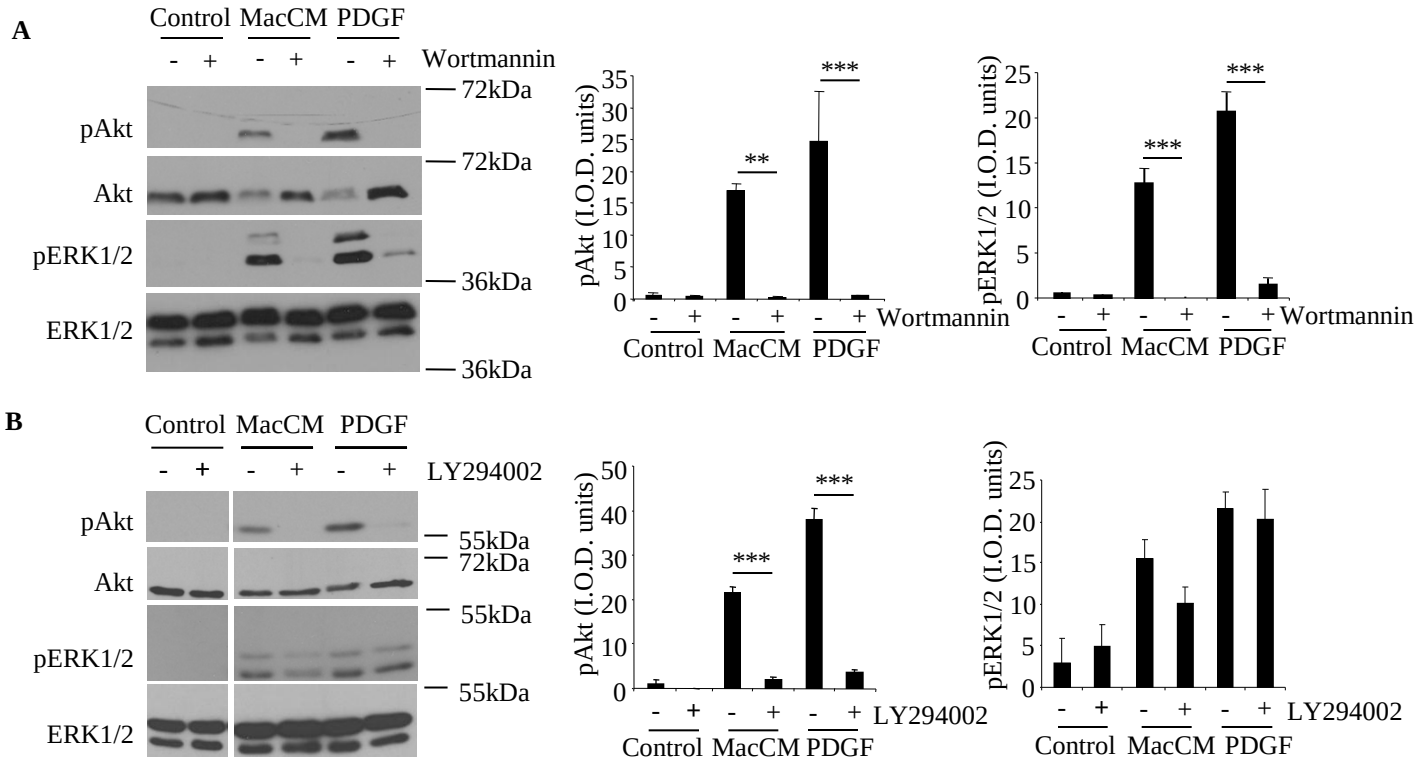
A
Control
MacCM
PDGF
- + - + - +
Wortmannin
pAkt
Akt
pERK1/2
ERK1/2
72kDa
72kDa
36kDa
36kDa
pAkt (I.O.D. units)
pERK1/2 (I.O.D. units)
**
***
***
***
Control MacCM PDGF
B
LY294002
55kDa
72kDa
55kDa
55kDa

Figure 1. Wortmannin or LY294002 inhibits MacCM-stimulated preadipocyte survival signaling. 3T3-L1 preadipocytes were pretreated with 100 nM wortmannin (15 min) (A), 10 μM LY294002 (30 min) (B), or vehicle as described, and then treatments were continued in the indicated serum-free medium (15 min). Cellular proteins were separated by SDS-PAGE and immunoblotted as indicated. Representative immunoblots are shown. Densitometric data are expressed as mean ± SE (n=3 for *A* and *B*). ***p*<0.01, ****p*<0.001.

wortmannin (Fig. 1A; $p<0.001$). Similar results were seen for PDGF-stimulated responses with or without wortmannin (Fig. 1A; $p<0.001$). Preadipocytes treated with LY294002, a structurally distinct PI3K inhibitor, also exhibited a significant reduction in J774A.1-MacCM-stimulated or PDGF-stimulated Akt phosphorylation (Fig. 1B; $p<0.001$). A trend towards a reduction in ERK1/2 phosphorylation in response to J774A.1-MacCM, but not PDGF, was observed with LY294002 (Fig. 1B).

To test the effect of wortmannin on J774A.1-MacCM-induced preadipocyte survival, 3T3-L1 preadipocytes were serum-deprived for 6h in J774A.1-MacCM or control medium (Fig. 2A). In control medium, the number of viable cells was reduced by 37% ($p<0.01$), and as we have shown previously (Molgat et al., 2009), J774A.1-MacCM completely prevented cell death. However, when wortmannin was added to J774A.1-MacCM, the protective effect was blocked, and there was a 29% decrease in cell number ($p<0.01$; versus serum-free MacCM). Consistent with this wortmannin effect, the addition of LY294002 to J774A.1-MacCM caused an 18% reduction in cell number (Fig. 2B; $p<0.01$; versus serum-free MacCM).

These data were supported by staining serum-deprived preadipocytes with annexin V and PI (Fig. 2C). In control medium, a significant 3.8-fold increase in the percentage of early-stage apoptotic preadipocytes, defined as annexin V+/PI-, occurred ($p<0.001$). J774A.1-MacCM prevented this apoptotic response, but when wortmannin was present, there was a significant 2.2-fold increase in the percentage of early apoptotic preadipocytes ($p<0.05$; versus serum-free MacCM). The low annexin V signal of serum-free preadipocytes in the presence of PDGF rose by 5.6-fold when wortmannin was added ($p<0.001$).

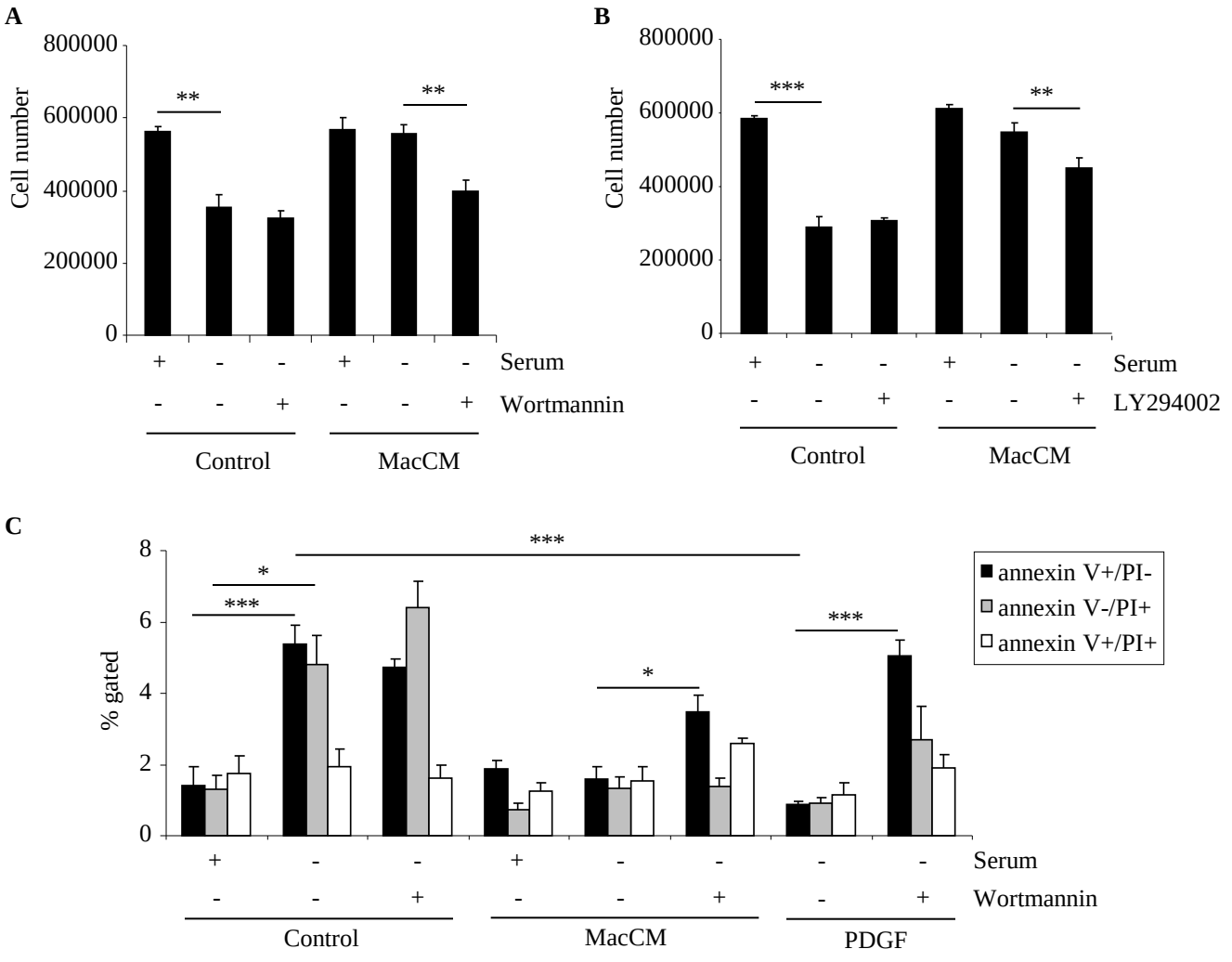
A
800000
600000
400000
200000
0
Cell number
**
**
+ - - + - - Serum
- - + - - + Wortmannin
Control
MacCM
B
800000
600000
400000
200000
0
Cell number
***
**
+ - - + - - Serum
- - + - - + LY294002
Control
MacCM
C
8
6
4
2
0
% gated
*
***
***
*
***
annexin V+/PI-
annexin V-/PI+
annexin V+/PI+
+ - - + - - - - Serum
- - + - - + - + Wortmannin
Control
MacCM
PDGF

Figure 2. Wortmannin or LY294002 inhibits MacCM-induced preadipocyte survival. A and B: 3T3-L1 preadipocytes were pretreated with 100 nM wortmannin (15 min) (A), 10 μM LY294002 (30 min) (B), or vehicle as described, and then treatments were continued in the indicated medium (6 h). Cells were trypsinized, stained with 0.2% trypan blue, and enumerated. Data are expressed as the number of viable cells (mean ± SE, n=3, each performed in triplicate). C: 3T3-L1 preadipocytes were pretreated with wortmannin or vehicle as in (A) and then treatment was continued in the indicated medium (3 h). Cells were stained with annexin V and PI. Data from flow cytometric analysis are expressed as the percentage of cells gated for each indicated population (mean ± SE, n=3, each performed in duplicate). *p<0.05, **p<0.01, ***p<0.001.

MacCM-induced preadipocyte survival is reduced by MEK1/2 inhibitors

UO126, a selective inhibitor of MEK1/2, and PD98059, a MEK1-selective inhibitor, reduced J774A.1-MacCM-stimulated ERK1/2 phosphorylation by 79% ($p<0.001$) and 44% ($p<0.05$), respectively (Fig. 3A). There was no effect on Akt phosphorylation. Studies with these inhibitors to examine PDGF-stimulated preadipocytes gave similar results. UO126 and PD98059 inhibited the pro-survival effect of J774A.1-MacCM on serum-deprived preadipocytes, as assessed by the 18% ($p<0.01$) and 21% ($p<0.05$) reductions in cell number, respectively (Fig. 3B; versus serum-free MacCM).

DPI and NAC modulate preadipocyte signaling and survival

ROS, generated by NADPH oxidases stimulated by cell surface receptors, are implicated in Akt and ERK1/2 signaling (Baumer et al., 2008; Svegliati et al., 2005). DPI is a widely used oxidase inhibitor that inhibits ROS production in 3T3-L1 adipocytes (Furukawa et al., 2004; Mahadev et al., 2001) and other cell types (Mochizuki et al., 2006; Sim et al., 2005). DPI treatment inhibited Akt and ERK1/2 phosphorylation by 88% ($p<0.01$) and 52% ($p<0.05$), respectively, in 3T3-L1 preadipocytes stimulated by J774A.1-MacCM (Fig. 4A). In contrast, DPI did not influence PDGF-stimulated Akt or ERK1/2 phosphorylation under these culture conditions. DPI did not significantly inhibit PDGFR tyrosine phosphorylation in response to either J774A.1-MacCM or PDGF (Fig. 4A).

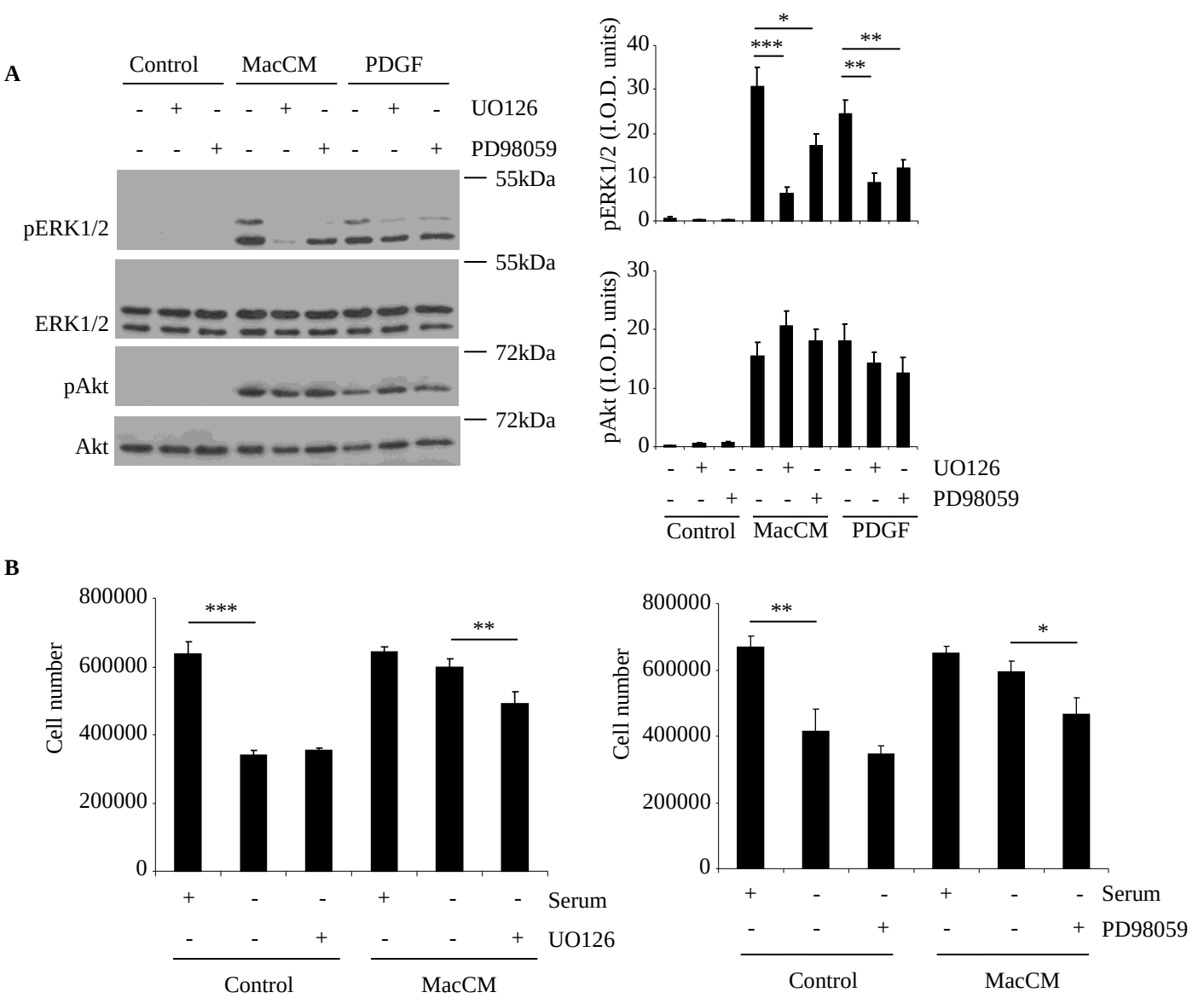
A
Control
MacCM
PDGF
UO126
PD98059
55kDa
pERK1/2
55kDa
ERK1/2
72kDa
pAkt
72kDa
Akt
pERK1/2 (I.O.D. units)
pAkt (I.O.D. units)
B
Cell number
Serum
Control
MacCM

Figure 3. UO126 or PD98059 inhibits MacCM-stimulated preadipocyte survival signaling and MacCM-induced preadipocyte survival. 3T3-L1 preadipocytes were pretreated with 10 µM UO126 (30 min), 50µM PD98059 (30 min), or vehicle as described, and then treatments were continued in the indicated serum-free medium (15 min) (A), or indicated medium (6 h) (B). A: Cellular proteins were separated by SDS-PAGE and immunoblotted as indicated. Representative immunoblots are shown. Densitometric data are expressed as mean ± SE (n=4). B: Cells were trypsinized, stained with 0.2% trypan blue, and enumerated. Data are expressed as number of viable cells (mean±SE; n=3, each performed in triplicate). *p<0.05, **p<0.01, ***p<0.001.

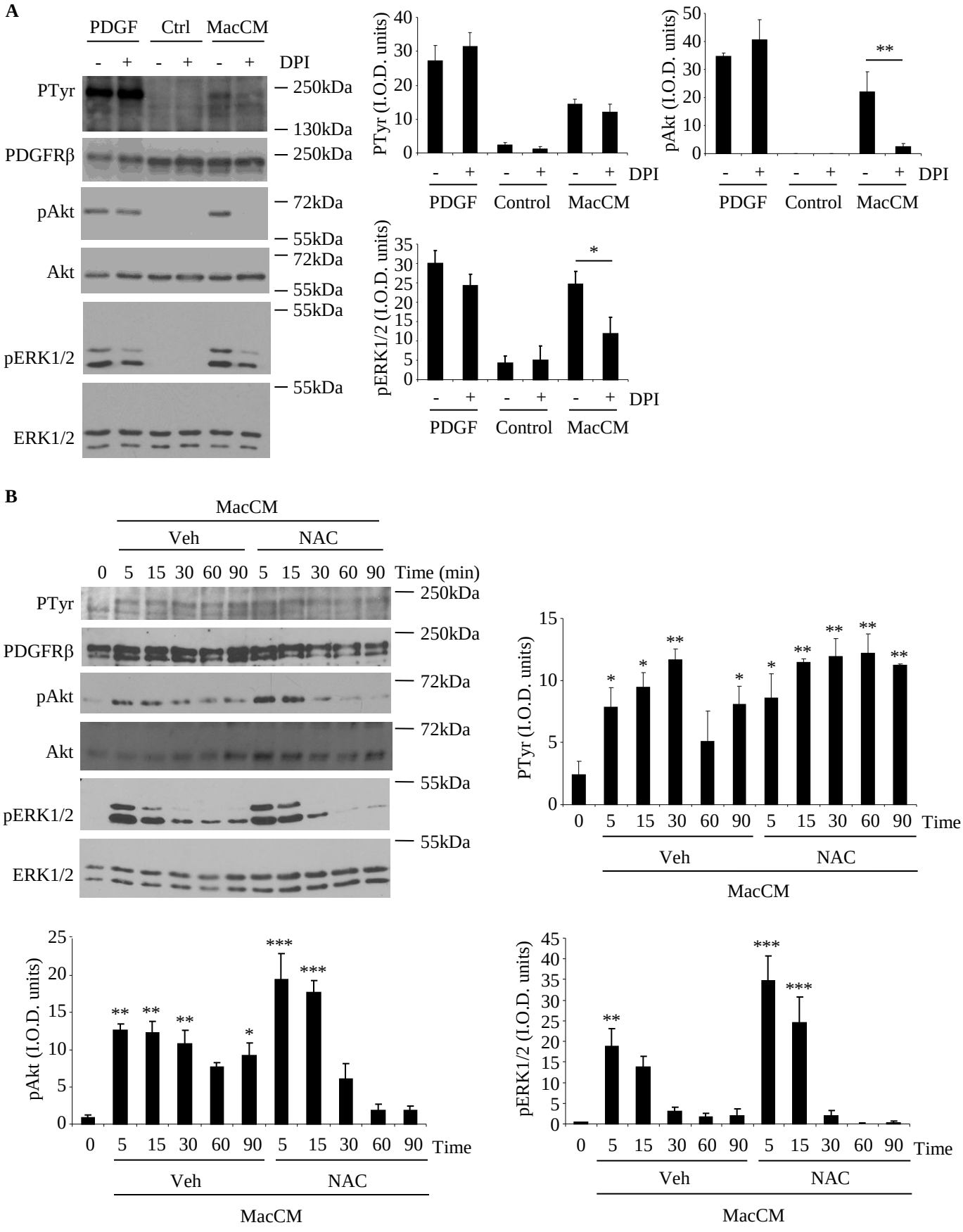
A
PDGF
Ctrl
MacCM
- + - + - + DPI
PTyr
PDGFRβ
pAkt
Akt
pERK1/2
ERK1/2
250kDa
130kDa
250kDa
72kDa
55kDa
72kDa
55kDa
55kDa
55kDa
PTyr (I.O.D. units)
pAkt (I.O.D. units)
pERK1/2 (I.O.D. units)
PDGF
Control
MacCM
DPI
B
MacCM
Veh
NAC
0 5 15 30 60 90 5 15 30 60 90 Time (min)
PTyr
PDGFRβ
pAkt
Akt
pERK1/2
ERK1/2
250kDa
250kDa
72kDa
72kDa
55kDa
55kDa
PTyr (I.O.D. units)
pAkt (I.O.D. units)
pERK1/2 (I.O.D. units)
Time

Figure 4. DPI or NAC inhibits MacCM-stimulated preadipocyte survival signaling. A and B: 3T3-L1 preadipocytes were pretreated with 10 μM DPI (30 min) (A), 10 mM NAC (2 h) (B), or vehicle as described, and then treatment was continued in the indicated serum-free medium for 15 min (A) or the times shown (B). Cellular proteins were separated by SDS-PAGE and immunoblotted as indicated. Representative immunoblots are shown. Densitometric data are expressed as mean ± SE (n=3 for all, except n=5, pERK1/2, in panel A). *p<0.05, **p<0.01, ***p<0.001 versus time 0 or between indicated pairs.

To interfere with ROS by another mechanism, we used NAC, which increases intracellular glutathione levels, thereby reducing ROS levels (Furukawa et al., 2004). This resulted in a delayed onset of inhibition of J774A.1-MacCM-stimulated Akt phosphorylation, becoming apparent from 30 min to 90 min (Fig. 4B). No NAC-related effect on PDGFR or ERK1/2 phosphorylation was observed.

These preadipocyte studies using DPI and NAC suggest that ROS may play a role in J774A.1-MacCM-stimulated cell signaling. We therefore examined ROS levels in 3T3-L1 preadipocytes after 15 minutes of serum deprivation in control medium versus MacCM. In serum-free control medium, ROS levels increased by 2.1-fold, as assessed by rhodamine 123 fluorescence (Fig. 5A; $p<0.001$). J774A.1-MacCM, which, in contrast to serum deprivation, promotes preadipocyte survival, generated a 3.4-fold increase in ROS ($p<0.001$; versus serum-containing MacCM) that was larger than the serum deprivation response ($p<0.05$). MacCM, immunodepleted of PDGF, which we have previously shown to be incapable of maintaining preadipocyte survival (Molgat et al., 2009), generated a significantly reduced level of ROS ($p<0.05$, versus serum-free MacCM) that was similar to the signal generated by apoptosis-promoting serum-free control medium. It would appear that regulation of ROS generation in preadipocytes is complex, in that conditions leading either to death or survival increase cellular ROS levels.

DPI significantly inhibited the pro-survival activity of J774A.1-MacCM in serum-deprived preadipocytes (Fig. 5B), resulting in a 57% reduction in cell number ($p<0.001$; versus serum-free MacCM), and a somewhat lower cell survival versus serum-free control medium ($p<0.05$). DPI increased the percentage of annexin V+/PI+ preadipocytes by 2.7-fold, representative of late-stage apoptosis (Fig. 5C; $p<0.05$; versus serum-free

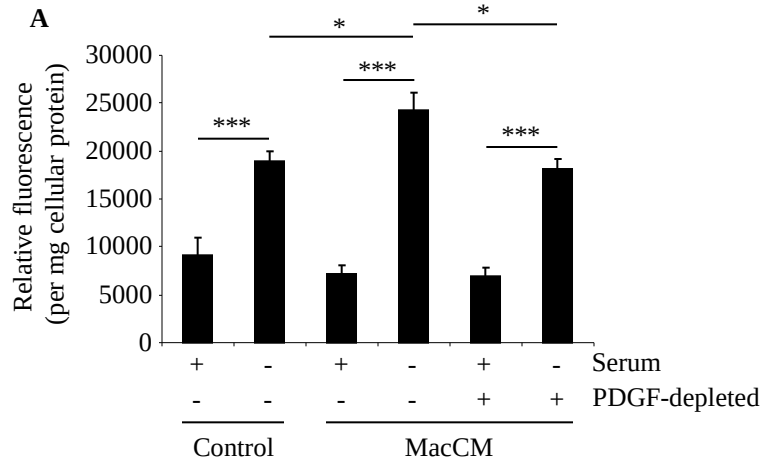
A
Relative fluorescence (per mg cellular protein)
30000
25000
20000
15000
10000
5000
0
*
*
***
***
***
Serum
PDGF-depleted
Control
MacCM

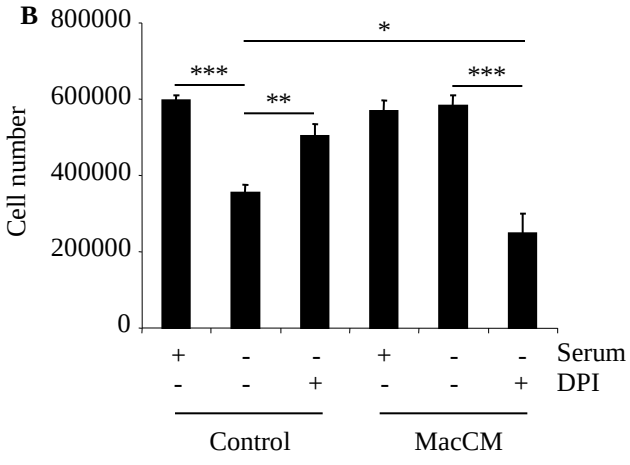
B
Cell number
800000
600000
400000
200000
0
*
***
**
***
Serum
DPI
Control
MacCM

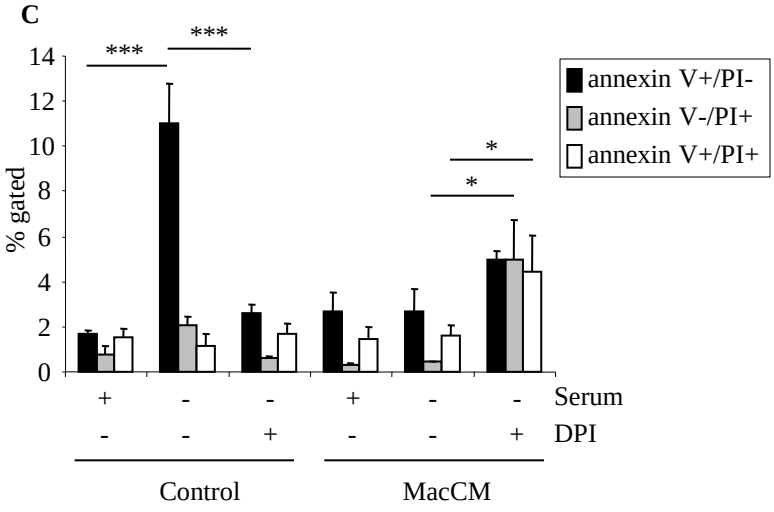
C
% gated
14
12
10
8
6
4
2
0
***
***
*
*
annexin V+/PI-
annexin V-/PI+
annexin V+/PI+
Serum
DPI
Control
MacCM

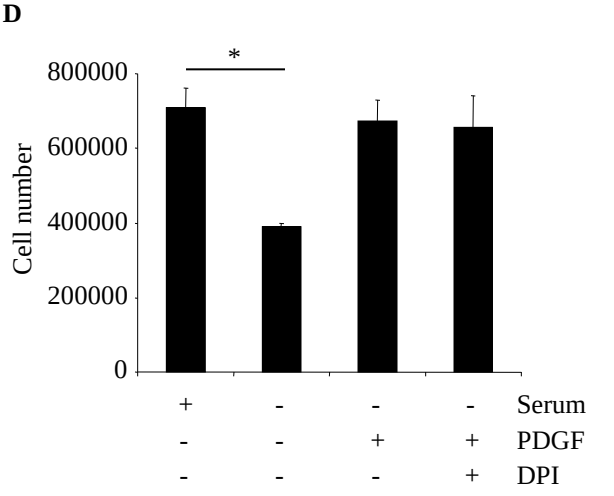
D
Cell number
800000
600000
400000
200000
0
*
Serum
PDGF
DPI

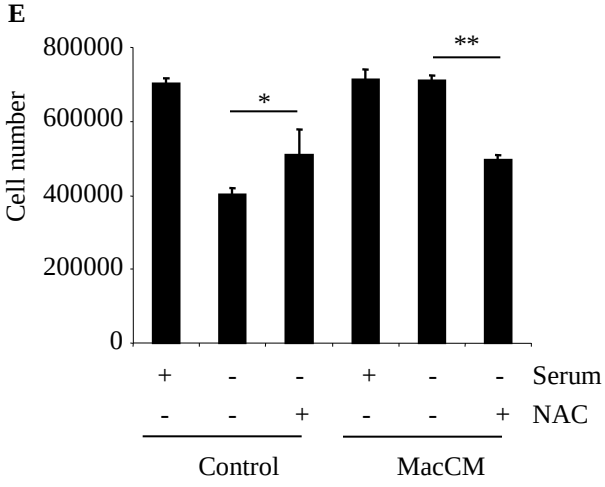
E
Cell number
800000
600000
400000
200000
0
*
**
Serum
NAC
Control
MacCM

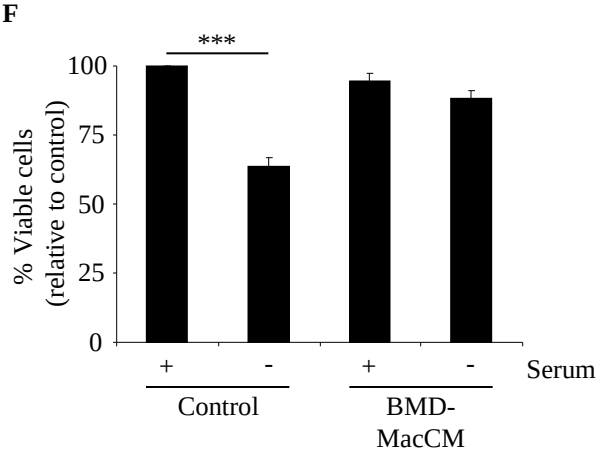
F
% Viable cells (relative to control)
100
75
50
25
0
***
Serum
Control
BMD-MacCM

Figure 5. DPI or NAC inhibits MacCM-induced preadipocyte survival. A: 3T3-L1 preadipocytes were placed in the indicated medium, supplemented with 10 μM DHR123, for 15 min. Cell lysates were collected and assayed for fluorescence. Data are expressed as mean ± SE of relative fluorescence intensity, normalized for cellular protein (n=3). B: 3T3-L1 preadipocytes were pretreated with 10 μM DPI (30 min) or vehicle as described, and then treatment was continued in the indicated medium (6 h). Cells were trypsinized, stained with 0.2% trypan blue, and enumerated. Data are expressed as number of viable cells (mean ± SE; n=6-7, each performed in triplicate). C: 3T3-L1 preadipocytes were pretreated with 10 μM DPI (1 h) or vehicle as described, and then treatment was continued in the indicated medium (3 h). Cells were stained with annexin V and PI. Data from flow cytometric analysis are expressed as the percentage of cells gated for each indicated population (mean ± SE; n=3, each performed in duplicate). D-E: 3T3-L1 preadipocytes were pretreated with 10 μM DPI (30 min) (D), or 10 mM NAC (2h) (E), or vehicle as described, and then treatment was continued in the indicated medium (6 h). Cells were trypsinized, stained with 0.2% trypan blue, and enumerated. Data are expressed as number of viable cells (mean ± SE; n=3, each performed in triplicate). F: 3T3-L1 preadipocytes were placed in the indicated medium for 6 h. Cells were trypsinized, stained with 0.2% trypan blue, and enumerated. Data are expressed as the percentage of viable cells relative to the control serum-containing condition (mean ± SE; n=3, each performed in duplicate). *p<0.05, **p<0.01, ***p<0.001.

MacCM). A 1.8-fold increase in the percentage of early-stage annexin V+/PI- apoptotic preadipocytes was also observed, but did not reach statistical significance**.** DPI did not alter PDGF-dependent preadipocyte survival (Fig. 5D), consistent with its lack of effect on PDGF-stimulated survival signaling pathways (Fig. 4A).

In addition to the inhibitory effect of DPI on J774A.1-MacCM-mediated survival, DPI also reduced preadipocyte cell death caused by serum deprivation in control medium, as assessed by cell enumeration (Fig. 5B; $p<0.05$). DPI completely eliminated annexin V staining of preadipocytes in serum-free control medium (Fig. 5C; $p<0.001$).

Similar to DPI, NAC significantly impaired J774A.1-MacCM-induced preadipocyte survival, resulting in a 30% reduction in cell number (Fig. 5E; $p<0.01$; versus serum-free MacCM). NAC also significantly reduced cell death induced by serum withdrawal in control medium ($p<0.05$). Taken together, these preadipocyte survival studies, using DPI and NAC, suggest a requirement for ROS in two distinct responses: 1) preadipocyte apoptosis induced by serum deprivation, and 2) preadipocyte survival induced by MacCM.

To evaluate whether MacCM generated from a primary macrophage cell model would exert pro-survival activity on preadipocytes, we investigated the effect of BMD-MacCM on preadipocyte survival. As shown in Fig. 5F, preadipocyte death induced by serum withdrawal was prevented by BMD-MacCM.

Discussion

We recently reported that J774A.1-MacCM prevents 3T3-L1 preadipocyte apoptosis due to serum deprivation, and identified PDGF as the principal responsible component (Molgat et al., 2009). We have now performed a detailed analysis of survival signaling pathways in preadipocytes that might be activated by J774A.1-MacCM. Although both MacCM and PDGF promote preadipocyte survival, our data reveal signal transduction patterns that differ in response to these two inducers.

We examined the PI3K-Akt and MEK-ERK1/2 pathways and their responses to PDGF versus J774A.1-MacCM. PDGF binds to its cognate receptor tyrosine kinase to induce dimerization and autophosphorylation of the cytoplasmic regions of each receptor, leading to a variety of downstream signaling pathways. PI3K is recruited to the PDGF receptor and generates PI(3,4,5)P3 that in turn attracts Akt to the cell membrane, where it is activated via phosphorylation of S473 and T308 by its upstream regulators, mTORC2 and PDK1, respectively (Park et al., 2003). Akt promotes cell survival via its inhibitory phosphorylation of pro-apoptotic Bad, and FOXO3a (Vantler et al., 2005). PI3K/PI(3,4,5)P3/Akt signaling has been shown to protect preadipocytes from serum withdrawal induced apoptosis (Gagnon et al., 2001; Niesler et al., 2000). The ligand-bound PDGF receptor can also interact with the Grb2-Sos complex to switch on Ras. This in turn activates ERK1/2 due to phosphorylation of T202 and Y204 by upstream kinases MEK1/2 (Bonni et al., 1999). ERK1/2 mediates cell survival via transcriptional and post-transcriptional regulation of Bcl-2 proteins (Ballif and Blenis, 2001). Whether MEK/ERK1/2 mediates 3T3-L1 preadipocyte survival is unclear. We found no role for

MEK/ERK1/2 in IGF-1 survival signaling with 18 h of serum withdrawal (Gagnon et al., 2001), whereas a positive role for the MEK/ERK1/2 pathway was reported with 24 h of serum withdrawal (Niesler et al., 2000).

Akt phosphorylation stimulated by J774A.1-MacCM or PDGF was equally sensitive to PI3K inhibitors wortmannin or LY294002. However, we observed a difference between the two inhibitors with respect to the ERK1/2 phosphorylation response, with only wortmannin causing inhibition. PI3K has been positioned upstream of ERK1/2 in some cell systems. For example, in NIH 3T3 cells, a systematic quantitative analysis in combination with kinetic modeling indicates PI3K signaling activates ERK1/2 through interactions that are proximal and distal to Ras activation (Wang et al., 2009). Furthermore, in HL-60 cells and in mouse embryonic stem cells, inhibitors of Akt reduced ERK1/2 phosphorylation (Kim et al., 2009; Patel et al., 2010). The irreversible nature of the wortmannin inhibition possibly explains the more potent effect on ERK1/2 phosphorylation that we observed versus LY294002. Alternatively, wortmannin or LY294002 may inhibit targets, other than PI3K, that might regulate ERK1/2 (Gharbi et al., 2007). Inhibition of J774A.1-MacCM- or PDGF-stimulated ERK1/2 phosphorylation also occurred either with UO126 or PD98509, with no effect on Akt phosphorylation. The apparent greater inhibition of ERK1 may reflect the weaker intensity of the stimulated phospho-ERK1 signal, relative to that of phospho-ERK2.

Preadipocyte survival induced by J774A.1-MacCM, assessed both by cell enumeration of adherent viable cells as well as by flow cytometric analysis of annexin V staining, was substantially impaired by wortmannin or LY294002. Inhibition of the ERK1/2 pathway, by either UO126 or PD98509, was also sufficient to block the pro-

survival activity of J774A.1-MacCM on 3T3-L1 preadipocytes. It would seem that these two pathways are each required for preadipocyte survival. Wortmannin (29% cell loss) caused a greater disruption of MacCM-induced preadipocyte survival than did LY294002 (18% cell loss), perhaps due to its ability to inhibit phosphorylation of ERK1/2 in addition to Akt. It remains to be determined whether combined PI3K and ERK1/2 inhibition with LY294002 and UO126/PD98059 would augment the inhibition of J774A.1-MacCM-dependent preadipocyte survival.

We have evaluated the complex role of ROS in preadipocyte survival signaling and cell death. Using the general oxidase inhibitor DPI, we examined J774A.1-MacCM- versus PDGF-stimulated signaling pathways. DPI strongly inhibited J774A.1-MacCM-stimulated Akt and ERK1/2 phosphorylation, however, PDGF-stimulated Akt and ERK1/2 phosphorylation responses were unaffected, even when examined at longer stimulation times and with lower concentrations of PDGF (data not shown). The inhibition of J774A.1-MacCM-stimulated Akt phosphorylation by NAC versus DPI occurred later, consistent with NAC acting as a scavenger to accelerate the clearance of ROS compared to direct inhibition of ROS generation by DPI. Taken together, these results suggest that in preadipocytes, ROS is required for Akt and ERK1/2 signaling in response to J774A.1-MacCM, but not to PDGF. Activation of Akt and ERK1/2 by PDGF was also found to be independent ROS in vascular smooth muscle cells (ten Freyhaus et al., 2006).

Our results raise the possibility that DPI may prevent the reversible oxidation of PTEN due to localized generation of ROS by factors within the MacCM (Woo et al., 2010). This regional ROS generation by membrane-localized NADPH oxidase normally

attenuates PTEN 3-phosphatase action on PI(3,4,5)P3, thereby contributing to net PI(3,4,5)P3 accumulation and activation of Akt (Kwon et al., 2004). Inhibition of this process by DPI would result in a fully active PTEN, lowering PI(3,4,5)P3 levels and reducing Akt activation. Indeed, we detected an increase in ROS levels when serum-deprived preadipocytes were treated with J774A.1-MacCM. Our data indicate ROS are essential for Akt and ERK1/2 phosphorylation and 3T3-L1 preadipocyte survival in response to J774A.1-MacCM.

Additional studies will be needed to learn more about the role of ROS in preadipocyte survival signaling, and to understand why it is specific for MacCM and not PDGF. We did confirm there was a 2.9-fold increase in ROS in PDGF-stimulated preadipocytes under the same experimental conditions as the MacCM studies. A significant reduction in MacCM-dependent ROS production was observed following PDGF immunodepletion, consistent with PDGF contributing to this response. It is possible that factors other than PDGF within the J774A.1-MacCM may influence preadipocyte survival signaling, resulting in a greater sensitivity to ROS inhibition.

ROS levels in preadipocytes also rose in response to serum deprivation, and addition of DPI or NAC actually protected the preadipocytes from apoptosis during the period of serum deprivation. Recently, 3T3-L1 preadipocytes have been shown to be highly susceptible to ROS-induced apoptosis (Kojima et al., 2010). In PC12 cells, serum-withdrawal induced apoptosis was reduced by antioxidant treatment (Satoh et al., 1996), consistent with our data for 3T3-L1 preadipocytes. In contrast to NADPH oxidase-stimulated ROS generation near the membrane by growth factor receptors, this mode of ROS generation involves mitochondrial oxidases, and is associated with apoptosis in

other cell systems (Lee et al., 2006). Recent work has identified Romo1, a mitochondrial protein, as an essential player linking the serum deprivation signal to mitochondrial ROS production (Lee et al., 2010). Intracellular localization of ROS generated in response to serum withdrawal versus survival factors is needed to support this conceptual model. The level of ROS generated in response to PDGF-depleted MacCM was comparable in magnitude to the levels generated by serum-free control medium. As both of these treatments induce preadipocyte apoptosis (Molgat et al., 2009), it is possible both of these ROS responses arise from common pro-apoptotic mitochondrial origins. Alternatively, other as yet unidentified factors present in PDGF-depleted MacCM may be responsible for stimulating the production of these ROS.

Our data demonstrate that J774A.1-MacCM can prevent serum withdrawal-induced 3T3-L1 preadipocyte apoptosis through Akt and ERK1/2 signaling pathways. Although a pharmacological inhibitor strategy can never be completely specific, we have used structurally unrelated compounds to target each of the pathways that we have implicated here. More work will be needed to determine if our observations will apply to human macrophage and preadipocyte models. Recent studies have found specific evidence of adipocyte apoptosis and turnover in humans, but little is known about in vivo preadipocyte turnover (Alkhouri et al., 2010; Arner and Spalding, 2010; Maumus et al., 2008; Spalding et al., 2008). Attempts to measure the number of preadipocytes in obesity have been hindered by a lack of specific human preadipocyte markers, and instead, quantification of adipose stromal cells as a whole has been reported. Numbers of adipose stromal cells correlate positively with BMI, consistent with increased preadipocyte proliferation and/or survival (van Harmelen et al., 2003).

Growing evidence supports a role for macrophages in the regulation of preadipocyte fate. We and others have reported that MacCM prevents adipocyte differentiation using several *in vitro* and in vivo models (Constant et al., 2006; Constant et al., 2008; Keophiphath et al., 2009; Lacasa et al., 2007; Lu et al., 2010; Stienstra et al., 2008; Yarmo et al., 2009). The effect of MacCM on preadipocyte proliferation has been variable, with both positive and negative regulation reported (Lacasa et al., 2007; Maumus et al., 2008). Preadipocyte survival is another potential route by which the preadipocyte pool can be modulated. At this point, it can only be speculated that adipose tissue macrophages, when activated to produce PDGF, might promote preadipocyte survival to maintain or expand the preadipocyte pool as adipose tissue is remodeled. PDGF is present in the adipose tissue of mice and humans, with higher concentrations in the obese state, and macrophages are a principal source of PDGF that is produced by adipose tissue (Pang et al., 2008). The overall effect of MacCM is likely to be influenced by whether macrophages are classically or alternatively activated, and this should be explored in future studies.

Acknowledgments

This work was supported by a grant-in-aid NA 6634 from the Heart and Stroke Foundation of Ontario to A.S. A.S.D.M. is the recipient of an Alexander Graham Bell Canada Graduate Scholarship from the National Sciences and Engineering Research Council of Canada.

4.0 MANUSCRIPT #3

The activation state of macrophages alters their ability to suppress preadipocyte apoptosis.

STATEMENT OF AUTHOR CONTRIBUTIONS

André S.D. Molgat is the first author on this publication. He performed the experiments and the data analysis, participated in the design of the experiments, and wrote the manuscript. **Dr. AnneMarie Gagnon** is the research associate in Dr. Alexander Sorisky`s laboratory. She participated in the design of the experiments, performed data analysis, and assisted in the editing and revising of the manuscript. **Charlie Foster** was an undergraduate research student in the laboratory of Dr. Alexander Sorisky. He assisted in performing experiments and data analysis. **Dr. Alexander Sorisky** is the PhD supervisor of André Molgat. He contributed to the design of the experiments, analysis of results, and revising the manuscript.

SUMMARY

The following manuscript entitled "The activation state of macrophages alters their ability to suppress preadipocyte apoptosis" was published in J Endocrinol [(2012) 214, 21-29]. The objective of manuscript #3 was to determine the effect of macrophage activation on macrophage-dependent preadipocyte survival, and to extend the findings

from objectives #1 and 2 into a primary human cell model. This study was conducted using both 3T3-L1 and human primary preadipocyte models, as well as J774A.1, THP-1, and human primary MD-macrophage cell models. MacCM was prepared and applied to confluent preadipocyte cultures. 3T3-L1 preadipocytes were induced to undergo apoptosis by serum withdrawal. Human preadipocytes were induced to undergo apoptosis by serum withdrawal in the presence of cycloheximide (CHX) and TNF-α. Preadipocyte apoptosis was assessed by enumeration of viable cells and by quantification of apoptotic nuclei. Macrophages were activated towards pro-inflammatory, and towards anti-inflammatory phenotypes by incubation with LPS and IL-4, respectively. This study revealed that the anti-apoptotic effect of MacCM was lost following the pro-inflammatory activation of macrophages, yet retained with anti-inflammatory activation. Furthermore, this study revealed that human macrophages also suppress apoptosis of human primary preadipocytes.

The Activation State of Macrophages Alters Their Ability to Suppress Preadipocyte Apoptosis

ANDRÉ S.D. MOLGAT, ANNEMARIE GAGNON, CHARLIE FOSTER, ALEXANDER SORISKY*

Chronic Disease Program, Ottawa Hospital Research Institute; and Departments of Medicine and of Biochemistry, Microbiology & Immunology, University of Ottawa, Ottawa, Canada.

*Correspondence to: Alexander Sorisky, Ottawa Hospital Research Institute, General campus, 501 Smyth Road, Ottawa, Ontario, Canada, K1H 8L6, Phone: 613-737-8899 #73320; Fax: 613-737-8803; E-mail asorisky@ohri.ca

Short title: Macrophage activation and preadipocyte apoptosis

Keywords

- preadipocyte
- macrophage
- apoptosis
- inflammation
- platelet-derived growth factor
- tumor-necrosis factor α

Abstract

Adipose tissue contains macrophages whose state of activation is regulated as obesity develops. Macrophage-secreted factors influence critical processes involved in adipose tissue homeostasis, including preadipocyte proliferation and differentiation into adipocytes. Macrophage-conditioned medium (MacCM) from J774A.1 macrophages protects 3T3-L1 preadipocytes from apoptosis through platelet-derived growth factor (PDGF) signaling. Here we have investigated the effect of macrophage activation on MacCM-dependent preadipocyte survival. MacCM was prepared following activation of either J774A.1 macrophages with lipopolysaccharide (LPS), or human primary monocyte-derived macrophages (MD-macrophages) with LPS or IL-4. 3T3-L1 and human primary preadipocytes were induced to undergo apoptosis in MacCM, and apoptosis was quantified by cell enumeration or Hoechst nuclear staining. Preadipocyte PDGF signaling was assessed by immunoblot analysis of phosphorylated PDGF receptor, Akt and ERK1/2. Pro-inflammatory activation of J774A.1 macrophages with LPS inhibited the pro-survival activity of MacCM on 3T3-L1 preadipocytes, despite intact PDGF signaling. Upregulation of macrophage TNF-α expression occurred in response to LPS, and TNF-α was demonstrated to be responsible for the inability of LPS-J774A.1-MacCM to inhibit preadipocyte apoptosis. Furthermore, MacCM from human MD-macrophages (MD-MacCM) inhibited apoptosis of primary human preadipocytes. MD-MacCM from LPS-treated macrophages, but not IL-4-treated anti-inflammatory macrophages, was unable to protect human preadipocytes from cell death. In both murine cell lines and human primary cells, pro-inflammatory activation of macrophages inhibits

their pro-survival activity, favouring preadipocyte death. These findings may be relevant to preadipocyte fate and adipose tissue remodeling in obesity.

Introduction

Obesity is a major risk factor for insulin resistance, type 2 diabetes and cardiovascular disease. Adipose tissue expansion, due to chronic positive energy balance, occurs via coordinated increases in adipocyte size (hypertrophy) and number (hyperplasia). Hyperplastic obesity, associated with insulin sensitivity in humans and in animal models (Arner et al., 2010; Kim et al., 2007), depends on an adequate number of functional preadipocytes that can differentiate into adipocytes to meet the energy storage demand (adipogenesis). In contrast, hypertrophic obesity is linked to adipose tissue inflammation and insulin resistance (Arner et al., 2010; Heilbronn et al., 2004), and results from insufficient adipogenic capacity.

In addition to preadipocytes and adipocytes, adipose tissue contains macrophages (adipose tissue macrophages; ATM). Their number and activation state vary with extent of adiposity (Lumeng et al., 2007a; Weisberg et al., 2003; Xu et al., 2003). In the lean state, resident ATM account for ~10% of stromal cells, and are in a M2 anti-inflammatory activation state. In obesity, due to infiltration and differentiation of circulating monocytes, ATMs comprise ~50% of stromal cells, and many display a pro-inflammatory M1 activation state. These dynamic changes in macrophage activation alter adipose tissue function. Obese mice subjected to conditional ablation of CD11c-positive cells fail to accumulate M1 ATMs and are not susceptible to diet-induced insulin resistance (Patsouris et al., 2008). Mice with a macrophage-specific PPARγ deletion do not generate M2 macrophages, and are predisposed to obesity-associated insulin resistance (Odegaard et al., 2007). Furthermore, depending on the macrophage model

used, the anti-adipogenic activity of macrophage-conditioned medium (MacCM) on cultured preadipocytes, reported by us and others (Constant et al., 2006; Ide et al., 2011; Lacasa et al., 2007), can be regulated by macrophage activation (Lu et al., 2010; Lumeng et al., 2008; Stienstra et al., 2008).

Our previous investigations into macrophage-adipose cell interactions revealed that MacCM, collected under basal conditions, protects 3T3-L1 preadipocytes from apoptosis in a platelet-derived growth factor (PDGF)-dependent manner (Molgat et al., 2009, 2011). Pro-inflammatory environments, induced by a high fat diet, or cytokines, such as IL-6, IL-1β, and TNF-α, have been associated with adipose cell death, *in vitro* and *in vivo* (Alkhouri et al., 2010; Keuper et al., 2011; Niesler et al., 2000; Tchkonia et al., 2005). Therefore, we have now investigated the effect of pro-inflammatory macrophage activation on the pro-survival activity of MacCM on preadipocytes, using mouse cell lines and human cells in primary culture.

Materials and Methods

Preparation of MacCM.

J774A.1-MacCM was prepared from J774A.1 mouse macrophages (from ATCC, Manasas, VA) that were grown in DMEM supplemented with 10% FBS (Hyclone; South Logan, UT), 100 U/ml penicillin, and 0.1 mg/ml streptomycin (Gibco; Gathersburg, MD). Confluent cells were placed in serum-free medium that was collected 24 h later. LPS-J774A.1-MacCM was prepared by treating confluent cells for 0.5 – 6 h with 100

ng/ml lipopolysaccharide (LPS; from Sigma Aldrich; Saint Louis, MO) or vehicle (HBSS; Hank's buffered salt solution); cells were then placed in serum-free medium for 24 h of conditioning prior to collection. In some experiments, where indicated, J774A.1 macrophages in serum-free medium were treated with a lower dose of LPS (10 ng/ml) during the 24 h conditioning period. For these studies, to control for any residual LPS bioactivity in the medium after collection, 3T3-L1 preadipocytes were treated with serum-free control medium supplemented with 10 ng/ml LPS. There was no effect of LPS control conditions on cell signaling or cell death responses. To neutralize TNF-α, LPS-J774A.1-MacCM or J774A.1-MacCM was incubated with either 2 μg/ml rat-anti-mouse TNF-α neutralizing antibody (R&D Systems, Minneapolis, MN) or control non-specific rat IgG for 1 h prior to use**.**

To prepare MacCM from human monocyte-derived macrophages, peripheral blood mononuclear cells (PBMCs) were isolated from blood donated by 6 healthy volunteers (3 male and 3 female; mean age was 29.7 ± 7.5 years; approved by The Ottawa Hospital Research Ethics Board #2008445-01H). Blood was centrifuged (500 x g) with Ficoll-Hypaque (GE Healthcare; Uppsala, Sweden), and PBMCs were seeded at a density of 1 x 10^7 cells/well in 12 well culture dishes. Monocytes were allowed to adhere for 1 h in serum-free RPMI, and subsequently differentiated into macrophages over either 7 or 14 days in RPMI supplemented with 10% FBS, 100 U/ml penicillin, and 0.1 mg/ml streptomycin (Daigneault et al., 2010; Mayi et al., 2010). Where indicated, macrophage differentiation was also induced in RPMI supplemented with 20% FBS, 100 U/ml penicillin, 0.1 mg/ml streptomycin , and 100 ng/ml M-CSF for either 7 or 14 days (Franco et al., 2006). Differentiated human macrophages were placed in serum-free

medium, and treated either with 100 ng/ml LPS (M1 activation), or 20 ng/ml human recombinant IL-4 (M2 activation; R&D Systems); the medium was collected 24 h later (monocyte-derived-MacCM; MD-MacCM) (Franco et al., 2006). To control for any potential residual bioactivity in the medium during preadipocyte studies, unconditioned control medium supplemented with corresponding concentrations of LPS or IL-4 was evaluated; no effect on preadipocyte responses was noted.

THP-1 monocytes (ATCC) were cultured as described (Constant et al., 2006). They were grown to a density of 1 x 10^6 cells/ml and then treated with 100 nM 12-O-tetradecanoylphorbol-13-acetate (TPA) for 24 h to induce macrophage differentiation. The resulting macrophages were placed in serum-free medium without TPA, and the THP-1-MacCM was collected 24 h later.

MacCM, generated from each macrophage model, was centrifuged at 200 ×g for 5 min, and the supernatant was stored at −20 °C until use for preadipocyte studies.

Isolation and culture of human preadipocytes.

Subcutaneous adipose tissue was obtained from healthy volunteers undergoing elective abdominal surgery (approved by The Ottawa Hospital Research Ethics Board #1995023-01H). Mean age was 52.2 ± 12 years, and mean body mass index was 31.2 ± 11.4 kg/m^2 (±SD). Preadipocytes were isolated as described (Artemenko et al., 2005). Adipose tissue was separated from connective tissue and capillaries by dissection, then digested with collagenase CLS type I (600 U/g of tissue; Worthington, Lakewood, NJ). The digested tissue was subjected to progressive size filtration and centrifugation,

followed by incubation in erythrocyte lysis buffer. Preadipocytes were seeded at a density of 3.5 x 10^5 cells/35mm dish, cultured in DMEM supplemented with 10% FBS, 100 U/ml penicillin, 0.1 mg/ml streptomycin, and 50 U/ml nystatin (Calbiochem, Merck KGaA; Darmstadt, Germany), and grown for 24-48 h until confluent.

Preadipocyte signal transduction studies.

Low-passage 3T3-L1 mouse preadipocytes (ATCC) were grown in DMEM supplemented with 10% calf serum, 100 U/ml penicillin, and 0.1 mg/ml streptomycin (growth medium). Confluent 3T3-L1 preadipocytes, pretreated where indicated for 90 min with 10 μM imatinib or vehicle (0.1% DMSO), were placed in serum-free J774A.1-MacCM, LPS-J774A.1-MacCM, or control medium (supplemented with 10 ng/ml LPS where indicated), for 15 min. Preadipocytes were then processed for immunoblot analysis.

Immunoblot analysis.

Cells were lysed in 1X Laemmli buffer (Laemmli, 1970) supplemented with 5% β-mercaptoethanol, 1 mM sodium orthovanadate, 5 mM EGTA (pH 8.0), 50 mM sodium fluoride, and 5 mM sodium pyrophosphate. Protein was measured using the Dc Protein Assay (Bio-Rad, Hercules, CA) with BSA as a standard. Equal amounts (20-25 μg) of solubilized protein were resolved by SDS-PAGE and transferred to a nitrocellulose membrane. Membranes were incubated for 1 h in 5% skim milk or 3% BSA to block

non-specific binding sites, and then probed as indicated with the following primary antibodies directed against: PDGF receptor (PDGFR)-β (rabbit polyclonal; 1 μg/ml; Santa Cruz Biotechnology, Santa Cruz, CA), phosphotyrosine (PY20; mouse monoclonal; 1:1000; BD Biosciences, Mississauga, ON, Canada), ERK1/2 (rabbit polyclonal; 0.25 μg/ml; Upstate Biotechnology, Charlottesville, VA), phospho-ERK1/2 (pERK1/2; Thr202/Tyr204; rabbit polyclonal; 1:2000), Akt (rabbit polyclonal; 1:1000), or phospho-Akt (pAkt; Ser473; rabbit polyclonal; 1:1000; all from Cell Signaling Technology, Beverly, MA). After incubation with the appropriate horseradish peroxidase (HRP)-conjugated secondary antibody, signal detection was performed using the Immobilon Western chemiluminescence HRP Substrate kit (Millipore). Relative intensity of the bands was quantified using AlphaEaseFC software (Alpha Innotech, San Leandro, CA) and expressed as integrated optical density (I.O.D.) units.

Cell death analysis.

For cell enumeration studies, confluent 3T3-L1 preadipocytes, pretreated where indicated for 90 min with 10 μM imatinib or vehicle (0.1% DMSO), were placed in control medium (supplemented or not with 10% FBS, 1-100 ng/ml recombinant mouse TNF-α (R&D Systems), or 20 ng/ml recombinant human PDGF BB (Calbiochem)), serum-free J774A.1-MacCM, or serum-free LPS-J774A.1-MacCM. After 6 h, floating cells were removed, and adherent cells were trypsinized and stained with 0.2% trypan blue dye. Viable cells (trypan blue exclusion) were counted in duplicate using a Neubauer hemacytometer. Each treatment was performed in duplicate.

For Hoechst staining, primary human preadipocytes grown on coverslips were placed in serum-free medium (control or MacCM) supplemented with either 10 μg/ml cycloheximide (CHX; Calbiochem), 10 ng/ml recombinant human TNF-α (R&D Systems), or both, for 6 h to induce apoptosis (Fischer-Posovszky et al., 2011a; Fischer-Posovszky et al., 2004; Tchoukalova et al., 2007). Cells were then fixed in 10% formaldehyde for 1 h, followed by staining for 10 min with 1 μg/ml Hoechst 33342 in a humid chamber. Individual coverslips were mounted onto glass slides using Moviol. Cells were visualized and photographed (400 x mag) with a Zeiss Axio Imager.M1 microscope equipped with an Axiocam HRm digital camera (Carl Zeiss, Toronto, Canada). Ten random fields, equivalent to a minimum of approximately 200 cells, were photographed for each of the three coverslips used per treatment. Percent apoptosis was calculated by dividing the total number of apoptotic nuclei by the total number of nuclei (counted by two independent observers), multiplied by 100.

RT-PCR.

J774A.1 macrophages were treated with 100 ng/ml LPS or vehicle (0.1% HBSS) for 2 or 6 h. RNA, extracted with Qiazol (Qiagen; Missisauga, ON), was processed and analyzed by RT-PCR as described (Ide et al., 2011). Data were analyzed using Light Cycler Software 3.0 (Roche; Mannheim, Germany), and are expressed as the fold increase of the relative quantification (RQ) of LPS-treated cells vs. time-matched controls. TNF-α-specific primer pairs were: forward, 5'-ACGGCATGGATCTCAAAGAC-3', and reverse, 5'-AGATAGCAAATCGGCTGACG-

3', with 18S used as an internal control. The relative expression of PDGF A and B mRNA was calculated by comparing the RQ values for each gene, normalized to 18S, in untreated J774A.1 macrophages. Primer pairs for PDGF were: PDGF A forward, 5'-GGAGCCAGGTGGACCCCACA-3', and reverse, 5'-TGGCCACCTTGACACTGCGG-3'; and PDGF B forward, 5'-CCACTCCATCCGCTCCTTT-3', reverse, 5'-AAGTCCAGCTCAGCCCCAT-3'.

MD-macrophages, treated with 100 ng/ml LPS or 20 ng/ml IL-4 for 24 h, were processed for RT-PCR analysis, as above. TNF-α-specific primer pairs were: forward, 5'-GCCCCCAGAGGGAAGAGTTCCC-3', and reverse, 5'-CAGCTCCACGCCATTGGCCA-3'. CD206-specific primer pairs were: forward, 5'-GGAAGGCGGTGACCTCACAAGT-3', and reverse, 5'-TGCCCAGTACCCATCCTTGCCTT-3'. 18S was used as an internal control.

ELISA.

PDGF BB content in basal J774A.1- and LPS-J774A.1-MacCM (prepared following treatment with 100 ng/ml LPS or vehicle for 2 or 6 h in serum-free medium) was assayed using the Quantikine mouse/rat PDGF-BB ELISA (R&D Systems). TNF-α and IL-1β were quantified in THP-1-MacCM using Quantikine human IL-1β and human TNF-α ELISA (R&D Systems).

Statistical analysis.

One-way ANOVA followed by the post-hoc Newman Keuls test was used to assess differences between means using GraphPad InStat v3.05 (GraphPad Software Inc., San Diego, CA). For imatinib studies, two-way ANOVA followed by the post-hoc Tukey's test was used. A value of $P<0.05$ was considered significant.

Results

Pro-inflammatory macrophage activation reduces the survival activity of J774A.1-MacCM

We previously reported that J774A.1-MacCM, in a PDGF-dependent manner, inhibits apoptosis of serum-deprived 3T3-L1 preadipocytes, and this was documented by cell enumeration, Hoescht staining, and annexin V detection by flow cytometry (Molgat et al., 2009, 2011). We have now investigated, for the first time, the effect of pro-inflammatory macrophage activation, induced by LPS treatment, on the preadipocyte survival activity of MacCM. As before, basal J774A.1-MacCM prevented serum withdrawal-induced death of 3T3-L1 preadipocytes, assessed by enumeration of viable cells (Fig. 1A). Addition of LPS to J774A.1 macrophages for 6 h prior to the conditioning period inhibited survival activity of the MacCM by 50% (Fig. 1A). Shorter durations of LPS treatment were less effective.

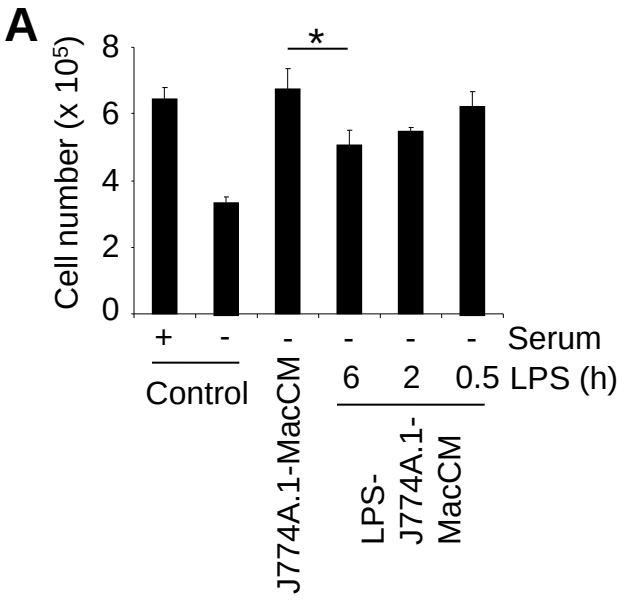
A
Cell number (x 10^5)
8
6
4
2
0
*
+
-
-
-
-
-
Serum
Control
6
2
0.5
LPS (h)
J774A.1-MacCM
LPS-J774A.1-MacCM

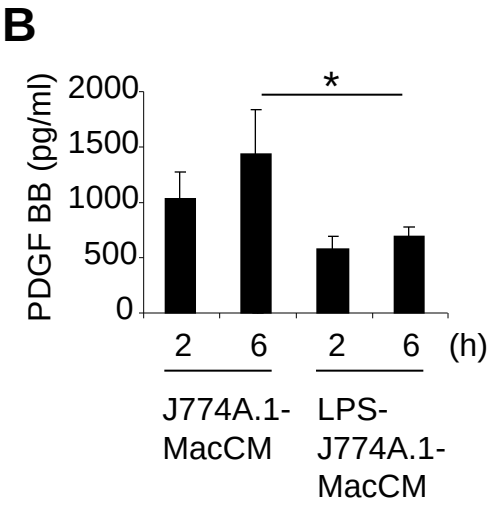
B
PDGF BB (pg/ml)
2000
1500
1000
500
0
*
2
6
2
6
(h)
J774A.1-MacCM
LPS-J774A.1-MacCM

Figure 1. Pro-inflammatory macrophage activation, PDGF release, and survival activity of J774A.1-MacCM. (A) 3T3-L1 preadipocytes were incubated for 6 h in serum-free control medium, J774A.1 MacCM, or LPS-J774A.1 MacCM generated by LPS pre-treatment of macrophages for the times indicated. Viable adherent cells (trypan blue negative) were enumerated and expressed as mean cell number ± SEM. n=4, **P*<0.05. (B) PDGF BB in J774A.1-MacCM or LPS-J774A.1-MacCM, treated with vehicle or LPS for the indicated period of time prior to preparation of MacCM, was quantified by ELISA. Data are expressed in pg/ml. n=3; **P*<0.05.

To investigate the mechanism by which LPS reduces the pro-survival activity of MacCM, we measured the amount of PDGF released into J774A.1-MacCM, since its ability to suppress preadipocyte apoptosis is dependent on this growth factor (Molgat et al., 2009). RT-PCR comparative cycle number analysis indicated PDGF B mRNA is 19-fold more abundant than PDGF A in unactivated macrophages (data not shown), in agreement with other observations (Nagaoka et al., 1992). J774A.1-MacCM contained 1034 or 1443 pg/ml of PDGF BB, following 2 or 6 h of vehicle treatment, respectively (Fig. 1B). Treatment of macrophages with LPS for 2 or 6 h decreased PDGF BB levels in the MacCM by 44 or 52%, respectively (Fig. 1B).

Given the lower level of PDGF protein released by the J774A.1 macrophages in response to LPS, we determined whether the reduced survival activity of LPS-J774A.1-MacCM might be due to attenuated PDGF signaling in 3T3-L1 preadipocytes. We examined the phosphorylation responses of PDGFR, Akt, and ERK1/2, since we have previously reported that these pathways mediate the pro-survival effect of MacCM (Molgat et al., 2011). There was no difference in PDGFR or Akt phosphorylation in response to LPS-J774A.1-MacCM vs. J774A.1-MacCM (Fig. 2A). Therefore, LPS-J774A.1-MacCM survival signaling in preadipocytes, as assessed by these two PDGFR-dependent parameters, was unaffected despite the LPS-associated reduction of PDGF protein levels in the MacCM (Fig. 1B).

ERK1/2 phosphorylation in 3T3-L1 preadipocytes treated with LPS-J774A.1-MacCM vs J774A.1-MacCM was actually enhanced (Fig. 2A). The augmented ERK1/2 signaling with LPS-J774A.1-MacCM was not altered by pre-treating preadipocytes with

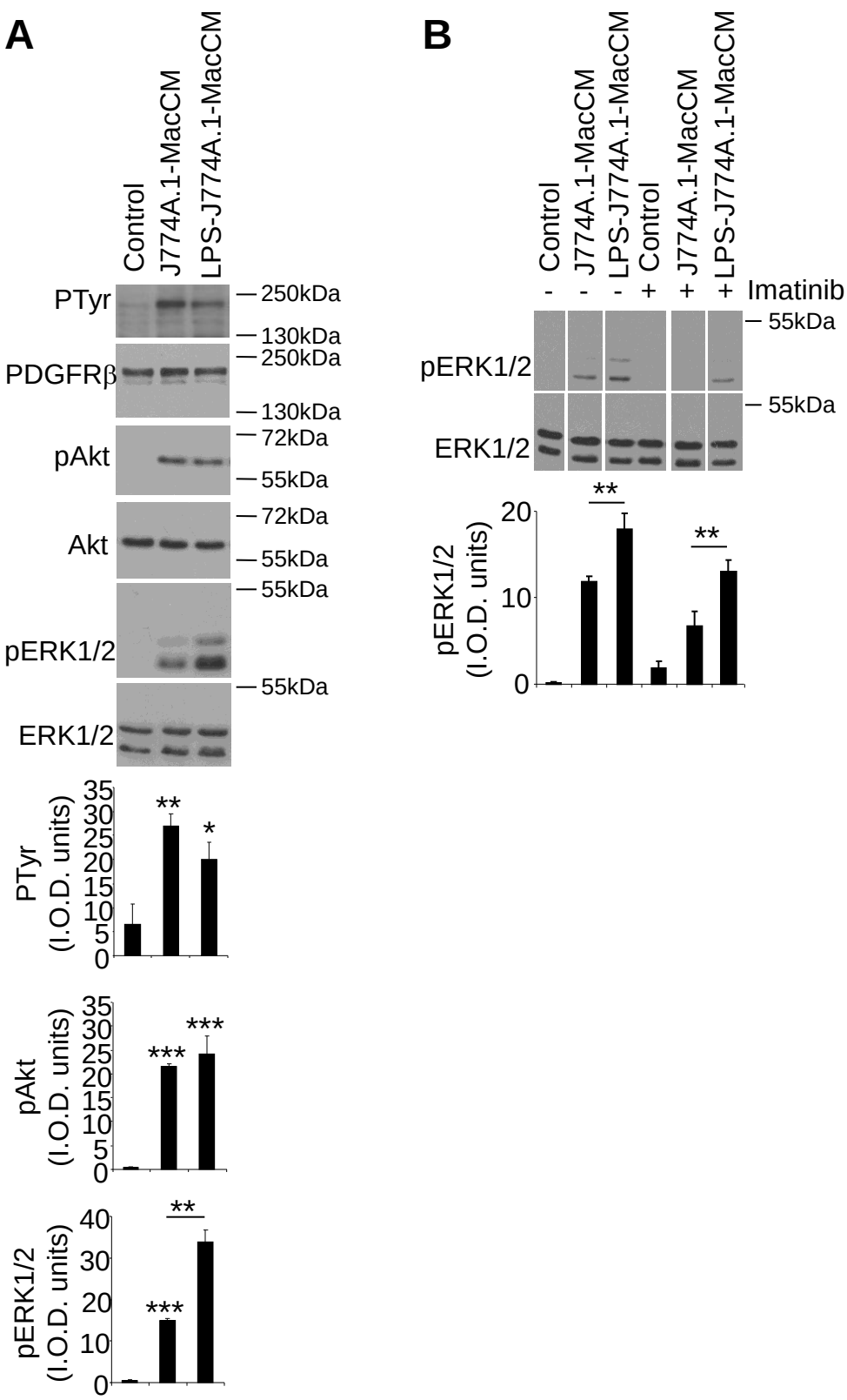
A
Control
J774A.1-MacCM
LPS-J774A.1-MacCM
PTyr
250kDa
130kDa
PDGFRβ
250kDa
130kDa
pAkt
72kDa
55kDa
Akt
72kDa
55kDa
pERK1/2
55kDa
ERK1/2
55kDa
PTyr (I.O.D. units)
35
30
25
20
15
10
5
0
**
*
pAkt (I.O.D. units)
35
30
25
20
15
10
5
0
***
***
pERK1/2 (I.O.D. units)
40
30
20
10
0
**
***
B
Control
J774A.1-MacCM
LPS-J774A.1-MacCM
Control
J774A.1-MacCM
LPS-J774A.1-MacCM
- - - + + +
Imatinib
pERK1/2
55kDa
ERK1/2
55kDa
pERK1/2 (I.O.D. units)
20
10
0
**
**

Figure 2. LPS-J774A.1-MacCM, PDGF signaling and 3T3-L1 preadipocyte death. 3T3-L1 preadipocytes, pretreated or not with 10 μM imatinib, as in indicated, were incubated for 15 min in serum-free control medium, J774A.1-MacCM, or LPS-J774A.1-MacCM (generated by LPS pretreatment of macrophages for 6 h). Whole cell lysates were immunoblotted with the indicated antibodies. n=3 (A), n=4 (B), **P*<0.05, ***P*<0.01, ****P*<0.001 vs. control medium, or indicated pairs.

imatinib (Fig. 2B), suggesting PDGF was not responsible for the enhanced ERK1/2 signal.

LPS-induced macrophage TNF-α production reduces the survival activity of J774A.1-MacCM

Since PDGF survival signaling remained intact in LPS-J774A.1-MacCM, we considered whether a pro-apoptotic factor was induced by LPS treatment. A 20- or 40-fold increase in TNF-α mRNA expression in J774A.1 macrophages occurred by 2 or 6 h of LPS treatment, respectively (data not shown). TNF-α promotes 3T3-L1 preadipocyte apoptosis when added to standard cell culture medium (Niesler et al., 2000). Therefore, we determined whether LPS-induced TNF-α was responsible for the inhibition of MacCM pro-survival activity using an immunoneutralization strategy.

In this case, LPS-J774A.1-MacCM was collected after 24 h of 10 ng/ml LPS treatment, and then added to 3T3-L1 preadipocytes. A similar increase in phosphorylation of PDGFR, Akt, and ERK1/2 occurred with this LPS protocol (Fig. 3A vs. Fig. 2A). LPS alone had no effect on 3T3-L1 preadipocyte signaling (Fig. 3A) or survival (data not shown). LPS-J774A.1-MacCM inhibited the pro-survival effect of unstimulated J774A.1-MacCM by 62%, and TNF-α immunoneutralization almost fully restored the pro-survival activity to 89% of the basal J774A.1-MacCM effect (Fig. 3B). The anti-TNF-α antibody alone had no effect on cell death induced by serum withdrawal in the presence or absence of LPS (data not shown). When TNF-α was added to basal J774A.1-MacCM (no LPS treatment), it inhibited the ability of MacCM to suppress preadipocyte cell death (Fig. 3C). Therefore, TNF-α appears to be a critical component of

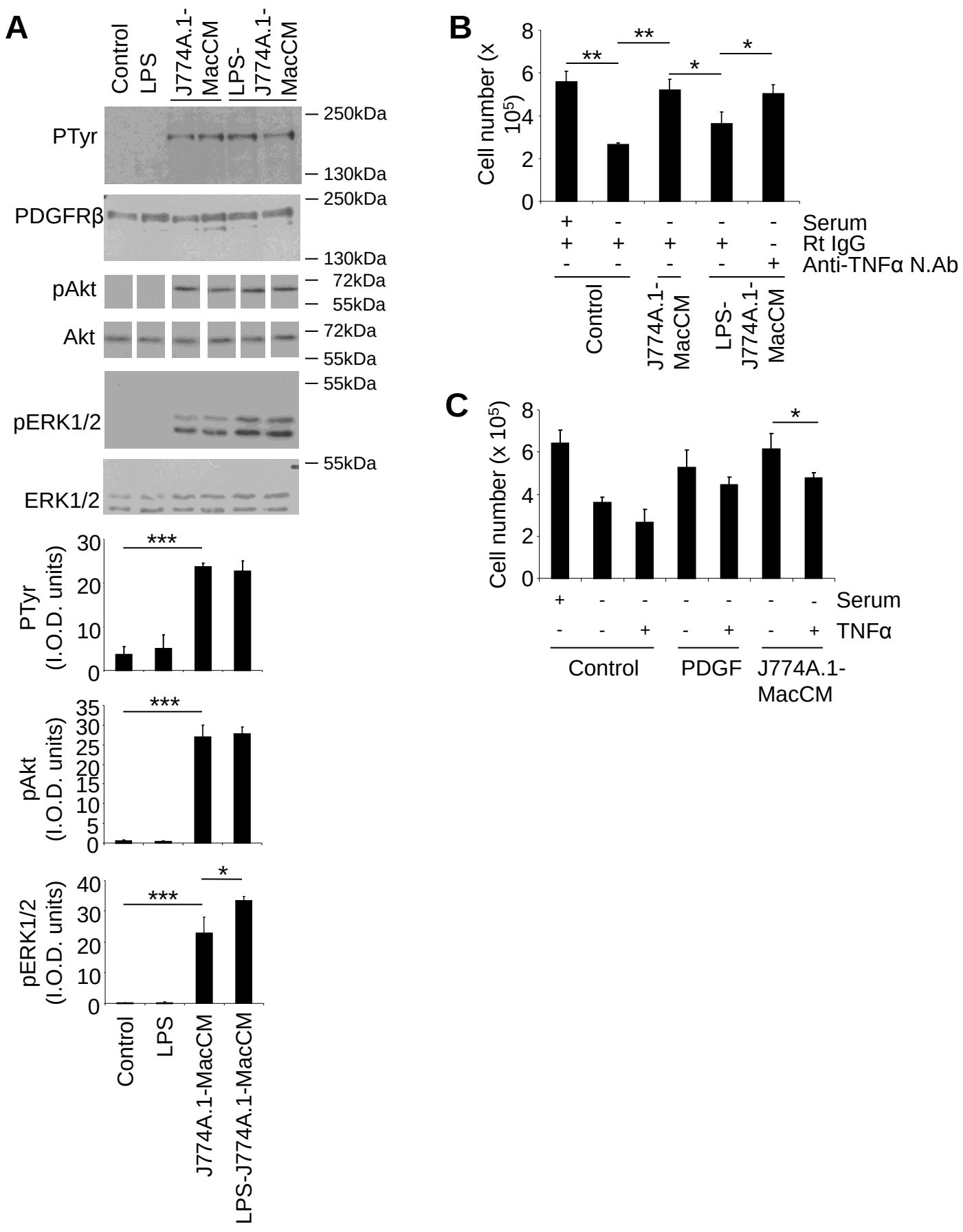
A
Control
LPS
J774A.1-MacCM
LPS-J774A.1-MacCM
PTyr
PDGFRβ
pAkt
Akt
pERK1/2
ERK1/2
250kDa
130kDa
72kDa
55kDa
PTyr (I.O.D. units)
pAkt (I.O.D. units)
pERK1/2 (I.O.D. units)
***
*
Control
LPS
J774A.1-MacCM
LPS-J774A.1-MacCM
B
Cell number (x 10^5)
**
*
Serum
Rt IgG
Anti-TNFα N.Ab
Control
J774A.1-MacCM
LPS-J774A.1-MacCM
C
Cell number (x 10^5)
Serum
TNFα
Control
PDGF
J774A.1-MacCM

Figure 3. LPS-induced macrophage TNF-α and survival activity of MacCM. (A) 3T3-L1 preadipocytes were incubated for 15 min in serum-free control medium, LPS-control medium, J774A.1-MacCM, or LPS-J774A.1-MacCM, prepared following 24 h incubation with 10 ng/ml LPS. Whole cell lysates were immunoblotted with the indicated antibodies. n=3, **P*<0.05, ****P*<0.001. (B) 3T3-L1 preadipocytes were incubated for 6 h in serum-free control medium, J774A.1-MacCM, or LPS-J774A.1-MacCM, following preincubation of the media with anti-TNF-α neutralizing antibody or control non-specific rat IgG. Viable adherent cells (trypan blue negative) were enumerated and data expressed as mean cell number ± SEM. n=3, **P*<0.05, ***P*<0.01. (C) 3T3-L1 preadipocytes were incubated for 6 h with serum-free control medium, 20 ng/ml PDGF BB, or J774A.1-MacCM, each supplemented or not with 10 ng/ml TNF-α. Viable adherent cells (trypan blue negative) were enumerated and data expressed as mean cell number ± SEM. n=3, **P*<0.05.

the LPS-J774A.1-MacCM that overcomes the pro-survival effect of the J774A.1 macrophage-derived PDGF on 3T3-L1 preadipocytes. TNF-α, when added to J774A.1-MacCM, is also sufficient to mimic the negative effect of LPS-J774A.1-MacCM on 3T3-L1 preadipocyte survival.

MD-MacCM promotes the survival of human primary preadipocytes

We evaluated whether the MacCM pro-survival effect observed with the J774A.1 and 3T3-L1 cell line models extends to interactions between human monocyte-derived macrophages and human stromal-vascular preadipocytes. However, compared to 3T3-L1 preadipocytes, human preadipocytes are much less susceptible to apoptosis induced solely by serum withdrawal (Papineau et al., 2003). To induce adequate cell death, it was necessary to supplement the serum-free medium with CHX and TNF-α, apoptotic inducers used together by others (Fischer-Posovszky et al., 2011a; Fischer-Posovszky et al., 2004; Tchoukalova et al., 2007). An approximate 20-fold induction of human preadipocyte apoptosis occurred with this combination (Fig. 4A).

To investigate whether MacCM from primary macrophages would reduce preadipocyte apoptosis, we differentiated human blood monocytes into macrophages over 7 or 14 days in 10% FBS, and then conditioned serum-free medium for 24 h. This MD-MacCM suppressed human preadipocyte apoptosis by either 41 or 55%, respectively (Fig. 4B). A similar 36 or 55% suppression of apoptosis was also observed with MD-MacCM generated from macrophages that were differentiated as above but supplemented with M-CSF (Fig. 4B). Therefore, we have established for the first time that the pro-

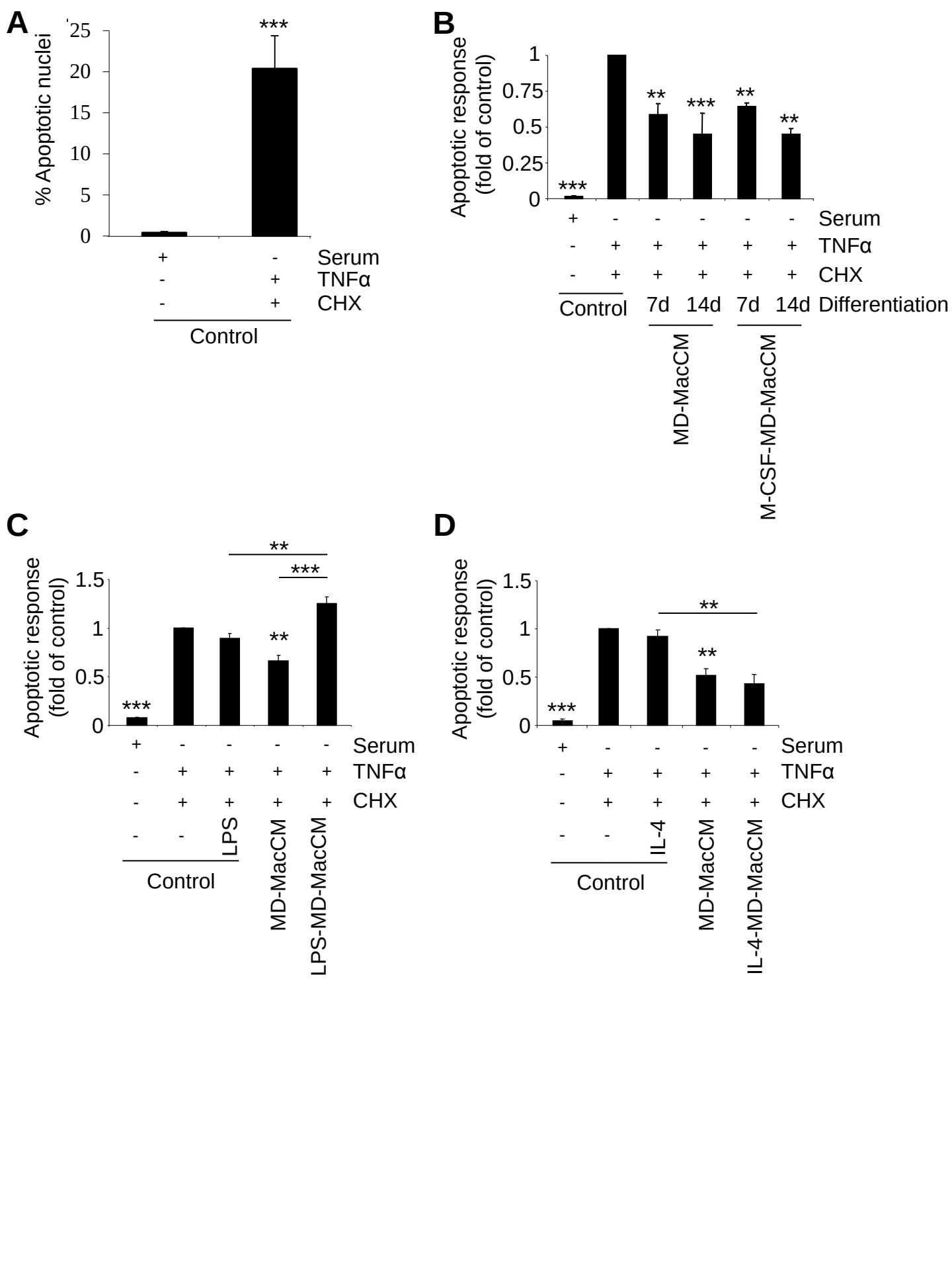
A
% Apoptotic nuclei
25
20
15
10
5
0
***
+ -
- +
- +
Serum
TNFα
CHX
Control
B
Apoptotic response (fold of control)
1
0.75
0.5
0.25
0
***
**
***
**
**
+ - - - - - Serum
- + + + + + TNFα
- + + + + + CHX
Control
7d
14d
7d
14d
Differentiation
MD-MacCM
M-CSF-MD-MacCM
C
Apoptotic response (fold of control)
1.5
1
0.5
0
**
***
***
**
+ - - - - Serum
- + + + + TNFα
- + + + + CHX
- - LPS
Control
MD-MacCM
LPS-MD-MacCM
D
Apoptotic response (fold of control)
1.5
1
0.5
0
**
***
**
+ - - - - Serum
- + + + + TNFα
- + + + + CHX
- - IL-4
Control
MD-MacCM
IL-4-MD-MacCM

Figure 4. MD-MacCM survival activity and human preadipocytes. (A) Human primary preadipocytes were incubated for 6 h with serum-containing or serum-free medium supplemented with 10 μg/ml CHX and 10 ng/ml TNF-α, as indicated. Cell death was assessed by quantification of Hoechst-stained apoptotic nuclei. n=9, ***P<0.001. (B) Human primary preadipocytes were induced to undergo apoptosis as described in (A), in the presence of control medium or MD-MacCM, prepared following differentiation of human blood monocytes for 7 or 14 days in serum-containing medium supplemented or not with M-CSF. Cell death was assessed as in (A). Data are expressed as the fold of the control apoptotic response ± SEM. n=4; **P<0.01, ***P<0.001 vs. serum-free control. (C,D) Human primary preadipocytes were induced to undergo apoptosis as described in (A) in the presence of MD-MacCM that was either unactivated, or activated with either LPS (C) or IL-4 (D). Cell death was assessed as in (A). Data are expressed as the fold of the control apoptotic response ± SEM. n=3. **P<0.01 and ***P<0.001 vs. serum-free control, or indicated pairs.

survival effect of macrophages on preadipocytes that occurs in murine cell lines is valid for primary human cells.

We examined whether the pro-survival effect on preadipocytes might be altered by macrophages that were in a pro-inflammatory M1 versus anti-inflammatory M2 macrophage activation state. Either 100 ng/ml LPS (M1) or 20 ng/ml IL-4 (M2) was added to serum-free medium during the 24 h conditioning period, resulting in a 5-fold increase in TNF-α mRNA ($P<0.05$) or a 4-fold increase in CD206 mRNA ($P<0.01$), respectively. LPS-MD-MacCM not only lost its pro-survival effect, it exacerbated preadipocyte apoptosis by 1.4-fold (Fig. 4C). In contrast, IL-4-MD-MacCM and basal MD-MacCM had similar pro-survival activities towards human preadipocytes (Fig. 4D). Neither LPS nor IL-4, when added alone to control medium, affected human preadipocyte viability.

Discussion

Proliferation and differentiation of preadipocytes are influenced by macrophage-secreted factors (Constant et al., 2006; Ide et al., 2011; Lacasa et al., 2007; Maumus et al., 2008). We have studied another cell fate, survival, and have previously reported that MacCM from J774A.1 macrophages protects 3T3-L1 preadipocytes from apoptosis in a PDGF-dependent manner, measured by cell enumeration, Hoescht staining, and annexin V detection by flow cytometry (Molgat et al., 2009, 2011). Here, we report that pro-inflammatory macrophage activation reduces the pro-survival activity of J774A.1-MacCM for 3T3-L1 preadipocytes. Furthermore, we have now demonstrated that human

primary monocyte-derived macrophages exert a similar anti-apoptotic effect on human primary preadipocytes that is also dependent on state of macrophage activation.

MacCM from LPS-treated versus basal J774A.1 macrophages displayed a reduced preadipocyte pro-survival activity. This occurred despite the ability of LPS-J774A.1-MacCM to fully activate PDGFR signaling pathways. The steady level of PDGF signaling, despite the reduced levels of PDGF, is consistent with the notion that PDGF levels produced by LPS-treated J774A.1 macrophages exceed a threshold concentration of PDGF sufficient for complete receptor activation and downstream signaling in 3T3-L1 cells. The pro-inflammatory state was associated with a significant upregulation of TNF-α. This cytokine is expressed at very low levels in J774A.1 cells under basal conditions, and is rapidly upregulated by LPS to reach concentrations in the ng/ml range (Jozefowski et al., 2010; Telepnev et al., 2003). Exogenous addition of TNF-α in this concentration range was sufficient to inhibit the anti-apoptotic effect of J774A.1-MacCM on 3T3-L1 preadipocytes. Immunoneutralization of TNF-α in the MacCM demonstrated this cytokine is responsible for the inhibition of the pro-survival activity. Our data indicate that TNF-α interferes with the pro-survival effect of PDGF in the context of murine macrophage and preadipocyte models. This action on preadipocyte fate may potentially represent another mechanism by which TNF-α, emanating either from activated macrophages or inflamed hypertrophied adipocytes *in vivo*, can act as a local adipostat to limit adipose tissue expansion (Skolnik and Marcusohn, 1996; Zhang et al., 2001).

Until now, our investigations on the pro-survival effect of MacCM on preadipocytes were based on studies using mouse 3T3-L1 preadipocytes and mouse macrophage cell models (Molgat et al., 2009, 2011). Here, we have taken the important

step to demonstrate that human MD-MacCM also prevents apoptosis of human preadipocytes. Compared to 3T3-L1 preadipocytes, human preadipocytes are relatively resistant to apoptosis induced by serum deprivation (Papineau et al., 2003). Therefore, we used an apoptotic trigger that consists of serum deprivation in the presence of CHX and TNF-α (Fischer-Posovszky et al., 2011a; Fischer-Posovszky et al., 2004; Tchoukalova et al., 2007). TNF-α activates the extrinsic apoptosis pathway through caspase 8 activation; versus the intrinsic mitochondria-dependent apoptotic pathway induced by serum deprivation. CHX treatment inhibits pro-survival protein synthesis and has been shown to promote the association of caspase 8 with the TNF receptor, which enhances the death-inducing activity of TNF-α (Chau et al., 2011). In preadipocytes, CHX has been shown to selectively downregulate FLICE-like inhibitory protein, enhancing the sensitivity of these cells to death ligand-dependent apoptosis (Fischer-Posovszky et al., 2011a). Our finding that MD-MacCM is capable of preventing CHX/TNF-α- and serum deprivation–dependent preadipocyte apoptosis suggests it impedes intrinsic and extrinsic apoptotic pathways.

The significant suppression of apoptosis of human preadipocytes by basal MD-MacCM was absent in LPS-MD-MacCM. Therefore, as for J774A.1 macrophages, pro-inflammatory M1 activation of MD-macrophages interferes with the pro-survival effect of MD-MacCM. Moreover, in the case of LPS-MD-MacCM, an augmentation of human preadipocyte apoptosis was observed, possibly arising from differences in the primary human macrophage model, from the higher LPS concentration used, or from the exogenous TNF-α already present in the apoptosis-induction medium. The effect of an anti-inflammatory M2 stimulus on MD-macrophages was studied using IL-4 (Gordon and

Martinez, 2010). IL-4-activated MD-MacCM or basal untreated MD-MacCM each exerted similar anti-apoptotic effects on human preadipocytes. Therefore, the influence of MD-MacCM on human preadipocyte apoptosis appears to be activation-dependent, as observed with J774A.1-MacCM.

Future investigations will be necessary to elucidate the pro-survival mechanism in greater detail. As an initial step, we have determined that Akt and ERK1/2 activation occurs in human preadipocytes in response to MD-MacCM (n=3, data not shown). These signaling responses were unaffected by the activation state of the macrophages, consistent with what we observed for the murine macrophage-preadipocyte studies. It will be important to directly assess whether Akt and ERK1/2 are implicated in MD-MacCM-dependent human preadipocyte survival, and to identify the pro-survival factor(s) secreted by human macrophages in the basal or IL-4-treated state. Furthermore, the basis of the blockade of the pro-survival effect of LPS-MD-MacCM on human preadipocytes remains to be determined. As noted, in contrast to the 3T3-L1 model in which apoptosis was triggered with serum-deprivation alone, a more complex apoptotic induction was required for the human preadipocytes. The ability of basal and IL-4-treated human MD-MacCM to protect human preadipocytes from death, despite the presence of exogenous TNF-α in the treatment medium, will require further investigation. For example, human MD-macrophages may secrete a variety of pro-survival factors.

In contrast to the anti-apoptotic effect of MD-MacCM that we observed with primary human preadipocytes, a pro-apoptotic effect of THP-1-MacCM with the Simpson-Golabi-Behmel syndrome human preadipocyte model has been described (Keuper et al., 2011). Several reasons might account for this difference. The

differentiation of THP-1 macrophages with 200 nM phorbol myristate acetate by that group occurred over 48 h, and elevated mRNA expression of IL-6, IL-1β, and TNF-α was noted, indicative of a pro-inflammatory state. We have generated THP-1-MacCM derived from THP-1 macrophages that were differentiated with 100 nM TPA over 24 h, and observed a 30 % reduction in human preadipocyte apoptosis. With respect to cytokines released, our THP-1-MacCM contained similar levels of IL-1β (447 ± 59 pg/ml, n=3), but levels of TNF-α (21 ± 10 pg/ml TNF-α, n=3) were much lower compared to the ng/ml levels observed by Keuper et al. We do note that different commercial ELISA systems were used, and perhaps that may have contributed in part to the variation in TNF-α values. In addition, compared to the primary human preadipocytes used in our studies, Simpson-Golabi-Behmel syndrome preadipocytes have a greater adipogenic capacity and higher sensitivity to apoptosis (Fischer-Posovszky et al., 2004).

Macrophage activation states could potentially alter the balance between adipocyte hypertrophy and hyperplasia through the control of preadipocyte survival and/or cell number. Hypertrophic adipose tissue growth is associated with insulin resistance and adipose tissue inflammation; whereas hyperplastic growth maintains adipose tissue insulin sensitivity. Our novel data, demonstrating pro-inflammatory activation interferes with the anti-apoptotic activity of macrophages, are derived from cell culture models. Future studies are needed to address whether preadipocyte survival is regulated by adipose tissue macrophages *in vivo*, and whether the pro-inflammatory activation of ATMs in the pathological state of obesity regulates preadipocyte viability.

Funding

This work was supported by Heart and Stroke Foundation of Canada (Ontario) grant-in-aid NA6634 to A.S. A.S.D.M. is the recipient of an Alexander Graham Bell Canada Doctoral Research Scholarship from the National Sciences and Engineering Research Council of Canada.

Acknowledgements

We thank the patients and surgeons of The Ottawa Hospital for their participation in this study.

5.0 GENERAL DISCUSSION

SUMMARY OF RESEARCH FINDINGS

My research has revealed a novel function of macrophage-secreted factors in the prevention of preadipocyte apoptosis, advancing our understanding of this complex paracrine interaction (summarized in Figure 5.1). Using MacCM from three tumor cell lines (RAW264.7, J774A.1, and THP-1), and primary cells (murine BMD-macrophages and human MD-macrophages), I have observed inhibition of apoptosis in both murine 3T3-L1 preadipocytes and human primary preadipocytes. Apoptosis was quantified using several assays of cell death, including enumeration of viable adherent cells, Hoechst staining of apoptotic nuclei, and Annexin V/PI staining. Suppression of preadipocyte apoptosis was associated with MacCM-dependent activation of Akt and ERK1/2 signaling in both the 3T3-L1 and human preadipocyte models. PDGF/PDGFR, Akt, ERK1/2, and ROS were shown to be required for the survival of 3T3-L1 preadipocytes by J774A.1-MacCM. Finally, I have demonstrated that the activation state of the macrophage alters their ability to prevent preadipocyte apoptosis. Pro-inflammatory macrophages that were activated with LPS failed to suppress preadipocyte death, whereas anti-inflammatory macrophages that were activated with IL-4 retained pro-survival function.

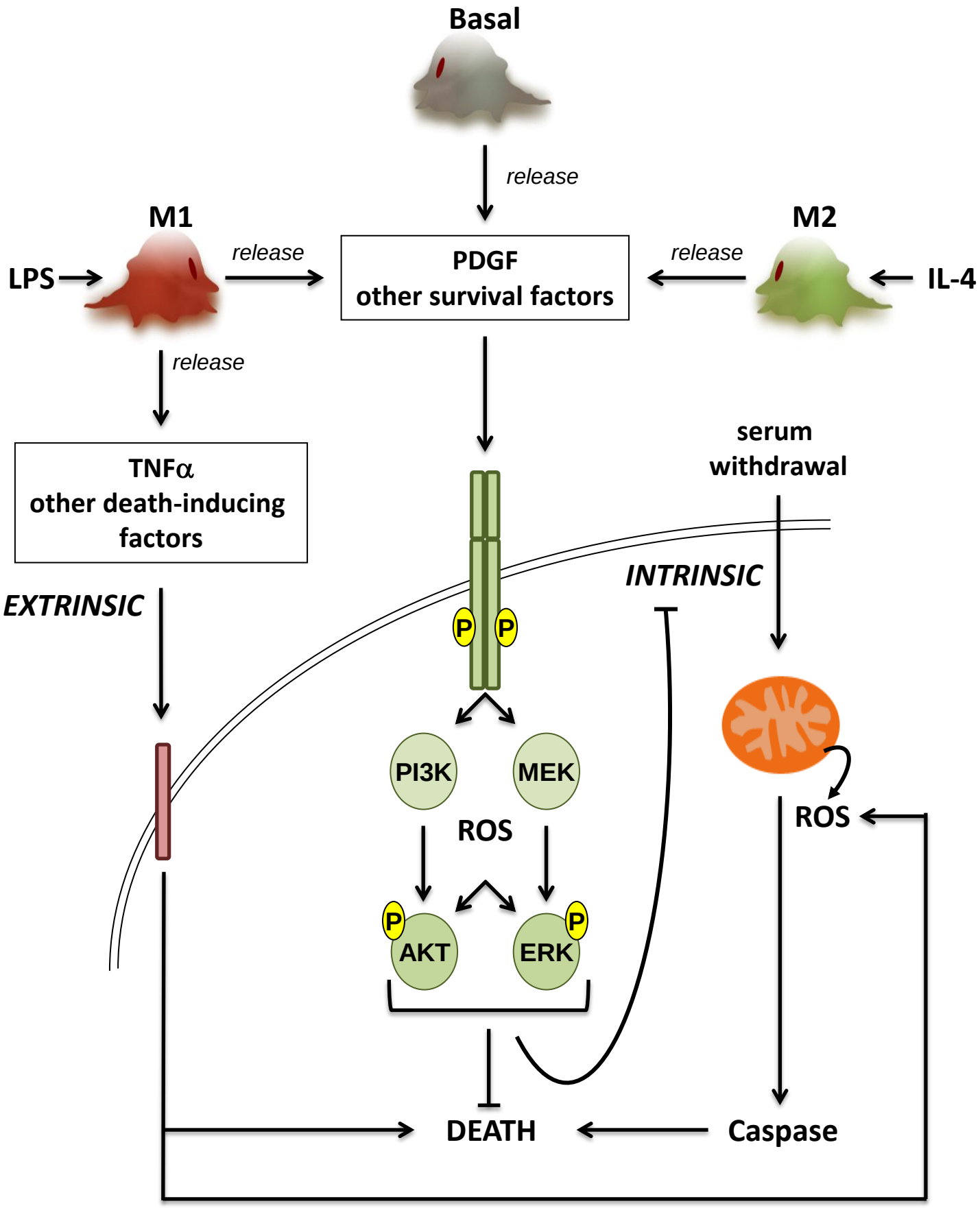
Basal
release
M1
LPS
release
PDGF
other survival factors
release
M2
IL-4
release
TNFα
other death-inducing
factors
serum
withdrawal
EXTRINSIC
INTRINSIC
P
P
PI3K
MEK
ROS
ROS
P
AKT
ERK
P
DEATH
Caspase

Figure 5.1 Proposed model of the anti-apoptotic effect of macrophage-secreted factors on preadipocytes. In the absence of macrophage-secreted factors, serum-withdrawal or TNF-α stimulation leads to preadipocyte death via intrinsic and extrinsic apoptosis pathways, respectively. In the presence of macrophage-secreted factors, derived from unactivated or IL-4-activated macrophages, pro-survival signaling pathways (PI3K/Akt, MEK/ERK1/2, and ROS) are activated resulting in maintained preadipocyte survival. In murine cells, macrophage-secreted PDGF is necessary for the activation of these pro-survival events. When macrophage-secreted factors derived from LPS-activated macrophages are present, despite the presence of pro-survival factors, TNF-α-mediated apoptosis is potentiated resulting in preadipocyte death.

MacCM stimulated Akt and ERK signaling

The first indication that macrophage-secreted factors may influence preadipocyte survival responses came from the observed activation of survival kinases, Akt and ERK1/2, following exposure to MacCM. Akt is activated by growth factors in a PI3K-dependent pathway involving mTOR-mediated phosphorylation of Ser473 and PDK1-mediated phosphorylation of Thr308. ERK1/2 is activated by phosphorylation of Thr202 and Tyr204 by MEK1/2. Akt phosphorylation of Ser473 and ERK1/2 phosphorylation of both sites was observed in 3T3-L1 and human primary preadipocytes following incubation with J774A.1-MacCM and MD-MacCM, respectively. Several studies have examined the influence of macrophages on Akt and ERK1/2 signaling in preadipocytes, and others have reported variable effects of MacCM on the phosphorylation of these kinases in differentiated adipocytes and other cell types.

In differentiated 3T3-L1 adipocytes, Lumeng et al. reported unactivated J774A.1-MacCM did not affect basal or insulin-stimulated Akt phosphorylation (Lumeng et al., 2007c). Pro-inflammatory LPS-J774A.1-MacCM, however, significantly suppressed the insulin-stimulated response. Pro-inflammatory LPS-THP-1-MacCM was also seen to suppress insulin-stimulated Akt phosphorylation in both undifferentiated and differentiated 3T3-L1 cells (Moreno-Navarrete et al., 2009). In SGBS adipocytes, differentiated from a highly proliferative and adipogenic human preadipocyte cell line isolated from the adipose tissue of a patient with Simpson-Golabi-Behmel syndrome, Keuper et al. reported a significant reduction of basal and insulin-stimulated Akt phosphorylation in the presence of untreated THP-1-MacCM. Characterization of the

MacCM cytokine content revealed elevated levels of TNF-α, indicating pro-inflammatory activation of the THP-1 cells (Keuper et al., 2011). Therefore, whereas my data suggest MacCM stimulates Akt phosphorylation in undifferentiated preadipocytes, MacCM may suppress Akt phosphorylation in differentiated adipocytes and preadipocytes, co-treated with insulin.

As mentioned, MacCM-dependent Akt phosphorylation responses have also been examined in non-adipose cells. Incubation of C6 myoblasts with RAW264.7-MacCM, following macrophage treatment with palmitic acid, suppressed insulin-dependent Akt phosphorylation, an effect not observed under basal conditions or with unactivated MacCM (Samokhvalov et al., 2009). Robust Akt phosphorylation was reported in CCL39 myofibroblasts exposed to BMD-MacCM, activated or not with either IL-4 or IFNγ (Wynes et al., 2004). Similarly, Akt phosphorylation has been noted in MCF-7 human breast adenocarcinoma cells, and primary murine cerebellar granule cells, incubated with THP-1-MacCM and primary murine microglia-CM, respectively (Lee et al., 2011; Morgan et al., 2004).

ERK1/2 phosphorylation was stimulated in 3T3-L1 preadipocytes treated with either THP-1-monocyte-CM or THP-1-MacCM (Constant et al., 2008); however this stimulatory effect may not persist during the course of 3T3-L1 adipogenesis, or in differentiated SGBS adipocytes (Keuper et al., 2011; Yarmo et al., 2009). ERK1/2 phosphorylation has been reported in direct co-culture experiments between 3T3-L1 adipocytes and RAW264.7 macrophages, though the source of the phosphorylated ERK1/2 was not identified (Suganami et al., 2005). ERK1/2 phosphorylation is

stimulated in MCF-7 and CCL39 cells exposed to THP-1-MacCM and primary murine microglia-CM, respectively (Lee et al., 2011; Morgan et al., 2004).

Therefore, variable effects of MacCM on Akt and ERK1/2 phosphorylation have been reported. This may be due to intrinsic differences in the cell models used, or the activation state of the macrophages. It would appear, however, that macrophages are capable of stimulating Akt and ERK1/2 signaling in a variety of cell types.

Macrophage-dependent PDGFR signaling

The Akt and ERK1/2 signaling responses I observed were not seen following inhibition of the PDGFR in 3T3-L1 preadipocytes; suggesting they are events downstream of PDGFR activation. Two PDGFRs are known, PDGFRα and PDGFRβ, which possess unique ligand specificity and expression patterns (Bonner, 2004). Though preadipocytes express both receptors, the PDGFRβ isoform is most abundant (Vaziri and Faller, 1996). Upon ligand binding, PDGFRs form homo- and heterodimers (α/α, α/β, β/β). PDGF ligands are synthesized from four separate genes: PDGFA, PDGFB, PDGFC, and PDGFD. The products of these four genes produce five PDGF protein isoforms: PDGF-AA, PDGF-AB, PDGF-BB, PDGF-CC, and PDGF-DD, all of which are detectable in most tissues. Ligand specificity follows that PDGFRα/α homodimers are activated following ligation with either PDGF-AA or -CC; PDGFRα/β heterodimers are activated by PDGF-AB, -BB, -CC, and -DD; and PDGFRβ/β homodimers are specifically activated by PDGF-BB and -DD (Fredriksson et al., 2004). PDGF binding to its cognate receptor activates intrinsic tyrosine kinase activity, creating phosphotyrosine

docking sites along the C-terminus of the receptor. PI3K and Grb2 bind to phosphorylated tyrosines on the PDGFR, initiating signaling that leads to Akt and ERK1/2 activation, respectively.

I found J774A.1-MacCM contains ~1ng/ml PDGF-BB, and my own unpublished RT-PCR analysis has shown PDGFB to be the most abundantly expressed PDGF isoform in J774A.1 cells. Macrophage PDGF expression has been previously reported and found to change upon monocyte to macrophage differentiation, as well as with macrophage activation (Allam et al., 1992; Kitamura et al., 2008; Kodelja et al., 1997; Kosaka et al., 1992; Kovacs and Vanstedum, 1995; Li et al., 1994; Nagaoka et al., 1992; Shanker et al., 1995; Song et al., 2000). J774A.1-secreted PDGF-BB has been shown to stimulate osteopontin expression in Swiss 3T3 cells, the parent cell line of 3T3-L1 preadipocytes (Mori et al., 2008). Evidence for murine microglia-secreted bioactive PDGF-BB has also been provided (Morgan et al., 2004). In murine AT, PDGF levels rise with obesity, and are downregulated by macrophage-selective depletion (Pang et al., 2008). This correlation between ATM content and AT PDGF expression is also seen in the sirtuin-1 deficient mouse which has reduced ATM content, and a corresponding lower level of AT PDGF expression (Xu et al., 2012).

In contrast to the activation of PDGF signaling in murine preadipocytes, I have not observed PDGFR phosphorylation in human primary preadipocytes following treatment with human MD-MacCM, despite MD-MacCM-dependent Akt and ERK1/2 signaling. Yarmo et al. previously showed that THP-1-MacCM-dependent signaling in human primary preadipocytes is insensitive to PDGFR-selective inhibition by imatinib (Yarmo et al., 2010). I am unable to detect PDGF-BB protein in MD-MacCM by

immunoassay (unpublished results). These findings suggest that macrophage-dependent pro-survival PDGF signaling may be specific to the mouse, and other as yet unidentified macrophage-derived factors act on human preadipocytes. Nevertheless, the pro-survival function of MacCM could be demonstrated in both murine and human primary preadipocytes.

ROS signaling in cell survival and death

I observed a significant increase in intracellular ROS levels in 3T3-L1 preadipocytes following either serum-withdrawal or incubation with serum-free J774A.1-MacCM. Since serum withdrawal and J744A.1-MacCM induced opposite effects on preadipocyte survival, these results raise the possibility that ROS are implicated in both preadipocyte survival and apoptosis. This hypothesis is supported by my studies using the general ROS inhibitor, DPI, and the anti-oxidant, NAC; both were found to reduce serum withdrawal-dependent apoptosis, and J774A.1-MacCM-dependent survival. The ability of ROS to possess dual functions on cell death and survival may be a result of localized subcellular production. Mitochondria are the major source of ROS produced in a cell, however membrane-localized ROS can also be generated in response to growth factors. Several studies support the concept that distinct pools of ROS may exert distinct functions.

Plasma membrane-localized ROS, generated in response to growth factor receptor stimulation, are produced from membrane-bound NADPH-oxidase (NOX) complexes. Growth factor signaling recruits cytosolic NOX subunits to membrane-bound $gp91^{phox}$, or

one of its homologs. Six gp91^{phox} homologs have been identified in mammalian cells, resulting in seven known NOX complexes (Sumimoto, 2008). The ROS generated by these enzymes are implicated in receptor tyrosine kinase signal transduction, in part through direct inhibition of phosphatase activity (Kwon et al., 2004). In non-adipose cells, PDGF generates intracellular ROS through the activity of NOX 1 and 4, which inactivate the lipid phosphatase PTEN, and the tyrosine phosphatase, protein phosphatase 2A (Kang, 2007). Insulin stimulates ROS production in preadipocytes through NOX4, which regulates preadipocyte proliferation and differentiation (Mouche et al., 2007). 3T3-L1 preadipocytes express three of the seven NOX isoforms (NOX 1, 2, 4) (Furukawa et al., 2004; Schroder et al., 2009). ROS are produced by NOX enzymes in response to growth factors within minutes of stimulation (Mouche et al., 2007).

In contrast, ROS-produced in response to serum-withdrawal are derived largely through mitochondrial generation. ROS modulator 1 (Romo1), a mitochondria-localized transmembrane protein, produces ROS from complex III of the mitochondrial electron transport chain (Chung et al., 2006). Romo1-dependent ROS is responsible for mediating serum withdrawal-induced apoptosis in HEK293, HeLa, and WI-35 VA-13 cells (Lee et al., 2010). The ROS produced in these cells occurred 6 h after treatment, in contrast to the ROS generated within 15 min in 3T3-L1 preadipocytes. This difference may reflect a relatively lower sensitivity to serum withdrawal-induced apoptosis in HEK293, HeLa, and WI-35 VA-13 cells, compared to 3T3-L1 preadipocytes. For example, 50% of HEK293 cells underwent apoptosis after 48 h of serum-withdrawal, whereas I observed a comparable degree of apoptosis with 3T3-L1 preadipocytes, after only 6 h of serum withdrawal.

Although I have not addressed ROS production in human primary preadipocytes undergoing apoptosis induced by extrinsic inducers CHX/TNF-α, ROS have been implicated in mediating extrinsic apoptosis induction (Basuroy et al., 2009). Romo1 has recently been found to generate ROS in response to these apoptotic inducers, with faster kinetics compared to serum withdrawal. Apoptotic induction and Romo1-ROS production was noted 15 minutes following CHX/TNF-α treatment of HEK293 cells (Kim et al., 2010).

Exceptions to the pro-death function of mitochondrial ROS have been reported. Firstly, treatment of adipocytes with insulin stimulates the phosphorylation and mitochondrial translocation of $p66^{Shc}$. There, $p66^{Shc}$ directly generates ROS that mediate downstream insulin-induced lipogenesis (Berniakovich et al., 2008). Secondly, Romo1-dependent ROS, produced in survival-promoting conditions (i.e. in the presence of serum and absence of apoptosis inducers), has been found to be indispensable for ERK1/2 phosphorylation and the proliferation of a variety of cell lines (Na et al., 2008). Additional studies will be necessary to identify the source and target of ROS produced in preadipocytes following serum withdrawal in the presence and absence of MacCM.

Macrophage-dependent preadipocyte survival

In contrast to the suppression of apoptosis in 3T3-L1 preadipocytes and human primary preadipocytes by unactivated or IL-4-MacCM, pro-inflammatory LPS-MacCM failed to support preadipocyte survival, and instead promoted cell death. One other study has examined the effect of MacCM on preadipocyte survival (Keuper et al., 2011). In

their study, Keuper et al. observed an increased rate of apoptosis in SGBS preadipocytes, following 24-72 h incubation with THP-1-MacCM. The model system used in my studies differs in several ways from theirs. Firstly, Keuper et al. used SGBS preadipocytes, a human preadipocyte cell line, whereas I assessed apoptosis in primary human preadipocytes. Of note, the apoptotic sensitivity of SGBS preadipocytes is much higher compared to human primary preadipocytes (Fischer-Posovszky et al., 2004). Secondly, Keuper et al. differentiated THP-1 monocytes into macrophages using 200nM TPA, versus 100nM used in my THP-1 experiments. Thirdly, THP-1 macrophage differentiation occurred over 48 h in the study by Keuper et al., versus 24 h in my study. Lastly, despite not being activated by known pro-inflammatory inducers, the THP-1 macrophages used by Keuper et al. secreted high levels of TNF-α; normally very low or undetectable in these cells. Indeed, although different assays were used, the THP-1-MacCM used in my studies contained approximately three orders of magnitude less TNF-α. The elevated production of TNF-α can be viewed as supporting my hypothesis that pro-inflammatory macrophages lose the ability to suppress preadipocyte apoptosis, and suggests that the pro-survival function of MacCM may be activation-dependent.

MACROPHAGE INVOLVEMENT IN ADIPOSE CELL DEATH

The results of my *in vitro* experiments suggest a close interplay between macrophages and adipose cell death, which is supported by a number of *in vivo* studies. In 2005, Cinti et al. were the first to report evidence of a link between macrophages and dying hypertrophied adipocytes in the AT of obese mice and humans. The dying

adipocytes, morphologically characterized as undergoing necrotic cell death, were surrounded by recruited ATMs, forming a CLS (Cinti et al., 2005). Adipocyte death during AT remodeling correlates with the infiltration of pro-inflammatory ATMs (Strissel et al., 2007). Alkhouri et al. demonstrated that AT of obese mice and humans has more apoptotic cells. Using a Bid-deficient mouse model, inhibition of adipose cell apoptosis was shown to reduce macrophage infiltration, suggesting adipocyte apoptosis governs macrophage recruitment (Alkhouri et al., 2010). Selective deletion of mature adipocytes in adult mice provoked the activation of a mixed-phenotype ATM subpopulation expressing high levels of TNF-α in combination with anti-inflammatory markers; suggesting adipocyte-derived factors regulate macrophage activation (Fischer-Posovszky et al., 2011b). The localization of ATMs around the apoptotic adipocytes suggests this unique subpopulation may be involved in apoptotic adipose cell clearance.

The interplay between adipose cell death and ATMs remains controversial. Using granulocyte-macrophage colony-stimulating factor (GM-CSF)-deficient mice, which contain a reduced number of ATMs in both the lean and obese states, Feng et al. examined the accompanying rate of adipose cell apoptosis. Comparable rates of apoptosis between either lean or obese GM-CSF-deficient and WT mice were found. The dissociation between ATM content and adipose cell apoptosis was further supported using pharmacological ATM depletion. Injection of liposome-encapsulated clodronate, which selectively kills phagocytic cells, did not influence the rate of adipose cell apoptosis in obese mice (Feng et al., 2011). Both of these strategies targeted the entire ATM population. It is possible that pro- and anti-inflammatory macrophages may serve

opposing functions with respect to the regulation of adipose cell survival *in vivo*; a more selective inhibition of ATM subpopulations would be necessary to test this.

Due to the lack of specific preadipocyte markers, it remains uncertain whether the apoptotic adipose cells detected *in vivo* are exclusively adipocytes. Feng et al. reported positive staining for apoptotic cell death in AT sections, in addition to *in vitro* evidence suggesting adipocytes are more prone to necrotic cell death, whereas preadipocytes more readily undergo apoptosis (Feng et al., 2011). It is possible preadipocytes and other stromal cells also undergo cell death *in vivo*, and so contribute to the total pool of apoptotic cells detected in the aforementioned studies.

GENERALIZED SURVIVAL FUNCTION OF MACROPHAGES

The results from my macrophage-preadipocyte *in vitro* experiments raise the question as to whether promoting cell survival may be a generalized function of tissue macrophages. In support of this, pro-survival effects of macrophages on non-adipose cells have been reported. Murine BMD-MacCM, either unactivated or activated with IL-4, was found to suppress CCL39 myofibroblast apoptosis, induced by serum-withdrawal (Wynes et al., 2004). While PDGF-BB was undetectable, BMD-macrophages were found to secrete IGF-1, which was demonstrated to mediate CCL39 survival, in a PI3K-, ERK1/2-dependent manner. Hayashi et al. reported a pro-survival function of rat cortical microglia on retinal ganglion cells, mediated through microglia-secreted ApoE-lipoproteins (Hayashi et al., 2007). Finally, Morgan et al. reported that rat microglia, which secrete a number of other survival factors including: PDGF, basic fibroblast

growth factor, transforming growth factor β, epidermal growth factor, and brain-derived neurotrophic factor, protect cerebellar granule cells from apoptosis, predominantly through the action of PDGF (Morgan et al., 2004). It is interesting to note the various macrophage models used in these studies mediated pro-survival effects through a variety of secreted factors. The different tissue environments, coupled with the reactive nature of the macrophage likely results in a variety of activation states, each capable of secreting different survival factors.

CONCLUSION

The *in vitro* preadipocyte survival function of macrophage-secreted factors raises the possibility that ATMs may function to promote preadipocyte survival *in vivo*. My data suggest that the pro-survival function may be carried out by anti-inflammatory ATMs; whereas, when a pro-inflammatory activation state predominates, the pro-survival function is reduced. AT expansion relies on an adequate number of differentiation-competent preadipocytes to maintain adipocyte function by preventing excessive adipocyte hypertrophy. My results support a model in which a resident population of anti-inflammatory ATMs serves to maintain a healthy population of preadipocytes, permitting AT hyperplasia. With obesity, the local AT environment changes, such that a pro-inflammatory milieu develops, and pro-inflammatory ATMs accumulate. The apoptotic effects of pro-inflammatory cytokines, such as TNF-α, overcome the pro-survival effect of other ATM-derived factors; consequently, preadipocyte survival may no longer be maintained. A loss in functional preadipocytes could contribute to adipocyte hypertrophy

and AT dysfunction - hallmarks of obesity. This study implicates the macrophage as a potential regulator of preadipocyte fate.

6.0 REFERENCES

Alkhouri, N., Gornicka, A., Berk, M.P., Thapaliya, S., Dixon, L.J., Kashyap, S., Schauer, P.R., and Feldstein, A.E. (2010). Adipocyte apoptosis, a link between obesity, insulin resistance, and hepatic steatosis. J Biol Chem 285, 3428-3438.

Allam, M., Martinet, N., Gallati, H., and Martinet, Y. (1992). Differential expression of PDGF A- and B-chain genes and production of AA and AB dimers by activated human blood monocytes. Biochimie 74, 1097-1101.

Alligier, M., Meugnier, E., Debard, C., Lambert-Porcheron, S., Chanseaume, E., Sothier, M., Loizon, E., Hssain, A.A., Brozek, J., Scoazec, J.Y., Morio, B., Vidal, H., and Laville, M. (2012). Subcutaneous adipose tissue remodeling during the initial phase of weight gain induced by overfeeding in humans. J Clin Endocrinol Metab 97, E183-192.

Arase, Y., Hiwasa, T., Hasegawa, R., Nomura, J., Ito, H., and Suzuki, N. (2000). Prevention of v-Ha-Ras-dependent apoptosis by PDGF coordinates in phosphorylation of ERK and Akt. Biochem Biophys Res Commun 267, 33-39.

Armulik, A., Genove, G., and Betsholtz, C. (2011). Pericytes: developmental, physiological, and pathological perspectives, problems, and promises. Dev Cell 21, 193-215.

Arner, E., Westermark, P.O., Spalding, K.L., Britton, T., Ryden, M., Frisen, J., Bernard, S., and Arner, P. (2010). Adipocyte turnover: relevance to human adipose tissue morphology. Diabetes 59, 105-109.

Arner, P., and Spalding, K.L. (2010). Fat cell turnover in humans. Biochem Biophys Res Commun 396, 101-104.

Artemenko, Y., Gagnon, A., Aubin, D., and Sorisky, A. (2005). Anti-adipogenic effect of PDGF is reversed by PKC inhibition. J Cell Physiol 204, 646-653.

Ballif, B.A., and Blenis, J. (2001). Molecular mechanisms mediating mammalian mitogen-activated protein kinase (MAPK) kinase (MEK)-MAPK cell survival signals. Cell Growth Differ 12, 397-408.

Basuroy, S., Bhattacharya, S., Leffler, C.W., and Parfenova, H. (2009). Nox4 NADPH oxidase mediates oxidative stress and apoptosis caused by TNF-alpha in cerebral vascular endothelial cells. Am J Physiol Cell Physiol 296, C422-432.

Baumer, A.T., Ten Freyhaus, H., Sauer, H., Wartenberg, M., Kappert, K., Schnabel, P., Konkol, C., Hescheler, J., Vantler, M., and Rosenkranz, S. (2008). Phosphatidylinositol 3-kinase-dependent membrane recruitment of Rac-1 and p47phox is critical for alpha-platelet-derived growth factor receptor-induced production of reactive oxygen species. J Biol Chem 283, 7864-7876.

Berniakovich, I., Trinei, M., Stendardo, M., Migliaccio, E., Minucci, S., Bernardi, P., Pelicci, P.G., and Giorgio, M. (2008). p66Shc-generated oxidative signal promotes fat accumulation. J Biol Chem 283, 34283-34293.

Bjorbaek, C., and Kahn, B.B. (2004). Leptin signaling in the central nervous system and the periphery. Recent Prog Horm Res 59, 305-331.

Bluher, M. (2010). The distinction of metabolically 'healthy' from 'unhealthy' obese individuals. Curr Opin Lipidol 21, 38-43.

Boden, G. (2009). Endoplasmic reticulum stress: another link between obesity and insulin resistance/inflammation? Diabetes 58, 518-519.

Bonner, J.C. (2004). Regulation of PDGF and its receptors in fibrotic diseases. Cytokine Growth Factor Rev 15, 255-273.

Bonni, A., Brunet, A., West, A.E., Datta, S.R., Takasu, M.A., and Greenberg, M.E. (1999). Cell survival promoted by the Ras-MAPK signaling pathway by transcription-dependent and -independent mechanisms. Science 286, 1358-1362.

Bourlier, V., Zakaroff-Girard, A., Miranville, A., De Barros, S., Maumus, M., Sengenes, C., Galitzky, J., Lafontan, M., Karpe, F., Frayn, K.N., and Bouloumié, A. (2008). Remodeling phenotype of human subcutaneous adipose tissue macrophages. Circulation 117, 806-815.

Bradley, R.L., Fisher, F.F., and Maratos-Flier, E. (2008). Dietary fatty acids differentially regulate production of TNF-alpha and IL-10 by murine 3T3-L1 adipocytes. Obesity 16, 938-944.

Bremer, A.A., Mietus-Snyder, M., and Lustig, R.H. (2012). Toward a unifying hypothesis of metabolic syndrome. Pediatrics 129, 557-570.

Brozek, J., Grande, F., Anderson, J.T., and Keys, A. (1963). Densitometric analysis of body composition: revision of some quantitative assumptions. Ann N Y Acad Sci 110, 113-140.

Buchdunger, E., O'Reilly, T., and Wood, J. (2002). Pharmacology of imatinib (STI571). Eur J Cancer 38, S28-36.

Cannon, B., Hedin, A., and Nedergaard, J. (1982). Exclusive occurrence of thermogenin antigen in brown adipose tissue. FEBS Lett 150, 129-132.

Chau, H., Mirtsos, C., and Huang, H.L. (2011). Regulation of death complexes formation in tumor necrosis factor receptor signaling. Exp Cell Res 317, 1841-1850.

Chen, Z., Torrens, J.I., Anand, A., Spiegelman, B.M., and Friedman, J.M. (2005). Krox20 stimulates adipogenesis via C/EBPbeta-dependent and -independent mechanisms. Cell Metab 1, 93-106.

Chung, Y.M., Kim, J.S., and Yoo, Y.D. (2006). A novel protein, Romo1, induces ROS production in the mitochondria. Biochem Biophys Res Commun 347, 649-655.

Cinti, S., Mitchell, G., Barbatelli, G., Murano, I., Ceresi, E., Faloia, E., Wang, S., Fortier, M., Greenberg, A.S., and Obin, M.S. (2005). Adipocyte death defines macrophage localization and function in adipose tissue of obese mice and humans. J Lipid Res 46, 2347-2355.

Coleman, D.L. (1973). Effects of parabiosis of obese with diabetes and normal mice. Diabetologia 9, 294-298.

Constant, V.A., Gagnon, A., Landry, A., and Sorisky, A. (2006). Macrophage-conditioned medium inhibits the differentiation of 3T3-L1 and human abdominal preadipocytes. Diabetologia 49, 1402-1411.

Constant, V.A., Gagnon, A., Yarmo, M., and Sorisky, A. (2008). The antiadipogenic effect of macrophage-conditioned medium depends on ERK1/2 activation. Metabolism 57, 465-472.

Conway, B., and Rene, A. (2004). Obesity as a disease: no lightweight matter. Obesity 5, 145-151.

Cypess, A.M., Lehman, S., Williams, G., Tal, I., Rodman, D., Goldfine, A.B., Kuo, F.C., Palmer, E.L., Tseng, Y.H., Doria, A., Kolodny, G.M., and Kahn, C.R. (2009). Identification and importance of brown adipose tissue in adult humans. N Engl J Med 360, 1509-1517.

Daigneault, M., Preston, J.A., Marriott, H.M., Whyte, M.K., and Dockrell, D.H. (2010). The identification of markers of macrophage differentiation in PMA-stimulated THP-1 cells and monocyte-derived macrophages. PLoS one 5, e8668.

Danforth, E., Jr. (2000). Failure of adipocyte differentiation causes type II diabetes mellitus? Nat Genet 26, 13.

Davies, L.C., Rosas, M., Smith, P.J., Fraser, D.J., Jones, S.A., and Taylor, P.R. (2011). A quantifiable proliferative burst of tissue macrophages restores homeostatic macrophage populations after acute inflammation. Eur J Immunol 41, 2155-2164.

Decaunes, P., Esteve, D., Zakaroff-Girard, A., Sengenes, C., Galitzky, J., and Bouloumie, A. (2011). Adipose-derived stromal cells: cytokine expression and immune cell contaminants. Methods Mol Biol 702, 151-161.

Despres, J.-P., and Lemieux, I. (2006). Abdominal obesity and metabolic syndrome. Nature 444, 881-887.

Divoux, A., Tordjman, J., Lacasa, D., Veyrie, N., Hugol, D., Aissat, A., Basdevant, A., Guerre-Millo, M., Poitou, C., Zucker, J.D., Bedossa, P., and Clément, K. (2010). Fibrosis in human adipose tissue: composition, distribution, and link with lipid metabolism and fat mass loss. Diabetes 59, 2817-2825.

Duffaut, C., Galitzky, J., Lafontan, M., and Bouloumie, A. (2009). Unexpected trafficking of immune cells within the adipose tissue during the onset of obesity. Biochem Biophys Res Commun 384, 482-485.

Dunay, I.R., Damatta, R.A., Fux, B., Presti, R., Greco, S., Colonna, M., and Sibley, L.D. (2008). Gr1(+) inflammatory monocytes are required for mucosal resistance to the pathogen Toxoplasma gondii. Immunity 29, 306-317.

Farmer, S.R. (2006). Transcriptional control of adipocyte formation. Cell Metab 4, 263-273.

Farooqi, I.S., Keogh, J.M., Yeo, G.S., Lank, E.J., Cheetham, T., and O'Rahilly, S. (2003). Clinical spectrum of obesity and mutations in the melanocortin 4 receptor gene. N Engl J Med 348, 1085-1095.

Farooqi, I.S., Matarese, G., Lord, G.M., Keogh, J.M., Lawrence, E., Agwu, C., Sanna, V., Jebb, S.A., Perna, F., Fontana, S., Lechler, R.I., DePaoli, A.M., and O'Rahilly, S. (2002). Beneficial effects of leptin on obesity, T cell hyporesponsiveness, and neuroendocrine/metabolic dysfunction of human congenital leptin deficiency. J Clin Invest 110, 1093-1103.

Feng, D., Tang, Y., Kwon, H., Zong, H., Hawkins, M., Kitsis, R.N., and Pessin, J.E. (2011). High-fat diet-induced adipocyte cell death occurs through a cyclophilin D intrinsic signaling pathway independent of adipose tissue inflammation. Diabetes 60, 2134-2143.

Fenstermaker, R.A., Poptic, E., Bonfield, T.L., Knauss, T.C., Corsillo, L., Piskurich, J.F., Kaetzel, C.S., Jentoft, J.E., Gelfand, C., and DiCorleto, P.E. (1993). A cationic region of the platelet-derived growth factor (PDGF) A-chain (Arg159-Lys160-Lys161) is required for receptor binding and mitogenic activity of the PDGF-AA homodimer. J Biol Chem 268, 10482-10489.

Festa, E., Fretz, J., Berry, R., Schmidt, B., Rodeheffer, M., Horowitz, M., and Horsley, V. (2011). Adipocyte lineage cells contribute to the skin stem cell niche to drive hair cycling. Cell 146, 761-771.

Feuerer, M., Herrero, L., Cipolletta, D., Naaz, A., Wong, J., Nayer, A., Lee, J., Goldfine, A.B., Benoist, C., Shoelson, S., and Mathis, D. (2009). Lean, but not obese, fat is

enriched for a unique population of regulatory T cells that affect metabolic parameters. Nat Med 15, 930-939.

Fischer-Posovszky, P., Keuper, M., Nagel, S., Hesse, D., Schurmann, A., Debatin, K.M., Strauss, G., and Wabitsch, M. (2011a). Downregulation of FLIP by cycloheximide sensitizes human fat cells to CD95-induced apoptosis. Exp Cell Res 317, 2200-2209.

Fischer-Posovszky, P., Tornqvist, H., Debatin, K.M., and Wabitsch, M. (2004). Inhibition of death-receptor mediated apoptosis in human adipocytes by the insulin-like growth factor I (IGF-I)/IGF-I receptor autocrine circuit. Endocrinology 145, 1849-1859.

Fischer-Posovszky, P., Wang, Q.A., Asterholm, I.W., Rutkowski, J.M., and Scherer, P.E. (2011b). Targeted deletion of adipocytes by apoptosis leads to adipose tissue recruitment of alternatively activated M2 macrophages. Endocrinology 152, 3074-3081.

Franco, M., Martinez, F., Rodriguez-Iturbe, B., Johnson, R.J., Santamaria, J., Montoya, A., Nepomuceno, T., Bautista, R., Tapia, E., and Herrera-Acosta, J. (2006). Angiotensin II, interstitial inflammation, and the pathogenesis of salt-sensitive hypertension. Am J Physiol Renal Physiol 291, F1281-1287.

Frayling, T.M., Timpson, N.J., Weedon, M.N., Zeggini, E., Freathy, R.M., Lindgren, C.M., Perry, J.R., Elliott, K.S., Lango, H., Rayner, N.W., Shields, B., Harries, L.W., Barrett, J.C., Ellard, S., Groves, C.J., Knight, B., Patch, A.M., Ness, A.R., Ebrahim, S., Lawlor, D.A., Ring, S.M., Ben-Shlomo, Y., Jarvelin, M.R., Sovio, U., Bennett, A.J., Melzer, D., Ferrucci, L., Loos, R.J., Barroso, I., Wareham, N.J., Karpe, F., Owen, K.R., Cardon, L.R., Walker, M., Hitman, G.A., Palmer, C.N., Doney, A.S., Morris, A.D., Smith, G.D., Hattersley, A.T., and McCarthy, M.I. (2007). A common variant in the FTO gene is associated with body mass index and predisposes to childhood and adult obesity. Science 316, 889-894.

Frayn, K.N., Karpe, F., Fielding, B.A., Macdonald, I.A., and Coppack, S.W. (2003). Integrative physiology of human adipose tissue. Int J Obes 27, 875-888.

Fredriksson, L., Li, H., and Eriksson, U. (2004). The PDGF family: four gene products form five dimeric isoforms. Cytokine Growth Factor Rev 15, 197-204.

Fujisaka, S., Usui, I., Bukhari, A., Ikutani, M., Oya, T., Kanatani, Y., Tsuneyama, K., Nagai, Y., Takatsu, K., Urakaze, M., Kobayashi, M., and Tobe, K. (2009). Regulatory mechanisms for adipose tissue M1 and M2 macrophages in diet-induced obese mice. Diabetes 58, 2574-2582.

Furukawa, S., Fujita, T., Shimabukuro, M., Iwaki, M., Yamada, Y., Nakajima, Y., Nakayama, O., Makishima, M., Matsuda, M., and Shimomura, I. (2004). Increased oxidative stress in obesity and its impact on metabolic syndrome. J Clin Invest 114, 1752-1761.

Gagnon, A., Dods, P., Roustan-Delatour, N., Chen, C.S., and Sorisky, A. (2001). Phosphatidylinositol-3,4,5-trisphosphate is required for insulin-like growth factor 1-mediated survival of 3T3-L1 preadipocytes. Endocrinology 142, 205-212.

Gesta, S., Bluher, M., Yamamoto, Y., Norris, A.W., Berndt, J., Kralisch, S., Boucher, J., Lewis, C., and Kahn, C.R. (2006). Evidence for a role of developmental genes in the origin of obesity and body fat distribution. Proc. Natl. Acad. Sci. USA 103, 6676-6681.

Gesta, S., Tseng, Y.H., and Kahn, C.R. (2007). Developmental origin of fat: tracking obesity to its source. Cell 131, 242-256.

Gharbi, S.I., Zvelebil, M.J., Shuttleworth, S.J., Hancox, T., Saghir, N., Timms, J.F., and Waterfield, M.D. (2007). Exploring the specificity of the PI3K family inhibitor LY294002. Biochem J 404, 15-21.

Gordon, S. (2003). Alternative activation of macrophages. Nat Rev Immunol 3, 23-35.

Gordon, S., and Martinez, F.O. (2010). Alternative activation of macrophages: mechanism and functions. Immunity 32, 593-604.

Green, H., and Goldberg, B. (1964). Collagen and cell protein synthesis by an established mammalian fibroblast line. Nature 204, 347-349.

Green, H., and Goldberg, B. (1965). Synthesis of collagen by mammalian cell lines of fibroblastic and nonfibroblastic origin. Proc. Natl. Acad. Sci. USA 53, 1360-1365.

Green, H., and Kehinde, O. (1975). An established preadipose cell line and its differentiation in culture. II. Factors affecting the adipose conversion. Cell 5, 19-27.

Green, H., and Meuth, M. (1974). An established pre-adipose cell line and its differentiation in culture. Cell 3, 127-133.

Guerre-Millo, M., Guesnet, P., Guichard, C., Durand, G., and Lavau, M. (1994). Alteration in membrane lipid order and composition in metabolically hyperactive fatty rat adipocytes. Lipids 29, 205-209.

Guo, W., Wong, S., Xie, W., Lei, T., and Luo, Z. (2007). Palmitate modulates intracellular signaling, induces endoplasmic reticulum stress, and causes apoptosis in mouse 3T3-L1 and rat primary preadipocytes. Am J Physiol Endocrinol Metab 293, E576-586.

Gupta, R.K., Mepani, R.J., Kleiner, S., Lo, J.C., Khandekar, M.J., Cohen, P., Frontini, A., Bhowmick, D.C., Ye, L., Cinti, S., and Spiegelman BM. (2012). Zfp423 expression identifies committed preadipocytes and localizes to adipose endothelial and perivascular cells. Cell Metab 15, 230-239.

Gustafson, B., Hammarstedt, A., Andersson, C.X., and Smith, U. (2007). Inflamed adipose tissue: a culprit underlying the metabolic syndrome and atherosclerosis. Arterioscler Thromb Vasc Biol 27, 2276-2283.

Hauner, H. (2005). Secretory factors from human adipose tissue and their functional role. Proc Nutr Soc 64, 163-169.

Hayashi, H., Campenot, R.B., Vance, D.E., and Vance, J.E. (2007). Apolipoprotein E-containing lipoproteins protect neurons from apoptosis via a signaling pathway involving low-density lipoprotein receptor-related protein-1. J Neurosci 27, 1933-1941.

Heilbronn, L., Smith, S.R., and Ravussin, E. (2004). Failure of fat cell proliferation, mitochondrial function and fat oxidation results in ectopic fat storage, insulin resistance and type II diabetes mellitus. Int J Obes 28 Suppl 4, S12-21.

Hirosumi, J., Tuncman, G., Chang, L., Gorgun, C.Z., Uysal, K.T., Maeda, K., Karin, M., and Hotamisligil, G.S. (2002). A central role for JNK in obesity and insulin resistance. Nature 420, 333-336.

Hotamisligil, G.S., Arner, P., Caro, J.F., Atkinson, R.L., and Spiegelman, B.M. (1995). Increased adipose tissue expression of tumor necrosis factor-alpha in human obesity and insulin resistance. J Clin Invest 95, 2409-2415.

Ichioka, M., Suganami, T., Tsuda, N., Shirakawa, I., Hirata, Y., Satoh-Asahara, N., Shimoda, Y., Tanaka, M., Kim-Saijo, M., Miyamoto, Y., Kamei, Y., Sata, M., and Ogawa, Y. (2011). Increased expression of macrophage-inducible C-type lectin in adipose tissue of obese mice and humans. Diabetes 60, 819-826.

Ide, J., Gagnon, A., Molgat, A.S., Landry, A., Foster, C., and Sorisky, A. (2011). Macrophage-conditioned medium inhibits the activation of cyclin-dependent kinase 2 by adipogenic inducers in 3T3-L1 preadipocytes. J Cell Physiol 226, 2297-2306.

Ilan, Y., Maron, R., Tukpah, A.M., Maioli, T.U., Murugaiyan, G., Yang, K., Wu, H.Y., and Weiner, H.L. (2010). Induction of regulatory T cells decreases adipose inflammation and alleviates insulin resistance in ob/ob mice. Proc. Natl. Acad. Sci. USA 107, 9765-9770.

Ingalls, A.M., Dickie, M.M., and Snell, G.D. (1950). Obese, a new mutation in the house mouse. J Hered 41, 317-318.

Jenkins, S.J., Ruckerl, D., Cook, P.C., Jones, L.H., Finkelman, F.D., van Rooijen, N., MacDonald, A.S., and Allen, J.E. (2011). Local macrophage proliferation, rather than recruitment from the blood, is a signature of Th2 inflammation. Science 332, 1284-1288.

Ji, Y., Sun, S., Xia, S., Yang, L., Li, X., and Qi, L. (2012). Short term high fat diet challenge promotes alternative macrophage polarization in adipose tissue via natural killer T cells and interleukin-4. J Biol Chem 287, 24378-24386.

Jiang, C., Qu, A., Matsubara, T., Chanturiya, T., Jou, W., Gavrilova, O., Shah, Y.M., and Gonzalez, F.J. (2011). Disruption of hypoxia-inducible factor 1 in adipocytes improves insulin sensitivity and decreases adiposity in high-fat diet-fed mice. Diabetes 60, 2484-2495.

Jiao, P., Chen, Q., Shah, S., Du, J., Tao, B., Tzameli, I., Yan, W., and Xu, H. (2008). Obesity-related upregulation of monocyte chemotactic factors in adipocytes: involvement of NF-kappaB and JNK pathways. Diabetes 58, 104-115.

Jiao, P., Ma, J., Feng, B., Zhang, H., Diehl, J.A., Chin, Y.E., Yan, W., and Xu, H. (2011). FFA-induced adipocyte inflammation and insulin resistance: involvement of ER stress and IKKbeta pathways. Obesity 19, 483-491.

Johnson, W.D., Jr., Mei, B., and Cohn, Z.A. (1977). The separation, long-term cultivation, and maturation of the human monocyte. J Exp Med 146, 1613-1626.

Jozefowski, S., Czerkies, M., Lukasik, A., Bielawska, A., Bielawski, J., Kwiatkowska, K., and Sobota, A. (2010). Ceramide and ceramide 1-phosphate are negative regulators of TNF-alpha production induced by lipopolysaccharide. J Immunol 185, 6960-6973.

Kanda, H., Tateya, S., Tamori, Y., Kotani, K., Hiasa, K., Kitazawa, R., Kitazawa, S., Miyachi, H., Maeda, S., Egashira, K., and Kasuga, M. (2006). MCP-1 contributes to macrophage infiltration into adipose tissue, insulin resistance, and hepatic steatosis in obesity. J Clin Invest 116, 1494-1505.

Kang, K., Reilly, S.M., Karabacak, V., Gangl, M.R., Fitzgerald, K., Hatano, B., and Lee, C.H. (2008). Adipocyte-derived Th2 cytokines and myeloid PPARdelta regulate macrophage polarization and insulin sensitivity. Cell Metab 7, 485-495.

Kang, S.W. (2007). Two axes in platelet-derived growth factor signaling: tyrosine phosphorylation and reactive oxygen species. Cell Mol Life Sci 64, 533-541.

Keophiphath, M., Achard, V., Henegar, C., Rouault, C., Clement, K., and Lacasa, D. (2009). Macrophage-secreted factors promote a profibrotic phenotype in human preadipocytes. Mol Endocrinol 23, 11-24.

Keuper, M., Bluher, M., Schon, M.R., Moller, P., Dzyakanchuk, A., Amrein, K., Debatin, K.M., Wabitsch, M., and Fischer-Posovszky, P. (2011). An inflammatory micro-environment promotes human adipocyte apoptosis. Mol Cell Endocrinol 339, 105-113.

Khandekar, M.J., Cohen, P., and Spiegelman, B.M. (2011). Molecular mechanisms of cancer development in obesity. Nat Rev Cancer 11, 886-895.

Kim, J.J., Lee, S.B., Park, J.K., and Yoo, Y.D. (2010). TNF-alpha-induced ROS production triggering apoptosis is directly linked to Romo1 and Bcl-X(L). Cell Death Differ 17, 1420-1434.

Kim, J.Y., van de Wall, E., Laplante, M., Azzara, A., Trujillo, M.E., Hofmann, S.M., Schraw, T., Durand, J.L., Li, H., Li, G., Jelicks, L.A., Mehler, M.F., Hui, D.Y., Deshaies, Y., Shulman, G.I., Schwartz, G.J., and Scherer, P.E. (2007). Obesity-associated improvements in metabolic profile through expansion of adipose tissue. J Clin Invest 117, 2621-2637.

Kim, M.O., Kim, M.H., Lee, S.H., Suh, H.N., Lee, Y.J., Lee, M.Y., and Han, H.J. (2009). 5′-N-ethylcarboxamide induces IL-6 expression via MAPKs and NF-kappaB activation through Akt, Ca2+/PKC, cAMP signaling pathways in mouse embryonic stem cells. J Cell Physiol 219, 752-759.

Kintscher, U., Hartge, M., Hess, K., Foryst-Ludwig, A., Clemenz, M., Wabitsch, M., Fischer-Posovszky, P., Barth, T.F., Dragun, D., Skurk, T., Hauner, H., Blüher, M., Unger, T., Wolf, A.M., Knippschild, U., Hombach, V., and Marx, N. (2008). T-lymphocyte infiltration in visceral adipose tissue: a primary event in adipose tissue inflammation and the development of obesity-mediated insulin resistance. Arterioscler Thromb Vasc Biol 28, 1304-1310.

Kitade, H., Sawamoto, K., Nagashimada, M., Inoue, H., Yamamoto, Y., Sai, Y., Takamura, T., Yamamoto, H., Miyamoto, K., Ginsberg, H.N., Mukaida, N., Kaneko, S., and Ota, T. (2012). CCR5 plays a critical role in obesity-induced adipose tissue inflammation and insulin resistance by regulating both macrophage recruitment and M1/M2 status. Diabetes 61, 1680-1690.

Kitamura, H., Ito, M., Yuasa, T., Kikuguchi, C., Hijikata, A., Takayama, M., Kimura, Y., Yokoyama, R., Kaji, T., and Ohara, O. (2008). Genome-wide identification and characterization of transcripts translationally regulated by bacterial lipopolysaccharide in macrophage-like J774.1 cells. Physiol Genomics 33, 121-132.

Kloting, N., Fasshauer, M., Dietrich, A., Kovacs, P., Schon, M.R., Kern, M., Stumvoll, M., and Bluher, M. (2010). Insulin-sensitive obesity. Am J Physiol Endocrinol Metab 299, E506-515.

Kodelja, V., Muller, C., Tenorio, S., Schebesch, C., Orfanos, C.E., and Goerdt, S. (1997). Differences in angiogenic potential of classically vs alternatively activated macrophages. Immunobiology 197, 478-493.

Kojima, T., Norose, T., Tsuchiya, K., and Sakamoto, K. (2010). Mouse 3T3-L1 cells acquire resistance against oxidative stress as the adipocytes differentiate via the transcription factor FoxO. Apoptosis 15, 83-93.

Kosaka, C., Masuda, J., Shimokado, K., Zen, K., Yokota, T., Sasaguri, T., and Ogata, J. (1992). Interferon-gamma suppresses PDGF production from THP-1 cells and blood monocyte-derived macrophages. Atherosclerosis 97, 75-87.

Kovacs, E.J., and Vanstedum, S. (1995). Cyclic AMP stimulates platelet-derived growth factor B chain mRNA expression in murine macrophage cell lines. Mediators Inflamm 4, 293-297.

Krause, B.R., and Hartman, A.D. (1984). Adipose tissue and cholesterol metabolism. J Lipid Res 25, 97-110.

Kurokawa, J., Arai, S., Nakashima, K., Nagano, H., Nishijima, A., Miyata, K., Ose, R., Mori, M., Kubota, N., Kadowaki, T., Oike, Y., Koga, H., Febbraio, M., Iwanaga, T., and Miyazaki, T. (2010). Macrophage-derived AIM is endocytosed into adipocytes and decreases lipid droplets via inhibition of fatty acid synthase activity. Cell Metab 11, 479-492.

Kwon, J., Lee, S.R., Yang, K.S., Ahn, Y., Kim, Y.J., Stadtman, E.R., and Rhee, S.G. (2004). Reversible oxidation and inactivation of the tumor suppressor PTEN in cells stimulated with peptide growth factors. Proc. Natl. Acad. Sci. USA 101, 16419-16424.

Lacasa, D., Taleb, S., Keophiphath, M., Miranville, A., and Clement, K. (2007). Macrophage-secreted factors impair human adipogenesis: involvement of proinflammatory state in preadipocytes. Endocrinology 148, 868-877.

Lachman, L.B., and Metzgar, R.S. (1980). Characterization of high and low molecular weight lymphocyte-activating factor (interleukin I) from P388D and J774.1 mouse macrophage cell lines. J Reticuloendothel Soc 27, 621-629.

Laemmli, U.K. (1970). Cleavage of structural proteins during the assembly of the head of bacteriophage T4. Nature 227, 680-685.

Lago, F., Dieguez, C., Gomez-Reino, J., and Gualillo, O. (2007). The emerging role of adipokines as mediators of inflammation and immune responses. Cytokine Growth Factor Rev 18, 313-325.

Lau, D.C., Dhillon, B., Yan, H., Szmitko, P.E., and Verma, S. (2005). Adipokines: molecular links between obesity and atheroslcerosis. Am J Physiol Heart Circ Physiol 288, H2031-2041.

Le Lay, S., Krief, S., Farnier, C., Lefrere, I., Le Liepvre, X., Bazin, R., Ferre, P., and Dugail, I. (2001). Cholesterol, a cell size-dependent signal that regulates glucose metabolism and gene expression in adipocytes. J Biol Chem 276, 16904-16910.

Lee, C.C., Liu, K.J., Wu, Y.C., Lin, S.J., Chang, C.C., and Huang, T.S. (2011). Sesamin inhibits macrophage-induced vascular endothelial growth factor and matrix

metalloproteinase-9 expression and proangiogenic activity in breast cancer cells. Inflammation 34, 209-221.

Lee, S.B., Bae, I.H., Bae, Y.S., and Um, H.D. (2006). Link between mitochondria and NADPH oxidase 1 isozyme for the sustained production of reactive oxygen species and cell death. J Biol Chem 281, 36228-36235.

Lee, S.B., Kim, J.J., Kim, T.W., Kim, B.S., Lee, M.S., and Yoo, Y.D. (2010). Serum deprivation-induced reactive oxygen species production is mediated by Romo1. Apoptosis 15, 204-218.

Lei, H., and Kazlauskas, A. (2009). Growth factors outside of the platelet-derived growth factor (PDGF) family employ reactive oxygen species/Src family kinases to activate PDGF receptor alpha and thereby promote proliferation and survival of cells. J Biol Chem 284, 6329-6336.

Li, S.R., Forster, L., Anggard, E., and Ferns, G. (1994). The effects of LPS and probucol on interleukin 1 (IL-1) and platelet-derived growth factor (PDGF) gene expression in the human monocytic cell line U-937. Biochim Biophys Acta 1225, 271-274.

Lu, C., Kumar, P.A., Fan, Y., Sperling, M.A., and Menon, R.K. (2010). A novel effect of growth hormone on macrophage modulates macrophage-dependent adipocyte differentiation. Endocrinology 151, 2189-2199.

Lumeng, C.N., Bodzin, J.L., and Saltiel, A.R. (2007a). Obesity induces a phenotypic switch in adipose tissue macrophage polarization. J Clin Invest 117, 175-184.

Lumeng, C.N., DelProposto, J.B., Westcott, D.J., and Saltiel, A.R. (2008). Phenotypic switching of adipose tissue macrophages with obesity is generated by spatiotemporal differences in macrophage subtypes. Diabetes 57, 3239-3246.

Lumeng, C.N., Deyoung, S.M., Bodzin, J.L., and Saltiel, A.R. (2007b). Increased inflammatory properties of adipose tissue macrophages recruited during diet-induced obesity. Diabetes 56, 16-23.

Lumeng, C.N., Deyoung, S.M., and Saltiel, A.R. (2007c). Macrophages block insulin action in adipocytes by altering expression of signaling and glucose transport proteins. Am J Physiol Endocrinol Metab 292, E166-174.

Lumeng, C.N., Liu, J., Geletka, L., Delaney, C., Delproposto, J., Desai, A., Oatmen, K., Martinez-Santibanez, G., Julius, A., Garg, S., and Yung, R.L. (2011). Aging is associated with an increase in T cells and inflammatory macrophages in visceral adipose tissue. J Immunol 187, 6208-6216.

Lundberg, A.S., and Weinberg, R.A. (1998). Functional inactivation of the retinoblastoma protein requires sequential modification by at least two distinct cyclin-cdk complexes. Mol Cell Biol 18, 753-761.

Macotela, Y., Emanuelli, B., Mori, M.A., Gesta, S., Schulz, T.J., Tseng, Y.H., and Kahn, C.R. (2012). Intrinsic differences in adipocyte precursor cells from different white fat depots. Diabetes 61, 1691-1699.

Magun, R., Boone, D., Tsang, B., and Sorisky, A. (1998a). The effect of adipocyte differentiation on the capacity of 3T3-L1 cells to undergo apoptosis in response to growth factor deprivation. Int J Obes 22, 567-571.

Magun, R., Gagnon, A., Yaraghi, Z., and Sorisky, A. (1998b). Expression and regulation of neuronal apoptosis inhibitory protein during adipocyte differentiation. Diabetes 47, 1948-1952.

Mahadev, K., Wu, X., Zilbering, A., Zhu, L., Lawrence, J.T., and Goldstein, B.J. (2001). Hydrogen peroxide generated during cellular insulin stimulation is integral to activation of the distal insulin signaling cascade in 3T3-L1 adipocytes. J Biol Chem 276, 48662-48669.

Manninen, A.H. (2006). Very-low-carbohydrate diets and preservation of muscle mass. Nutr Metab 3, 9.

Martinez, F.O., Gordon, S., Locati, M., and Mantovani, A. (2006). Transcriptional profiling of the human monocyte-to-macrophage differentiation and polarization: new molecules and patterns of gene expression. J Immunol 177, 7303-7311.

Maumus, M., Peyrafitte, J.A., D'Angelo, R., Fournier-Wirth, C., Bouloumie, A., Casteilla, L., Sengenes, C., and Bourin, P. (2011). Native human adipose stromal cells: localization, morphology and phenotype. Int J Obes 35, 1141-1153.

Maumus, M., Sengenes, C., Decaunes, P., Zakaroff-Girard, A., Bourlier, V., Lafontan, M., Galitzky, J., and Bouloumie, A. (2008). Evidence of in situ proliferation of adult adipose tissue-derived progenitor cells: influence of fat mass microenvironment and growth. J Clin Endocrinol Metab 93, 4098-4106.

Mayi, T.H., Daoudi, M., Derudas, B., Gross, B., Bories, G., Wouters, K., Brozek, J., Caiazzo, R., Raverdi, V., Pigeyre, M., Allavena, P., Mantovani, A., Pattou, F., Staels, B., and Chinetti-Gbaguidi, G. (2012). Human adipose tissue macrophages display activation of cancer-related pathways. J Biol Chem 287, 21904-21913.

Mayi, T.H., Duhem, C., Copin, C., Bouhlel, M.A., Rigamonti, E., Pattou, F., Staels, B., and Chinetti-Gbaguidi, G. (2010). Visfatin is induced by peroxisome proliferator-activated receptor gamma in human macrophages. FEBS J 277, 3308-3320.

McCarthy, M.I. (2010). Genomics, type 2 diabetes, and obesity. N Engl J Med 363, 2339-2350.

McDonnell, M.E., Ganley-Leal, L.M., Mehta, A., Bigornia, S.J., Mott, M., Rehman, Q., Farb, M.G., Hess, D.T., Joseph, L., Gokce, N., and Apovian, C.M. (2012). B lymphocytes in human subcutaneous adipose crown-like structures. Obesity 20, 1372-1378.

Mochizuki, T., Furuta, S., Mitsushita, J., Shang, W.H., Ito, M., Yokoo, Y., Yamaura, M., Ishizone, S., Nakayama, J., Konagai, A., Hirose, K., Kiyosawa, K., and Kamata, T. (2006). Inhibition of NADPH oxidase 4 activates apoptosis via the AKT/apoptosis signal-regulating kinase 1 pathway in pancreatic cancer PANC-1 cells. Oncogene 25, 3699-3707.

Modolell, M., Corraliza, I.M., Link, F., Soler, G., and Eichmann, K. (1995). Reciprocal regulation of the nitric oxide synthase/arginase balance in mouse bone marrow-derived macrophages by Th1 and Th2 cytokines. Eur J Immunol 25, 1101-1104.

Molgat, A.S., Gagnon, A., and Sorisky, A. (2009). Preadipocyte apoptosis is prevented by macrophage-conditioned medium in a PDGF-dependent manner. Am J Physiol Cell Physiol 296, C757-765.

Molgat, A.S., Gagnon, A., and Sorisky, A. (2011). Macrophage-induced preadipocyte survival depends on signaling through Akt, ERK1/2, and reactive oxygen species. Exp Cell Res 317, 521-530.

Montague, C.T., Farooqi, I.S., Whitehead, J.P., Soos, M.A., Rau, H., Wareham, N.J., Sewter, C.P., Digby, J.E., Mohammed, S.N., Hurst, J.A., Cheetham, C.H., Earley, A.R., Barnett, A.H., Prins, J.B., and O'Rahilly, S. (1997). Congenital leptin deficiency is associated with severe early-onset obesity in humans. Nature 387, 903-908.

Mora, S., and Pessin, J.E. (2002). An adipocentric view of signaling and intracellular trafficking. Diabetes Metab Res Rev 18, 345-356.

Moreno-Navarrete, J.M., Ortega, F.J., Ricart, W., and Fernandez-Real, J.M. (2009). Lactoferrin increases (172Thr)AMPK phosphorylation and insulin-induced (p473Ser)AKT while impairing adipocyte differentiation. Int J Obes 33, 991-1000.

Morgan, S.C., Taylor, D.L., and Pocock, J.M. (2004). Microglia release activators of neuronal proliferation mediated by activation of mitogen-activated protein kinase, phosphatidylinositol-3-kinase/Akt and delta-Notch signalling cascades. J Neurochem 90, 89-101.

Mori, R., Shaw, T.J., and Martin, P. (2008). Molecular mechanisms linking wound inflammation and fibrosis: knockdown of osteopontin leads to rapid repair and reduced scarring. J Exp Med 205, 43-51.

Mouche, S., Mkaddem, S.B., Wang, W., Katic, M., Tseng, Y.H., Carnesecchi, S., Steger, K., Foti, M., Meier, C.A., Muzzin, P., Kahn, C.R., Ogier-Denis, E., and Szanto, I. (2007). Reduced expression of the NADPH oxidase NOX4 is a hallmark of adipocyte differentiation. Biochim Biophys Acta 1773, 1015-1027.

Muoio, D.M., and Newgard, C.B. (2005). Metabolism: A is for adipokine. Nature 436, 337-338.

Na, A.R., Chung, Y.M., Lee, S.B., Park, S.H., Lee, M.S., and Yoo, Y.D. (2008). A critical role for Romo1-derived ROS in cell proliferation. Biochem Biophys Res Commun 369, 672-678.

Nagaoka, I., Honma, S., Someya, A., Iwabuchi, K., and Yamashita, T. (1992). Differential expression of the platelet-derived growth factor-A and -B genes during maturation of monocytes to macrophages. Comp Biochem Physiol B 103, 349-356.

Neese, R.A., Misell, L.M., Turner, S., Chu, A., Kim, J., Cesar, D., Hoh, R., Antelo, F., Strawford, A., McCune, J.M., Christiansen, M., and Hellerstein, M.K. (2002). Measurement in vivo of proliferation rates of slow turnover cells by 2H2O labeling of the deoxyribose moiety of DNA. Proc. Natl. Acad. Sci. USA 99, 15345-15350.

Niesler, C.U., Urso, B., Prins, J.B., and Siddle, K. (2000). IGF-I inhibits apoptosis induced by serum withdrawal, but potentiates TNF-alpha-induced apoptosis, in 3T3-L1 preadipocytes. J Endocrinol 167, 165-174.

Nishimura, S., Manabe, I., Nagasaki, M., Eto, K., Yamashita, H., Ohsugi, M., Otsu, M., Hara, K., Ueki, K., Sugiura, S., Yoshimura, K., Kadowaki, T., and Nagai, R. (2009). CD8+ effector T cells contribute to macrophage recruitment and adipose tissue inflammation in obesity. Nat Med 15, 914-920.

Norris, D.A., Morris, R.M., Sanderson, R.J., and Kohler, P.F. (1979). Isolation of functional subsets of human peripheral blood monocytes. J Immunol 123, 166-172.

Odegaard, J.I., Ricardo-Gonzalez, R.R., Goforth, M.H., Morel, C.R., Subramanian, V., Mukundan, L., Red Eagle, A., Vats, D., Brombacher, F., Ferrante, A.W. Jr., and Chawla, A. (2007). Macrophage-specific PPARgamma controls alternative activation and improves insulin resistance. Nature 447, 1116-1120.

Oh, D.Y., Morinaga, H., Talukdar, S., Bae, E.J., and Olefsky, J.M. (2012). Increased macrophage migration into adipose tissue in obese mice. Diabetes 61, 346-354.

Onate, B., Vilahur, G., Ferrer-Lorente, R., Ybarra, J., Diez-Caballero, A., Ballesta-Lopez, C., Moscatiello, F., Herrero, J., and Badimon, L. (2012). The subcutaneous adipose tissue reservoir of functionally active stem cells is reduced in obese patients. FASEB J Jul 6. Epub ahead of print.

Ortega Martinez de Victoria, E., Xu, X., Koska, J., Francisco, A.M., Scalise, M., Ferrante, A.W., Jr., and Krakoff, J. (2009). Macrophage content in subcutaneous adipose tissue: associations with adiposity, age, inflammatory markers, and whole-body insulin action in healthy Pima Indians. Diabetes 58, 385-393.

Ouchi, N., Higuchi, A., Ohashi, K., Oshima, Y., Gokce, N., Shibata, R., Akasaki, Y., Shimono, A., and Walsh, K. (2010). Sfrp5 is an anti-inflammatory adipokine that modulates metabolic dysfunction in obesity. Science 329, 454-457.

Ouellet, V., Labbe, S.M., Blondin, D.P., Phoenix, S., Guerin, B., Haman, F., Turcotte, E.E., Richard, D., and Carpentier, A.C. (2012). Brown adipose tissue oxidative metabolism contributes to energy expenditure during acute cold exposure in humans. J Clin Invest 122, 545-552.

Ouimet, M., Wang, M.D., Cadotte, N., Ho, K., and Marcel, Y.L. (2008). Epoxycholesterol impairs cholesteryl ester hydrolysis in macrophage foam cells, resulting in decreased cholesterol efflux. Arterioscler Thromb Vasc Biol 28, 1144-1150.

Ozcan, U., Cao, Q., Yilmaz, E., Lee, A.H., Iwakoshi, N.N., Ozdelen, E., Tuncman, G., Gorgun, C., Glimcher, L.H., and Hotamisligil, G.S. (2004). Endoplasmic reticulum stress links obesity, insulin action, and type 2 diabetes. Science 306, 457-461.

Ozcan, U., Yilmaz, E., Ozcan, L., Furuhashi, M., Vaillancourt, E., Smith, R.O., Gorgun, C.Z., and Hotamisligil, G.S. (2006). Chemical chaperones reduce ER stress and restore glucose homeostasis in a mouse model of type 2 diabetes. Science 313, 1137-1140.

Pang, C., Gao, Z., Yin, J., Zhang, J., Jia, W., and Ye, J. (2008). Macrophage infiltration into adipose tissue may promote angiogenesis for adipose tissue remodeling in obesity. Am J Physiol Endocrinol Metab 295, E313-322.

Papineau, D., Gagnon, A., and Sorisky, A. (2003). Apoptosis of human abdominal preadipocytes before and after differentiation into adipocytes in culture. Metabolism 52, 987-992.

Park, C.S., Schneider, I.C., and Haugh, J.M. (2003). Kinetic analysis of platelet-derived growth factor receptor/phosphoinositide 3-kinase/Akt signaling in fibroblasts. J Biol Chem 278, 37064-37072.

Patel, S., Djerdjouri, B., Raoul-Des-Essarts, Y., Dang, P.M.-C., El-Benna, J., and Périanin, A. (2010). Protein kinase B (AKT) mediates phospholipase D activation via ERK1/2 and promotes respiratory burst parameters in formylpeptide-stimulated neutrophil-like HL-60 cells. J Biol Chem 285, 32055-32063.

Patel, Y.M., and Lane, M.D. (2000). Mitotic clonal expansion during preadipocyte differentiation: calpain-mediated turnover of p27. J Biol Chem 275, 17653-17660.

Patsouris, D., Li, P.P., Thapar, D., Chapman, J., Olefsky, J.M., and Neels, J.G. (2008). Ablation of CD11c-positive cells normalizes insulin sensitivity in obese insulin resistant animals. Cell Metab 8, 301-309.

Permana, P.A., Menge, C., and Reaven, P.D. (2006). Macrophage-secreted factors induce adipocyte inflammation and insulin resistance. Biochem Biophys Res Commun 341, 507-514.

Prins, J.B., Niesler, C.U., Winterford, C.M., Bright, N.A., Siddle, K., O'Rahilly, S., Walker, N.I., and Cameron, D.P. (1997). Tumor necrosis factor-alpha induces apoptosis of human adipose cells. Diabetes 46, 1939-1944.

Prins, J.B., and O'Rahilly, S. (1997). Regulation of adipose cell number in man. Clin Sci 92, 3-11.

Radhakrishnan, A., Goldstein, J.L., McDonald, J.G., and Brown, M.S. (2008). Switch-like control of SREBP-2 transport triggered by small changes in ER cholesterol: a delicate balance. Cell Metab 8, 512-521.

Ralph, P., and Nakoinz, I. (1975). Phagocytosis and cytolysis by a macrophage tumour and its cloned cell line. Nature 257, 393-394.

Ralph, P., and Nakoinz, I. (1977). Antibody-dependent killing of erythrocyte and tumor targets by macrophage-related cell lines: enhancement by PPD and LPS. J Immunol 119, 950-954.

Ralph, P., Prichard, J., and Cohn, M. (1975). Reticulum cell sarcoma: an effector cell in antibody-dependent cell-mediated immunity. J Immunol 114, 898-905.

Ramachandrappa, S., and Farooqi, I.S. (2011). Genetic approaches to understanding human obesity. J Clin Invest 121, 2080-2086.

Raschke, W.C., Baird, S., Ralph, P., and Nakoinz, I. (1978). Functional macrophage cell lines transformed by Abelson leukemia virus. Cell 15, 261-267.

Rausch, M.E., Weisberg, S., Vardhana, P., and Tortoriello, D.V. (2008). Obesity in C57BL/6J mice is characterized by adipose tissue hypoxia and cytotoxic T-cell infiltration. Int J Obes 32, 451-463.

Ray, S., Gao, C., Wyatt, K., Fariss, R.N., Bundek, A., Zelenka, P., and Wistow, G. (2005). Platelet-derived growth factor D, tissue-specific expression in the eye, and a key role in control of lens epithelial cell proliferation. J Biol Chem 280, 8494-8502.

Reichert, M., and Eick, D. (1999). Analysis of cell cycle arrest in adipocyte differentiation. Oncogene 18, 459-466.

Reshef, L., Olswang, Y., Cassuto, H., Blum, B., Croniger, C.M., Kalhan, S.C., Tilghman, S.M., and Hanson, R.W. (2003). Glyceroneogenesis and the triglyceride/fatty acid cycle. J Biol Chem 278, 30413-30416.

Richon, V.M., Lyle, R.E., and McGehee, R.E., Jr. (1997). Regulation and expression of retinoblastoma proteins p107 and p130 during 3T3-L1 adipocyte differentiation. J Biol Chem 272, 10117-10124.

Rigamonti, A., Brennand, K., Lau, F., and Cowan, C.A. (2011). Rapid cellular turnover in adipose tissue. PLoS one 6, e17637.

Rodeheffer, M.S., Birsoy, K., and Friedman, J.M. (2008). Identification of white adipocyte progenitor cells in vivo. Cell 135, 240-249.

Romashkova, J.A., and Makarov, S.S. (1999). NF-kappaB is a target of AKT in anti-apoptotic PDGF signalling. Nature 401, 86-90.

Romeo, G.R., Lee, J., and Shoelson, S.E. (2012). Metabolic syndrome, insulin resistance, and roles of inflammation - mechanisms and therapeutic targets. Arterioscler Thromb Vasc Biol 32, 1771-1776.

Rosen, E.D., Hsu, C.H., Wang, X., Sakai, S., Freeman, M.W., Gonzalez, F.J., and Spiegelman, B.M. (2002). C/EBPalpha induces adipogenesis through PPARgamma: a unified pathway. Genes Dev 16, 22-26.

Samokhvalov, V., Bilan, P.J., Schertzer, J.D., Antonescu, C.N., and Klip, A. (2009). Palmitate- and lipopolysaccharide-activated macrophages evoke contrasting insulin responses in muscle cells. Am J Physiol Endocrinol Metab 296, E37-46.

Satoh, T., Sakai, N., Enokido, Y., Uchiyama, Y., and Hatanaka, H. (1996). Survival factor-insensitive generation of reactive oxygen species induced by serum deprivation in neuronal cells. Brain Res 733, 9-14.

Schenk, S., Saberi, M., and Olefsky, J.M. (2008). Insulin sensitivity: modulation by nutrients and inflammation. J Clin Invest 118, 2992-3002.

Schroder, K., Wandzioch, K., Helmcke, I., and Brandes, R.P. (2009). Nox4 acts as a switch between differentiation and proliferation in preadipocytes. Arterioscler Thromb Vasc Biol 29, 239-245.

Seale, P., Conroe, H.M., Estall, J., Kajimura, S., Frontini, A., Ishibashi, J., Cohen, P., Cinti, S., and Spiegelman, B.M. (2011). Prdm16 determines the thermogenic program of subcutaneous white adipose tissue in mice. J Clin Invest 121, 96-105.

Shanker, G., Sorci-Thomas, M., and Adams, M.R. (1995). Estrogen modulates the inducible expression of platelet-derived growth factor mRNA by monocyte/macrophages. Life Sci 56, 499-507.

Shaul, M.E., Bennett, G., Strissel, K.J., Greenberg, A.S., and Obin, M.S. (2010). Dynamic, M2-like remodeling phenotypes of CD11c+ adipose tissue macrophages during high-fat diet--induced obesity in mice. Diabetes 59, 1171-1181.

Shields, M., Carroll, M.D., and Ogden, C.L. (2011). Adult obesity prevalence in Canada and the United States. NCHS data brief no 56.

Sim, S., Yong, T.S., Park, S.J., Im, K.I., Kong, Y., Ryu, J.S., Min, D.Y., and Shin, M.H. (2005). NADPH oxidase-derived reactive oxygen species-mediated activation of ERK1/2 is required for apoptosis of human neutrophils induced by Entamoeba histolytica. J Immunol 174, 4279-4288.

Skolnik, E.Y., and Marcusohn, J. (1996). Inhibition of insulin receptor signaling by TNF: potential role in obesity and non-insulin-dependent diabetes mellitus. Cytokine Growth Factor Rev 7, 161-173.

Skurk, T., and Hauner, H. (2012). Primary culture of human adipocyte precursor cells: expansion and differentiation. Methods Mol Biol 806, 215-226.

Song, E., Ouyang, N., Hörbelt, M., Antus, B., Wang, M., and Exton, M.S. (2000). Influence of alternatively and classically activated macrophages on fibrogenic activities of human fibroblasts. Cell Immunol 204, 19-28.

Spalding, K.L., Arner, E., Westermark, P.O., Bernard, S., Buchholz, B.A., Bergmann, O., Blomqvist, L., Hoffstedt, J., Naslund, E., Britton, T., Concha, H., Hassan, M., Rydén, M., Frisén, J., and Arner, P. (2008). Dynamics of fat cell turnover in humans. Nature 453, 783-787.

Stienstra, R., Duval, C., Keshtkar, S., van der Laak, J., Kersten, S., and Muller, M. (2008). Peroxisome proliferator-activated receptor gamma activation promotes infiltration of alternatively activated macrophages into adipose tissue. J Biol Chem 283, 22620-22627.

Strawford, A., Antelo, F., Christiansen, M., and Hellerstein, M.K. (2004). Adipose tissue triglyceride turnover, de novo lipogenesis, and cell proliferation in humans measured with 2H2O. Am J Physiol Endocrinol Metab 286, E577-588.

Strissel, K.J., DeFuria, J., Shaul, M.E., Bennett, G., Greenberg, A.S., and Obin, M.S. (2010). T-cell recruitment and Th1 polarization in adipose tissue during diet-induced obesity in C57BL/6 mice. Obesity 18, 1918-1925.

Strissel, K.J., Stancheva, Z., Miyoshi, H., Perfield, J.W., 2nd, DeFuria, J., Jick, Z., Greenberg, A.S., and Obin, M.S. (2007). Adipocyte death, adipose tissue remodeling, and obesity complications. Diabetes 56, 2910-2918.

Student, A.K., Hsu, R.Y., and Lane, M.D. (1980). Induction of fatty acid synthetase synthesis in differentiating 3T3-L1 preadipocytes. J Biol Chem 255, 4745-4750.

Suga, H., Eto, H., Aoi, N., Kato, H., Araki, J., Doi, K., Higashino, T., and Yoshimura, K. (2010). Adipose tissue remodeling under ischemia: death of adipocytes and activation of stem/progenitor cells. Plast Reconstr Surg 126, 1911-1923.

Suganami, T., Nishida, J., and Ogawa, Y. (2005). A paracrine loop between adipocytes and macrophages aggravates inflammatory changes: role of free fatty acids and tumor necrosis factor alpha. Arterioscler Thromb Vasc Biol 25, 2062-2068.

Sumimoto, H. (2008). Structure, regulation and evolution of Nox-family NADPH oxidases that produce reactive oxygen species. FEBS J 275, 3249-3277.

Sun, S., Ji, Y., Kersten, S., and Qi, L. (2012). Mechanisms of inflammatory responses in obese adipose tissue. Annu Rev Nutr 32, 261-286.

Svegliati, S., Cancello, R., Sambo, P., Luchetti, M., Paroncini, P., Orlandini, G., Discepoli, G., Paterno, R., Santillo, M., Cuozzo, C., Cassano, S., Avvedimento, E.V., and Gabrielli, A. (2005). Platelet-derived growth factor and reactive oxygen species (ROS) regulate Ras protein levels in primary human fibroblasts via ERK1/2. Amplification of ROS and Ras in systemic sclerosis fibroblasts. J Biol Chem 280, 36474-36482.

Tallquist, M., and Kazlauskas, A. (2004). PDGF signaling in cells and mice. Cytokine Growth Factor Rev 15, 205-213.

Tam, C.S., Tordjman, J., Divoux, A., Baur, L.A., and Clement, K. (2012). Adipose tissue remodeling in children: the link between collagen deposition and age-related adipocyte growth. J Clin Endocrinol Metab 97, 1320-1327.

Tang, Q.Q., Otto, T.C., and Lane, M.D. (2003). Mitotic clonal expansion: a synchronous process required for adipogenesis. Proc. Natl. Acad. Sci. USA 100, 44-49.

Tang, W., Zeve, D., Suh, J.M., Bosnakovski, D., Kyba, M., Hammer, R.E., Tallquist, M.D., and Graff, J.M. (2008). White fat progenitor cells reside in the adipose vasculature. Science 322, 583-586.

Tchkonia, T., Lenburg, M., Thomou, T., Giorgadze, N., Frampton, G., Pirtskhalava, T., Cartwright, A., Cartwright, M., Flanagan, J., Karagiannides, I., Gerry, N., Forse, R.A., Tchoukalova, Y., Jensen, M.D., Pothoulakis, C., and Kirkland, J.L. (2007). Identification of depot-specific human fat cell progenitors through distinct expression profiles and developmental gene patterns. Am J Physiol Endocrinol Metab 292, E298-307.

Tchkonia, T., Tchoukalova, Y.D., Giorgadze, N., Pirtskhalava, T., Karagiannides, I., Forse, R.A., Koo, A., Stevenson, M., Chinnappan, D., Cartwright, A., Jensen, M.D., and Kirkland, J.L. (2005). Abundance of two human preadipocyte subtypes with distinct capacities for replication, adipogenesis, and apoptosis varies among fat depots. Am J Physiol Endocrinol Metab 288, E267-277.

Tchoukalova, Y., Koutsari, C., and Jensen, M. (2007). Committed subcutaneous preadipocytes are reduced in human obesity. Diabetologia 50, 151-157.

Tchoukalova, Y.D., Koutsari, C., Votruba, S.B., Tchkonia, T., Giorgadze, N., Thomou, T., Kirkland, J.L., and Jensen, M.D. (2010a). Sex- and depot-dependent differences in adipogenesis in normal-weight humans. Obesity 18, 1875-1880.

Tchoukalova, Y.D., Votruba, S.B., Tchkonia, T., Giorgadze, N., Kirkland, J.L., and Jensen, M.D. (2010b). Regional differences in cellular mechanisms of adipose tissue gain with overfeeding. Proc. Natl. Acad. Sci. USA 107, 18226-18231.

Telepnev, M., Golovliov, I., Grundstrom, T., Tarnvik, A., and Sjostedt, A. (2003). Francisella tularensis inhibits Toll-like receptor-mediated activation of intracellular signalling and secretion of TNF-alpha and IL-1 from murine macrophages. Cell Microbiol 5, 41-51.

ten Freyhaus, H., Huntgeburth, M., Wingler, K., Schnitker, J., Bäumer, A.T., Vantler, M., Bekhite, M.M., Wartenberg, M., Sauer, H., and Rosenkranz, S. (2006). Novel Nox inhibitor VAS2870 attenuates PDGF-dependent smooth muscle cell chemotaxis, but not proliferation. Cardiovasc Res 71, 331-341.

Thiele, C., and Spandl, J. (2008). Cell biology of lipid droplets. Curr Opin Cell Biol 20, 378-385.

Tinsley, F.C., Taicher, G.Z., and Heiman, M.L. (2004). Evaluation of a quantitative magnetic resonance method for mouse whole body composition analysis. Obesity 12, 150-160.

Todaro, G.J., and Green, H. (1963). Quantitative studies of the growth of mouse embryo cells in culture and their development into established lines. J Cell Biol 17, 299-313.

Tran, K.V., Gealekman, O., Frontini, A., Zingaretti, M.C., Morroni, M., Giordano, A., Smorlesi, A., Perugini, J., De Matteis, R., Sbarbati, A., Corvera, S., and Cinti, S. (2012). The vascular endothelium of the adipose tissue gives rise to both white and brown fat cells. Cell Metab 15, 222-229.

Tran, T.T., and Kahn, C.R. (2010). Transplantation of adipose tissue and stem cells: role in metabolism and disease. Nat Rev Endocrinol. 6, 195-213.

Tran, T.T., Yamamoto, Y., Gesta, S., Kahn, C.R. (2008). Beneficial effects of subcutaneous fat transplantation on metabolism. Cell Metab 7, 410-420.

Trayhurn, P., Wang, B., and Wood, I.S. (2008). Hypoxia in adipose tissue: a basis for the dysregulation of tissue function in obesity? Br J Nutr 100, 227-235.

Tsuchiya, S., Kobayashi, Y., Goto, Y., Okumura, H., Nakae, S., Konno, T., and Tada, K. (1982). Induction of maturation in cultured human monocytic leukemia cells by a phorbol diester. Cancer Res 42, 1530-1536.

Tsuchiya, S., Yamabe, M., Yamaguchi, Y., Kobayashi, Y., Konno, T., and Tada, K. (1980). Establishment and characterization of a human acute monocytic leukemia cell line (THP-1). Int J Cancer 26, 171-176.

Tung, Y.C., and Yeo, G.S. (2011). From GWAS to biology: lessons from FTO. Ann N Y Acad Sci 1220, 162-171.

Turer, A.T., and Scherer, P.E. (2012). Adiponectin: mechanistic insights and clinical implications. Diabetologia.

van de Veerdonk, F.L., and Netea, M.G. (2010). Diversity: a hallmark of monocyte society. Immunity 33, 289-291.

van Harmelen, V., Skurk, T., Rohrig, K., Lee, Y.M., Halbleib, M., Aprath-Husmann, I., and Hauner, H. (2003). Effect of BMI and age on adipose tissue cellularity and differentiation capacity in women. Int J Obes 27, 889-895.

van Marken Lichtenbelt, W.D., Vanhommerig, J.W., Smulders, N.M., Drossaerts, J.M., Kemerink, G.J., Bouvy, N.D., Schrauwen, P., and Teule, G.J. (2009). Cold-activated brown adipose tissue in healthy men. N Engl J Med 360, 1500-1508.

Vantler, M., Caglayan, E., Zimmermann, W.H., Baumer, A.T., and Rosenkranz, S. (2005). Systematic evaluation of anti-apoptotic growth factor signaling in vascular smooth muscle cells. J Biol Chem 280, 14168-14176.

Vaziri, C., and Faller, D.V. (1996). Down-regulation of platelet-derived growth factor receptor expression during terminal differentiation of 3T3-L1 pre-adipocyte fibroblasts. J Biol Chem 271, 13642-13648.

Virtanen, K.A., Lidell, M.E., Orava, J., Heglind, M., Westergren, R., Niemi, T., Taittonen, M., Laine, J., Savisto, N.J., Enerback, S., and Nuutila, P. (2009). Functional brown adipose tissue in healthy adults. N Engl J Med 360, 1518-1525.

Wang, C.C., Cirit, M., and Haugh, J.M. (2009). PI3K-dependent cross-talk interactions converge with Ras as quantifiable inputs integrated by Erk. Mol Syst Biol 5, 246.

Weisberg, S.P., Hunter, D., Huber, R., Lemieux, J., Slaymaker, S., Vaddi, K., Charo, I., Leibel, R.L., and Ferrante, A.W., Jr. (2006). CCR2 modulates inflammatory and metabolic effects of high-fat feeding. J Clin Invest 116, 115-124.

Weisberg, S.P., McCann, D., Desai, M., Rosenbaum, M., Leibel, R.L., and Ferrante, A.W., Jr. (2003). Obesity is associated with macrophage accumulation in adipose tissue. J Clin Invest 112, 1796-1808.

Weischenfeldt, J., and Porse, B. (2008). Bone marrow-derived macrophages (BMM): isolation and applications. CSH protoc 12, pdb prot5080.

Wentworth, J.M., Naselli, G., Brown, W.A., Doyle, L., Phipson, B., Smyth, G.K., Wabitsch, M., O'Brien, P.E., and Harrison, L.C. (2010). Pro-inflammatory CD11c+CD206+ adipose tissue macrophages are associated with insulin resistance in human obesity. Diabetes 59, 1648-1656.

WHO (2004). The global burden of disease. Geneva, World Health Organization, 2004:2008 update.

Winer, D.A., Winer, S., Shen, L., Wadia, P.P., Yantha, J., Paltser, G., Tsui, H., Wu, P., Davidson, M.G., Alonso, M.N., Leong, H.X., Glassford, A., Caimol, M., Kenkel, J.A., Tedder, T.F., McLaughlin, T., Miklos, D.B., Dosch, H.M., and Engleman, E.G. (2011). B cells promote insulin resistance through modulation of T cells and production of pathogenic IgG antibodies. Nat Med 17, 610-617.

Winer, S., Chan, Y., Paltser, G., Truong, D., Tsui, H., Bahrami, J., Dorfman, R., Wang, Y., Zielenski, J., Mastronardi, F., Maezawa, Y., Drucker, D.J., Engleman, E., Winer, D., and Dosch, H.M. (2009). Normalization of obesity-associated insulin resistance through immunotherapy. Nat Med 15, 921-929.

Woo, H.A., Yim, S.H., Shin, D.H., Kang, D., Yu, D.Y., and Rhee, S.G. (2010). Inactivation of peroxiredoxin I by phosphorylation allows localized H2O2 accumulation for cell signaling. Cell 140, 517-528.

Wu, D., Molofsky, A.B., Liang, H.E., Ricardo-Gonzalez, R.R., Jouihan, H.A., Bando, J.K., Chawla, A., and Locksley, R.M. (2011). Eosinophils sustain adipose alternatively activated macrophages associated with glucose homeostasis. Science 332, 243-247.

Wu, H., Ghosh, S., Perrard, X.D., Feng, L., Garcia, G.E., Perrard, J.L., Sweeney, J.F., Peterson, L.E., Chan, L., Smith, C.W., and Ballantyne, C.M. (2007). T-cell accumulation and regulated on activation, normal T cell expressed and secreted upregulation in adipose tissue in obesity. Circulation 115, 1029-1038.

Wynes, M.W., Frankel, S.K., and Riches, D.W. (2004). IL-4-induced macrophage-derived IGF-I protects myofibroblasts from apoptosis following growth factor withdrawal. J Leukoc Biol 76, 1019-1027.

Xu, F., Burk, D., Gao, Z., Yin, J., Zhang, X., Weng, J., and Ye, J. (2012). Angiogenic deficiency and adipose tissue dysfunction are associated with macrophage malfunction in SIRT1-/- mice. Endocrinology 153, 1706-1716.

Xu, H., Barnes, G.T., Yang, Q., Tan, G., Yang, D., Chou, C.J., Sole, J., Nichols, A., Ross, J.S., Tartaglia, L.A., and Chen, H. (2003). Chronic inflammation in fat plays a crucial role in the development of obesity-related insulin resistance. J Clin Invest 112, 1821-1830.

Yang, X., Lu, X., Lombes, M., Rha, G.B., Chi, Y.I., Guerin, T.M., Smart, E.J., and Liu, J. (2010). The G(0)/G(1) switch gene 2 regulates adipose lipolysis through association with adipose triglyceride lipase. Cell Metab 11, 194-205.

Yarmo, M.N., Gagnon, A., and Sorisky, A. (2010). The anti-adipogenic effect of macrophage-conditioned medium requires the IKKbeta/NF-kappaB pathway. Horm Metab Res 42, 831-836.

Yarmo, M.N., Landry, A., Molgat, A.S., Gagnon, A., and Sorisky, A. (2009). Macrophage-conditioned medium inhibits differentiation-induced Rb phosphorylation in 3T3-L1 preadipocytes. Exp Cell Res 315, 411-418.

Zechner, R., Zimmermann, R., Eichmann, T.O., Kohlwein, S.D., Haemmerle, G., Lass, A., and Madeo, F. (2012). Fat signals - lipases and lipolysis in lipid metabolism and signaling. Cell Metab 15, 279-291.

Zeyda, M., Farmer, D., Todoric, J., Aszmann, O., Speiser, M., Gyori, G., Zlabinger, G.J., and Stulnig, T.M. (2007). Human adipose tissue macrophages are of an anti-inflammatory phenotype but capable of excessive pro-inflammatory mediator production. Int J Obes 31, 1420-1428.

Zeyda, M., Gollinger, K., Kriehuber, E., Kiefer, F.W., Neuhofer, A., and Stulnig, T.M. (2010). Newly identified adipose tissue macrophage populations in obesity with distinct chemokine and chemokine receptor expression. Int J Obes 34, 1684-1694.

Zhang, H.H., Kumar, S., Barnett, A.H., and Eggo, M.C. (2001). Dexamethasone inhibits tumor necrosis factor-alpha-induced apoptosis and interleukin-1 beta release in human subcutaneous adipocytes and preadipocytes. J Clin Endocrinol Metab 86, 2817-2825.

Zhang, Y., Proenca, R., Maffei, M., Barone, M., Leopold, L., and Friedman, J.M. (1994). Positional cloning of the mouse obese gene and its human homologue. Nature 372, 425-432.

Zimmerlin, L., Donnenberg, V.S., Pfeifer, M.E., Meyer, E.M., Peault, B., Rubin, J.P., and Donnenberg, A.D. (2010). Stromal vascular progenitors in adult human adipose tissue. Cytometry A 77, 22-30.

7.0 CURRICULUM VITAE

EDUCATION

Ph.D. Biochemistry
University of Ottawa, Ottawa, Ontario
Thesis: The effect of macrophage-secreted factors on fat cell progenitor survival.

B.Sc Honours Biochemistry
University of Ottawa, Ottawa, Ontario
Thesis: Macrophage foam cell formation
Graduated 2007 Magna cum laude

EMPLOYMENT HISTORY

Ph.D. student (Biochemistry) **September 2007-November 2012**
Ottawa Hospital Research Institute, Ottawa, ON
Supervisor: Dr. Alexander Sorisky

Teaching assistant BPS4102 **Fall 2012**
University of Ottawa, Ottawa, ON

Teaching assistant BCH2333 **Winter 2011**
University of Ottawa, Ottawa, ON

Honours student (Biochemistry) **September 2006-June 2007**
University of Ottawa Heart Institute, Ottawa, ON
Supervisor: Dr. Stewart Whitman

Research assistant (Lipid biochemistry) **May 2006- September 2006**
University of Ottawa Heart Institute, Ottawa, ON
Supervisor: Dr. Stewart Whitman

Research assistant (Microbiology) **May 2005- September 2005**
Public Health Agency of Canada, National Reference Centre for Mycobacteria, Winnipeg, MB
Supervisor: April Powell

ADDITIONAL TRAINING

Principles and theory of undergraduate teaching **Fall 2011**
University of Ottawa, Ottawa, Ontario

Stroke, Cardiovascular, Obesity, Lipids, Atherosclerosis Research program **May 2008**
University of Alberta, Edmonton, Alberta

PUBLICATIONS

Sorisky A, **Molgat AS**, Gagnon, A. Macrophage-induced adipose tissue dysfunction and the preadipocyte: should I stay (and differentiate) or should I go? Adv in Nutr. 2013 4: 1–9

Molgat AS, Gagnon A, Foster C, Sorisky A. The activation state of macrophages alters their ability to suppress preadipocyte apoptosis. J Endocrinol. 2012 Jul;214(1):21-9.

Ide J, Gagnon A, **Molgat AS**, Landry A, Foster C, Sorisky A. Macrophage-conditioned medium inhibits the activation of cyclin-dependent kinase 2 by adipogenic inducers in 3T3-L1 preadipocytes. J Cell Physiol. 2011 Sep;226(9):2297-306.

Molgat AS, Gagnon A, Sorisky A. Macrophage-induced preadipocyte survival depends on signaling through Akt, ERK1/2, and reactive oxygen species. Exp Cell Res. 2011 Feb 15;317(4):521-30.

Molgat AS, Gagnon A, Sorisky A. Preadipocyte apoptosis is prevented by macrophage-conditioned medium in a PDGF-dependent manner. Am J Physiol Cell Physiol. 2009 Apr;296(4):C757-65.

Yarmo MN, Landry A, **Molgat AS**, Gagnon A, Sorisky A. Macrophage-conditioned medium inhibits differentiation-induced Rb phosphorylation in 3T3-L1 preadipocytes. Exp Cell Res. 2009 Feb 1;315(3):411-8.

PRESENTATIONS & PUBLISHED ABSTRACTS

Molgat AS, Gagnon A, Sorisky A. June 2012. Activated macrophages regulate human preadipocyte apoptosis. 72nd Scientific Sessions – American Diabetes Association, Philadelphia PA. (refereed)

Molgat AS, Gagnon A, Sorisky A. November 2011. Preadipocyte apoptosis is regulated by macrophage secreted factors. 11th Annual Ottawa Hospital Research Institute Research Day, Ottawa ON.

Molgat AS, Gagnon A, Sorisky A. June 2011. Pro-survival activity of macrophage-conditioned medium on 3T3-L1 preadipocytes is impaired when macrophages are activated by LPS. 93rd Annual Meeting – The Endocrine Society, Boston MA. (refereed)

Molgat AS, Gagnon A, Sorisky A. February 2011. Macrophage-dependent preadipocyte survival: Influence of macrophage activation. University of Ottawa Seminar Day, Ottawa ON.

Molgat AS, Gagnon A, Sorisky A. May 2010. Macrophage-conditioned medium-dependent phosphorylation of Akt and ERK1/2 protects preadipocytes from apoptosis. University of Ottawa Poster Day, Ottawa ON.

Molgat AS, Gagnon A, Sorisky A. November 2010. Macrophage-induced preadipocyte survival depends on signaling through Akt, ERK1/2, and reactive oxygen species. 10th Annual Ottawa Hospital Research Institute Research Day, Ottawa ON.

Molgat AS, Gagnon A, Sorisky A. November 2009. The role of Akt and ERK1/2 phosphorylation in macrophage-conditioned medium-dependent preadipocyte survival. 9th Annual Ottawa Hospital Research Institute Research Day, Ottawa ON.

Molgat AS, Gagnon A, Sorisky A. June 2009. Macrophage-secreted PDGF protects 3T3-L1 preadipocytes from apoptosis. 91st Annual Meeting – The Endocrine Society, Washington DC. (refereed)

Molgat AS, Gagnon A, Sorisky A. May 2009. Macrophage-conditioned medium prevents 3T3-L1 preadipocytes from serum-withdrawal-induced apoptosis. University of Ottawa Poster Day, Ottawa ON.

Molgat AS, Gagnon A, Sorisky A. November 2008. Preadipocyte apoptosis is prevented by macrophage conditioned medium in a PDGF-dependent manner. 8th Annual Ottawa Hospital Research Institute Research Day, Ottawa ON.

Yarmo MN, **Molgat AS**, Landry A, Gagnon A, Sorisky A. June 2008. The inhibition of 3T3-L1 preadipocyte differentiation by macrophage-conditioned media. 90th Annual Meeting – The Endocrine Society, San Francisco CA. (refereed)

Molgat AS, Gagnon A, Sorisky A. November 2007. Anti-adipogenic signaling induced by macrophage secreted products. 7th Annual Ottawa Hospital Research Institute Research Day, Ottawa ON.

Molgat AS, Whitman, SC. March 2007. Macrophage foam cell formation: Assessment of cholesterol loading by the ACAT stimulation assay. Biochemistry Honours Research Day, Ottawa, ON.

SCHOLARSHIPS & AWARDS

Natural Sciences and Engineering Research Council of Canada - Alexander Graham Bell Canada Graduate Scholarship
Funding period: 2010-2013
Value: $105,000

Faculty of Medicine Award of Excellence in Graduate Studies
Award date: November 2011
Value: $500

11th Annual OHRI research day award (2nd place oral presentation)
Award date: November 2011
Value: $500

Heart & Stroke Foundation of Canada Doctoral Research Award (declined)
Funding period: 2010-2012
Value: $42,000

Ontario Graduate Scholarship (declined)
Funding period: 2010-2011
Value: $15,000

9th Annual OHRI research day award (3rd place oral presentation)
Award date: November 2009
Value: $50

University of Ottawa Excellence Scholarship
Funding period: 2008-2013

Heart & Stroke Foundation of Ontario Masters Studentship
Funding period: 2008-2010
Value: $36,000

Ontario Graduate Scholarship in Science and Technology (declined)
Funding period: 2008-2009
Value: $15,000

University of Ottawa Graduate Admission Scholarship
Funding period: 2007-2008

Dean's honour list
Award date: 2007

University of Ottawa Merit Scholarship
Funding period: 2005 – 2006
Value: $500

University of Ottawa Admission Scholarship
Funding period: 2003 – 2004
Value: $1,500